

## AN ABSTRACT OF THE THESIS OF

Hunseung Kang for the degree of Doctor of Philosophy in  
Biochemistry and Biophysics presented on November 22, 1993

Title : Base Inclinations for DNA in Solutions and Films  
as Revealed by Linear Dichroism.

\Redacted for Privacy

Abstract Approved by :

Dr. W. Curtis Johnson, Jr.

Linear dichroism (LD) is employed to investigate the inclination of bases for DNA in solutions and films. LD measurements are made in the vacuum uv region for the DNA samples in a flow cell, and a sophisticated algorithm, recently developed in our laboratory, is used to calculate specific inclination angles for the four individual bases. Vacuum uv flow LD demonstrates that the bases for poly[d(AC)]•poly[d(GT)] and poly[d(AG)]•poly[d(CT)] are inclined from perpendicular to the helix axis. The inclination angles are about 20-25° for purines and about 30-35° for pyrimidines in the B-form. The inclinations are increased in the A-form, as expected.

To obtain additional information about base inclinations, infrared (IR) LD of oriented films is employed for poly[d(AC)]•poly[d(GT)], poly[d(AG)]•poly[d(CT)], and natural DNAs (from *E. coli* and calf thymus). Using properly oriented samples on an IR transparent window, minimum angles of inclination are deduced from the dichroic ratios of each band arising from in-plane carbonyl bond and ring stretching vibrations. Infrared LD shows that the bases for B-DNA in films have sizable inclinations, which are comparable with those found in solution from uv LD. Poly[d(AG)]•poly[d(CT)] in the C-form has almost same inclinations as in B-DNA, and for the other DNAs the inclinations are increased slightly for the A-form. The average minimum inclinations for B- and

A-forms of DNA in film are, respectively, about 15-20° and 20-25°.

IR LD is also used to obtain conformational angles for phosphodiester backbone geometry of A-, B-, and C-DNA. The  $\theta_{\infty}$  angles for the A- and B-forms of synthetic polynucleotides and natural DNAs are about 63-65° and 54-55°, respectively. The  $\theta_{\text{opp}}$  angles for A- and B-form are, respectively, about 45-48° and 61-68°. For the C-DNA, the  $\theta_{\infty}$  and the  $\theta_{\text{opp}}$  angles are about 48° and 66°. All of these angles are well within the range of reported values obtained from IR LD, phosphorus NMR, and theoretical calculations. The orientation of the bases for DNA in solution and film revealed by LD using two different transition levels, electronic and vibronic, provide important clues to understanding the molecular structure of DNA in living cells.

In other work, stacking interactions of ApA analogues with modified backbones are studied as a function of temperature using CD measurements. Results of these studies show that when a carbonyl is substituted for the phosphate to produce an uncharged backbone, the analogues that have either a sugar or morpholino substitution do not stack. In contrast, when a morpholino group is substituted for the sugar and the phosphate is modified so as to be uncharged, there is strong base stacking. Singular value decomposition demonstrates that the stacking is two state, and Taylor series decomposition yields a coefficient that measures base stacking interactions. The van't Hoff equation is applied to the base stacking coefficient from the Taylor series fitting to give thermodynamic parameters.

**Base Inclinations for DNA in Solutions and Films  
as Revealed by Linear Dichroism.**

by

Hunseung Kang

A THESIS

submitted to

Oregon State University

in partial fulfillment of  
the requirements for the  
degree of  
Doctor of Philosophy

Completed November 22, 1993

Commencement June 1994

APPROVED :

Redacted for Privacy

Professor of Biochemistry and Biophysics in charge of major

Redacted for Privacy

---

Head of Department of Biochemistry and Biophysics

Redacted for Privacy

---

Dean of Graduate School

Date thesis is presented : November 22, 1993

Typed by Hunseung Kang for Hunseung Kang

## ACKNOWLEDGMENTS

First of all I would like to thank heartily my major professor Dr. W. Curtis Johnson, Jr. for his encouragement, guidance, and support. His advice in the laboratory as well as out of the laboratory have been greatly appreciated. He has taught me a simple but very powerful message to solve scientific problems, "Divide and Conquer!".

I would also like to thank other committee members, Dr. Sonia R. Anderson, Dr. George D. Pearson, Dr. Kensal E. van Holde, Dr. David E. Williams, and Dr. Malcolm Daniels, for their help and discussion in guiding my graduate program.

I would like to thank all members in our laboratory, Dr. Araz Toumadje, Dr. Vince Waterhous, and Mrs. Jeannine R. Lawrence for their help and discussion. Especially, I would like to thank Mr. Ping-Jung Chou in our laboratory for his friendship and discussion on many problems about computer programs. It was a great pleasure to work with people who are fun and have a sense of humor.

This dissertation is dedicated to my wife, Hoo-Joong Lee Kang, for her love, endurance, and support; to my lovely son, Ki-Hyun Kang; and to my parents for their love and prayers.

## TABLE OF CONTENTS

<b>SECTION I : INTRODUCTION</b>	<b>1</b>
Historical Background	1
Work on Linear Dichroism	6
 <b>SECTION II : LINEAR DICHROISM DEMONSTRATES THAT THE BASES IN POLY[d(AC)]•POLY[d(GT)] AND POLY[d(AG)]• POLY[d(CT)] ARE INCLINED FROM PERPENDICULAR TO THE HELIX AXIS</b>	 <b>10</b>
Abstract	11
Introduction	12
Materials and Methods	14
Sample Preparation	14
Spectroscopic Measurements	14
Data Analysis	15
Results	17
Discussion	33
Acknowledgements	36
References	37
 <b>SECTION III : INFRARED LINEAR DICHROISM REVEALS THAT A-, B-, AND C-DNA IN FILMS HAVE BASES HIGHLY INCLINED FROM PERPENDICULAR TO THE HELIX AXIS</b>	 <b>40</b>
Abstract	41
Introduction	42
Materials and Methods	45
Sample Preparation	45
Infrared Measurements	45
Theoretical	46
Data Analysis	48

Results and Discussion	51
Characterization of the A-, B-, and C-Forms	51
Estimation of the Orientation Parameter	61
Decomposition of Overlapping Bands	64
Inclination of the Bases	74
Conformation of Phosphodiester Backbone Geometry	76
Acknowledgements	84
References	85
SECTION IV : CONCLUSIONS	89
SECTION V : BIBLIOGRAPHY	91
APPENDIX : STACKING INTERACTIONS OF ApA ANALOGUES WITH MODIFIED BACKBONES	102
Abstract	103
Introduction	104
Materials and Methods	108
Materials	108
Spectroscopic Measurements	108
Singular Value Decomposition	108
Taylor Series Analysis	109
Fitting the Melting Data	110
Results and Discussion	114
Effect of Backbone Structure on CD	114
SVD and Taylor Series Fitting	123
Thermodynamics of Stacking	124
Fitting Straight Lines	125
Conformation of Stacked Dimers	126
Acknowledgements	140
References	141

## LIST OF FIGURES

Figure 2.1. Poly[d(AC)]•poly[d(GT)] in 10 mM sodium phosphate buffer, pH 7.0. (a) CD, (b) normalized LD, A, and reduced dichroism.	25
Figure 2.2. Poly[d(AC)]•poly[d(GT)] in 80 % trifluoroethanol, pH 7. (a) CD, (b) normalized LD, A, and reduced dichroism.	27
Figure 2.3. Poly[d(AG)]•poly[d(CT)] in 10 mM sodium phosphate buffer, pH 8.0. (a) CD, (b) normalized LD, A, and reduced dichroism.	29
Figure 2.4. Poly[d(AG)]•poly[d(CT)] in 80 % trifluoroethanol, pH 8. (a) CD, (b) normalized LD, A, and reduced dichroism.	31
Figure 3.1. Diagram showing sealed chamber.	50
Figure 3.2. Infrared spectra of (a) poly[d(AC)]•poly[d(GT)] in the B form at 94% r.h., (b) poly[d(AC)]•poly[d(GT)] in the A form at 75% r.h., (c) poly[d(AG)]•poly[d(CT)] in the B form at 94% r.h., and (d) poly[d(AG)]•poly[d(CT)] in the C form at 66% r.h.	55
Figure 3.3. Infrared spectra of (a) calf thymus DNA in the B form at 94% r.h., (b) calf thymus DNA in the A form at 75% r.h., (c) <i>E. coli</i> DNA in the B form at 94% r.h., and (d) <i>E. coli</i> DNA in the A form at 75% r.h.	57
Figure 3.4. Dichroic spectra in the PO <sub>2</sub> <sup>-</sup> stretching vibration region for the oriented DNA samples measured with the electric vector of the polarized light perpendicular and parallel to the helix axis.	59
Figure 3.5. Dependence of the $\theta$ angle on both the base inclination ( $\alpha$ ) and the relative angle between the transition dipole and the axis of inclination ( $\beta$ ).	63



Figure 3.6. Dichroic spectra for the in-plane double bond stretching region for the oriented films hydrated with D <sub>2</sub> O.	66
Figure 3.7. Dichroic spectra for the in-plane double bond stretching region for the oriented films hydrated with D <sub>2</sub> O.	68
Figure 3.8. (a) Dichroic spectra for the in-plane double bond stretching region for an oriented poly[d(AC)]•poly[d(GT)] film hydrated with D <sub>2</sub> O at 94% r.h.	70
Figure 3.9. (a) Dichroic spectra and (b) decomposition of overlapping bands for an oriented poly[d(AG)]•poly[d(CT)] film hydrated with D <sub>2</sub> O at 66% r.h.	72
Figure 4.1. Structures of the ApA analogues and their constituent monomers studied, showing the morpholino moiety and different linkage variations.	106
Figure 4.2. Variance of R <sup>2</sup> , SSQ, ΔS°, ΔH°, t <sub>ΔS</sub> , and t <sub>ΔH</sub> as a function of B <sub>st</sub> on fitting B(T) for ApA to the van't Hoff Equation.	112
Figure 4.3. Representative CD spectra of ApA, d(ApA), and dimer I in 10 mM sodium phosphate buffer, pH 7.0, between 2 and 90 °C.	115
Figure 4.4. Representative CD spectra of dimer II, III-fast, and III-slow in 10 mM sodium phosphate buffer, pH 7.0, between 2 and 90 °C.	117
Figure 4.5. Representative CD spectra of monomer VI, and dimers IV-fast and IV-slow in 10 mM sodium phosphate buffer, pH 7.0, between 5 and 90 °C.	119
Figure 4.6. Representative CD spectra of monomer VII, and dimers V-fast and V-slow in 10 mM sodium phosphate buffer, pH 7.0, between 5 and 85 °C.	121

Figure 4.7. The three most significant wavelength basis vectors (**US**) determined from singular value decomposition of CD spectra for (a) I, (b) III-slow, and (c) V-slow. 128

Figure 4.8. The three most significant temperature basis vectors (**SV<sup>T</sup>**) determined from singular value decomposition of CD spectra for (a) I, (b) III-slow, and (c) V-slow. 130

Figure 4.9. Taylor series coefficients A and B vs temperature for d(ApA), ApA, I, II, III-fast, III-slow, IV-fast, IV-slow, V-fast, and V-slow. 132

Figure 4.10. Percentage of stacking vs temperature for dimers that stack, calculated from the parameters of Table 4.1. 134

Figure 4.11. Taylor coefficient B vs Temperature for various straight lines with different slopes and intercepts. 136

## LIST OF TABLES

Table 2.1. Transition dipole directions.	20
Table 2.2. Simultaneous fitting of absorption and LD spectra for poly[d(AC)]•poly[d(GT)] in 10 mM sodium phosphate buffer, pH 7.0.	21
Table 2.3. Simultaneous fitting of absorption and LD spectra for poly[d(AC)]•poly[d(GT)] in 80 % TFE, pH 7.	22
Table 2.4. Simultaneous fitting of absorption and LD spectra for poly[d(AG)]•poly[d(CT)] in 10 mM sodium phosphate buffer, pH 8.0.	23
Table 2.5. Simultaneous fitting of absorption and LD spectra for poly[d(AG)]•poly[d(CT)] in 80 % TFE, pH 8.	24
Table 3.1. IR absorption bands observed for different DNA conformations in H <sub>2</sub> O.	54
Table 3.2. Dichroic ratios from various experiments and corresponding $\theta$ angles for poly[d(AC)]•poly[d(GT)] in films hydrated with D <sub>2</sub> O.	77
Table 3.3. Dichroic ratios from various experiments and corresponding $\theta$ angles for poly[d(AG)]•poly[d(CT)] in films hydrated with D <sub>2</sub> O.	78
Table 3.4. Dichroic ratios from various experiments and corresponding $\theta$ angles for <i>E.coli</i> DNA in film hydrated with D <sub>2</sub> O.	79
Table 3.5. Dichroic ratios from various experiments and corresponding $\theta$ angles for calf thymus DNA in film hydrated with D <sub>2</sub> O.	80
Table 3.6. Conformational angles for phosphodiester backbone of DNA in film hydrated with H <sub>2</sub> O.	83
Table 4.1. Thermodynamic parameters for intramolecular stacking.	138

Table 4.2. Results of fitting various straight lines (Figure 4.11) with different slopes and intercepts to the van't Hoff equation.

## PREFACE

This thesis comprises of three parts based on the manuscripts written for publication. The first manuscript has been published in *Biopolymers* (1993) **33**, pp. 245-253. The second manuscript has been submitted for publication (1993). These two manuscripts deal with base inclinations for DNA in solution and films using UV flow linear dichroism and infrared film linear dichroism, respectively. The third manuscript has been published in *Biopolymers* (1992) **32**, pp. 1351-1363. This manuscript deals with circular dichroism and thermodynamic analysis for stacking interactions of dinucleotides with a modified backbone. Since this work is not related to the first two manuscripts about base inclination, this manuscript has been included as the Appendix. The introduction section has been added to review the state of research on molecular structure of DNA. The other sections have been changed only slightly to meet the requirements of a thesis format.

# **Base Inclinations for DNA in Solutions and Films as Revealed by Linear Dichroism**

## **SECTION I INTRODUCTION**

### **Historical Background.**

The pioneering work on nucleic acid structure by Watson and Crick (1953), which deduced the double helical DNA model from X-ray fiber diffraction in the early fifties, opened a new research area in molecular biology. Since then research investigating the molecular structure of nucleic acids using different biophysical techniques has been extremely popular. Now it is well known that DNA can adopt many different conformations depending on sequence (Bram & Tougaard, 1972; Leslie et al., 1980; Dickerson & Drew, 1981; Sarai et al., 1988), salt (Fuller & Wilkins, 1965; Bram & Tougaard, 1972; Ivanov et al., 1973; Leslie et al., 1980), or solvent (Ivanov et al., 1973; Girod et al., 1973; Pohl, 1976). This polymorphic nature of DNA is regarded as very important to many biological processes, such as DNA-protein interactions, transcription, DNA-ligand interactions, and other DNA interactions.

The molecular structure of the canonical B- and A-forms of double helical DNA comes from analyses of the X-ray fiber diffraction (Arnott & Hukins, 1972, 1973; Arnott et al., 1974; Arnott & Selsing, 1974). From the regularly spaced diffraction pattern of the DNA fibers, important helical parameters for describing A- and B-DNA structures have emerged. The bases in canonical B-DNA are nearly perpendicular to the helix axis, and those in canonical A-DNA are inclined about 20° from perpendicular to the helix axis. Canonical A- and B-DNA are produced in the fibers of natural DNA equilibrated at low (75 %) and high (>94 %) relative humidity (r.h.), respectively. In addition to this canonical A- and B-DNA, several different conformations, such as C-, D-, and Z-forms, have been suggested for different DNA samples at specific environmental conditions. The C-form was first observed by Marvin et al. (1961) from X-ray

diffraction studies of fibers of LiDNA, and was regarded as a distorted form of B-DNA. The Z-form is a left-handed double helical conformation that can be produced for specific sequences with alternating purine-pyrimidine bases, G and C rich, and sequences with modified bases. The molecular structure and the possible biological roles of these unusual DNA conformations have been discussed by many workers (Johnston, 1992, and references therein).

As techniques in molecular biology have been developed to synthesize specific DNA oligomers of known sequence concomitant with progress in instrumentation to analyze biopolymers and progress to crystallize deoxyoligonucleotides, the research on DNA structure matured to investigate molecular structure of different conformations of DNA at high resolution. This progress in X-ray crystallography to deduce structure of known sequences of synthetic oligonucleotides tells us more accurately the helical parameters and the conformational angles of sugar, sugar-phosphate backbone, and glycosidic bonds for the different conformations of DNA. More than 100 deoxyoligonucleotide crystal structures have been solved for the A-, B-, and Z-forms of DNA (Wang et al., 1979; Drew & Dickerson, 1981a; Dickerson et al., 1982; Coll et al., 1988; Heinemann & Alings, 1989; Gessner et al., 1989; Larsen et al., 1991; Narayana et al., 1991; Jain et al., 1991; Yuan et al., 1992; Schneider et al., 1992; Bingman et al., 1992). The important message deduced from this work is that DNA can adopt many different conformations, depending on the sequence and crystallization conditions (Saenger et al., 1986; Digabriele et al., 1989).

Although the results of X-ray fiber and crystal diffraction analysis provide important clues to describe the molecular structure of DNA at the atomic level, they do not tell us about DNA structure in aqueous solution, which is the interior of living cells. Therefore, other methods of probing DNA structure in aqueous solution are required to understand the real nature of DNA in living cells. For this purpose, optical spectroscopy such as circular dichroism (CD), optical rotatory dispersion (ORD), and absorption spectroscopy have been widely used

to identify the A-, B-, and Z-forms of DNA in solution (Baase & Johnson, 1976, 1979; Sprecher et al., 1979; Woisard & Fazakerley, 1986; Bokma et al., 1987; Riazance et al., 1987; Gray et al., 1990; Zhong & Johnson, 1990; Gray et al., 1992). Although optical spectroscopy is useful to identify different conformations of DNA in solution with relatively simple measurements, they have not extracted quantitative structural parameters for the double helical structure of DNA.

During the last decade NMR spectroscopy has developed greatly and is used to investigate DNA structure in solution. The measurements of chemical shifts and coupling constants, and relaxation experiments have been used to study the structural and dynamic properties of oligonucleotides (Mirau & Kearns, 1984; Munt et al., 1984; Mirau et al., 1985; Behling & Kearns, 1986). In addition, the recent development of multi-dimensional NMR provides a powerful tool to deduce molecular structure of DNA in solution at high resolution. Helical parameters and the conformational and torsional angles for sugar, sugar-phosphate, or glycosidic bonds, have been investigated by using NMR and molecular dynamics (Clare et al., 1985; Hare & Reid, 1986; Nilsson et al., 1986; Nilges et al., 1987; Nerdal et al., 1988; Gronenborn & Clare, 1989). However, one of the problems with analyzing multi-dimensional NMR data is the starting DNA model used to fit the crosspeak pattern observed. The starting DNA models are usually obtained from the DNA structures deduced from the X-ray diffraction data. Thus it is not surprising to see that the structural parameters for DNA conformation deduced from NMR and X-ray data are quite similar. For example, the base inclinations for B-DNA are found to be less than  $6^\circ$  both in crystal from X-ray diffraction and in solution from NMR. Recently Cheng et al. (1992) have used NMR measurements together with distance geometry methods to obtain structural parameters for the B-form of synthetic oligonucleotides in solution, and have reported that the B-DNA had a somewhat strange A-DNA like inclination of about  $12^\circ$ . However, it should be noted that they used the NMR/distance geometry approach to elucidate the structural



features of double-stranded helical DNA in solution without resorting to empirical energy potentials and without using any structural assumptions from crystallographic data. More recently, Nibedita et al. (1993) have investigated the solution structure of a 14-mer DNA duplex by 2D NMR, molecular modeling, and distance geometry calculations, and have reported an interesting structural model with the sugars and many of the torsional angles belonging to the B-DNA family, but the base pairs inclined to the helical axis as is normally seen in A-DNA. It is, therefore, recognized that the structural parameters for the specific conformation of DNA in solid and solution states may be different each other.

Another useful way to probe the molecular structure of DNA in solution, as well as in gels or films, is infrared (IR) spectroscopy. IR spectroscopy has been used for a long time to study the solution structure of biopolymers such as proteins, nucleic acids, membranes, and protein-ligand and DNA-ligand complexes. The recent development of a Fourier transform IR spectrophotometer for rapid and accurate data collection, and the sophisticated software for efficient data management make IR spectroscopy a powerful tool to study the molecular structure of DNA. The principal use of IR spectroscopy has been to fingerprint different conformations of DNA. Many groups have reported IR spectra for synthetic polynucleotides, oligonucleotides, and natural DNAs in solution or films to determine characteristic marker bands for the A-, B-, C-, and Z-forms of DNA (for a review, see Taillandier & Liquier, 1992, and references therein). Recently, IR spectroscopy has also been used to detect the existence of a triple helix structure in specific sequences of synthetic polynucleotides (Liquier et al., 1991; Akhebat et al., 1992; Howard et al., 1992), and to study DNA-ligand or DNA-protein interactions (Liquier et al., 1975, 1979, 1989; Taillandier et al., 1984a; Dev & Walters, 1990; Pohle et al., 1990; Pohle & Fritzsche, 1990; Mohr et al., 1991; Adnet et al., 1992).

Our primary concern in using IR spectroscopy is to extract structural parameters, such as base inclination and conformational angles for the phosphodiester backbone, for nucleic acids in films using linear dichroism (IR

LD). Only a few references are available so far for the base inclination of DNA using IR LD measurements.

In addition to these experimental reports for probing the molecular structure of DNA in solid or solution states, model building studies may be used to supplement experimental data with detailed three-dimensional hypothetical models. The powerful methods of molecular mechanics and dynamics have been developed during the last 30 years. These methods use a so-called force field to calculate approximate internal energies of a given molecule as a function of the coordinates of its atoms. Here also a reasonable starting model DNA structure is required, and the coordinates obtained from X-ray fiber diffraction data are usually used. Interestingly, there are a lot of reports for energetically favorable B-DNA models with bases highly inclined from perpendicular to the helix axis (Levitt, 1978; Zhurkin et al., 1978; Singh et al., 1985; Rao et al., 1986; Ansevin & Wang, 1990; Srinivasan et al., 1990; Swaminathan et al., 1991). These authors have applied molecular mechanics or molecular dynamics to oligonucleotides to search for the energetically favorable conformation of DNA, and have reported sequence or charge dependent variations of the local conformation of DNA. From the results of modeling DNA structure by these authors, the base inclinations in the energetically favorable B-DNA are found to be about 15-25°. Edmondson (1987) used molecular mechanical energy minimization to construct model helices for poly(dA)•poly(dT), based on the base orientations determined by flow LD measurements, and has successfully produced an energetically stable conformation of B-DNA with the bases highly inclined from perpendicular to the helix axis. This modeling of DNA structures using molecular mechanics or molecular dynamics supplements the experimental results to give a detailed molecular structure of different conformations of DNA in solution.

## Work on Linear Dichroism

Linear dichroism (LD) is the anisotropic absorption of linearly polarized light by a chromophore, and is a useful way to get structural information about biopolymers in solution. LD can be expressed in a relatively simple analytical form in terms of the angles between the light-absorbing transition dipoles and the direction of polarization of the applied light. Of primary importance in LD is the transition dipoles for light absorbing components of the biomolecules; the direction of the transition dipoles must be known to deduce specific structural information from LD measurements. In the case of the DNA bases, the directions of the transition dipoles arising from  $\pi\text{-}\pi^*$  transitions in the uv absorption are known from other methods, such as polarized reflectance or absorption spectra of single crystals, fluorescence polarization, and polarized spectra of molecules oriented in stretched films or external electric fields (Chen & Clark, 1969, 1973; Hug & Tinoco, 1973; Clark, 1977, 1986, 1989, 1990; Matsuoka & Norden, 1982a; Zaloudek et al., 1985; Novros & Clark, 1986).

Several different LD techniques are named according to the specific method for orienting the sample molecules. These include flow fields, electric fields, magnetic fields, stretched films, compressed gels, photoselection, and crystals. A recent review by Norden et al. (1992a) discusses the theory and some practical aspects about these orientation techniques. Among them, electric dichroism (ED) is one of the most widely used methods due to its relatively easy orientation of the sample in an accurately controlled electric field. Many reports investigate base orientations of free DNA or DNA complexed with ligands or drugs (Ding et al., 1972; Yamaoka & Charney, 1973; Hogan et al., 1978; Wu et al., 1981; Yamaoka & Matsuda, 1981; Charney & Yamaoka, 1982; Lee & Charney, 1982; Charney et al., 1986; Charney & Chen, 1987; Schurr & Fujimoto, 1988). Since the measurements are usually made only at one specific wavelength in ED (at 260 nm for DNA), the information content from the ED measurements are limited; one can extract only the average minimum inclination of the DNA bases. In addition, the measured data have to be

extrapolated to infinite field where the orientation parameter ( $S$ ) is 1.0. If the molecules have a tertiary structure, the extrapolation may not be correct.

Another useful way to orient samples is to use the shear force of flow fields. Long oligomers of double helical DNA, other large molecules, or fibrous particles may be aligned by shear gradients. Flow LD also has been used to investigate the orientation of bases in free DNA, or DNA complexed with ligands or drugs (Rill, 1972; Matsuoka & Norden, 1982b, 1983; Geacintov et al., 1987; Eriksson et al., 1988; Forni et al., 1989a, 1989b; van Amerongen & van Grondelle, 1989; van Amerongen et al., 1988, 1990; Norden et al., 1990, 1992b; Swenberg et al., 1990; Clark & Gray, 1992). Our laboratory uses a short pathlength flow cell to produce a high enough shear force to align DNA oligomers in the flow field (recent investigations show that DNA fragments of about 150 base pairs in length are long enough to give proper orientation in our flow cell). In contrast to ED, which uses the data measured at only one specific wavelength, flow LD scans the spectrum. By extending LD measurements into the vacuum-uv region, we are able to greatly increase the information content of our LD data (Johnson, 1988). We use the high information content in the wavelength dependence of the absorption and the LD in the range of 320-175 nm to extract the orientation parameter, as well as the specific inclination angles and the axes of inclination for individual bases.

Our laboratory has used vacuum-uv flow LD to extract the inclination angles of each base for the synthetic polynucleotides, poly(dA)•poly(dT), poly(dG)•poly(dC), poly[d(AT)]•poly[d(AT)], and poly[d(GC)]•poly[d(GC)], and several natural DNAs in solution (Causley & Johnson, 1982; Dougherty et al., 1983; Edmondson & Johnson, 1985a, 1985b, 1986; Edmondson, 1987). Recently, a sophisticated algorithm has been developed in our laboratory to calculate the specific base inclinations for the DNA with four different types of bases (Chou & Johnson, 1993). The results obtained so far show that the bases are inclined about 20-25° in the B-DNA. The inclinations are increased in A-DNA, and in all cases the pyrimidines are more inclined than the purines.

Infrared linear dichroism (IR LD) is another method to study base inclination for DNA in solutions as well as fibers or films. The drawback of IR LD measurements, however, is that the specific inclination angles for individual bases cannot be extracted, since the directions of the transition dipoles due to the vibrational transitions are not known, and the information content is limited. One can only calculate minimum values of the average inclination angle for bases from the dichroic spectra of oriented DNA samples. Few references are available for the base inclinations of DNA revealed by IR LD. In the early sixties Bradbury et al. (1961) and Falk et al. (1963) measured dichroic spectra of calf thymus DNA in films hydrated with D<sub>2</sub>O, but they did not report any inclinations for the bases. The first systematic analysis of IR LD data related to base inclinations came from Baret et al. (1978) for oriented films of poly(dA)•poly(dT) and poly[d(AT)]•poly[d(AT)]. More recently, Flemming et al. (1988) used IR LD to obtain inclination angles of natural DNA in films. The IR results show that the bases in B-DNA are inclined about 15-25° with respect to the helical axis. They also found that the difference in base inclination between B- and A-DNA is not as large as that observed in fiber diffraction data (6° for B-DNA and 20° for A-DNA).

Another application of IR LD to reveal the molecular structure of DNA is to obtain conformational angles for the phosphate (PO<sub>2</sub><sup>-</sup>) geometry in the double helical structure of DNA. The geometry of the phosphodiester backbone in DNA is determined by the two conformational angles,  $\theta_{\text{oo}}$  and  $\theta_{\text{oop}}$ , which are defined as the angle between the helix axis and the transition moment vector along the O---O line and the OPO bisector, respectively. These conformational angles, together with the torsional angles for the sugar and glycosidic bonds, play a major role in determining the relative stability for specific conformations of DNA. X-ray diffraction, phosphorus NMR, IR LD, and theoretical calculations have been used to measure these conformational angles (Pohle et al., 1984, 1986, and references therein). Among them, IR LD is the only direct way to

extract the conformational angles by measuring the dichroic spectra of oriented fibers or films of DNA.

A lot of DNA samples (both synthetic polynucleotides and natural DNA) have been tested to get  $\theta_{\infty}$  and  $\theta_{\text{opo}}$  angles, and the similarities and differences in these angles determined by different methods are reviewed by Pohle et al. (1984, 1986). The results from IR LD, phosphorus NMR, and theoretical calculation agreed with each other quite well, but the results from X-ray fiber diffraction deviated somewhat, depending on the DNA model used to fit the diffraction data in the earlier analysis. But, in the review paper by Pohle et al. (1986), many different DNA models for X-ray diffraction data have been considered, and the coincidence of the angles for  $\text{PO}_2^-$  groups obtained by IR LD and X-ray diffraction analysis results has been discussed. It was also shown by Premilat and Albiser (1983) that the IR data for the  $\text{PO}_2^-$  group geometry are compatible with the same X-ray diffraction data, which had been misinterpreted previously. More recently, Chandrasekaran et al. (1989) have published model on A-DNA from X-ray data that are very similar to the IR results for the  $\text{PO}_2^-$  group geometry. Now, the average angles of  $\theta_{\infty}$  and  $\theta_{\text{opo}}$  for B-DNA are known to be in the range of 52-56° and 62-70°, respectively. A-DNA has the  $\theta_{\infty}$  and  $\theta_{\text{opo}}$  of 59-64° and 46-50°, respectively. For Z-DNA these two angles are found to be quite similar (about 58°) (Pohle et al, 1984, 1986, and references therein).

## **SECTION II**

**Linear Dichroism Demonstrates that the Bases in  
Poly[d(AC)]•Poly[d(GT)] and Poly[d(AG)]•Poly[d(CT)]  
Are Inclined from Perpendicular to the Helix Axis**

**Hunseung Kang and W. Curtis Johnson, Jr.**

Department of Biochemistry and Biophysics  
Oregon State University, Corvallis, OR 97331-6503.

Published in *Biopolymers* (1993) **33**, 245-253

## **ABSTRACT**

Flow linear dichroism is used to measure specific inclinations for each of the four bases in poly[d(AC)]•poly[d(GT)] and poly[d(AG)]•poly[d(CT)] in both the B and A forms. For the B form in solution the bases are found to have a sizable inclination. Inclination is increased in the A form, as expected. In all cases the pyrimidines are more inclined than the purines.



## INTRODUCTION

The well-defined conformation of DNA in living cells is very important for storing genetic information in a stable form and for sequence-specific DNA-protein interactions, and plays significant roles in several stages of gene expression. Since Watson and Crick proposed the helical structure of DNA, many efforts have been made to elucidate sequence-dependent secondary structure of natural or synthetic oligonucleotides by x-ray crystallography (Wang et al., 1979; Arnott et al., 1980; Drew et al., 1980; Fratini et al., 1982; Heinemann & Alings, 1989; Jain et al., 1991; Narayana et al., 1991). DNA is known to be polymorphic with the structure depending on sequence (Bram & Tougard, 1972; Leslie et al., 1980; Dickerson & Drew, 1981; Sarai et al., 1988), cation type (Fuller & Wilkins, 1965; Bram & Tougard, 1972; Ivanov et al., 1973; Leslie et al., 1982), and solvent (Ivanov et al., 1973; Girod et al., 1973; Pohl, 1976). The facility with which DNA assumes many different secondary structures means that structural models built on x-ray diffraction may well be different from the structures that actually exist in the aqueous environment of living cells. Therefore, it is important to study the structure of DNA in solution.

Linear dichroism (LD) spectroscopy is one technique for studying DNA structure in solution. The LD of DNA in the uv-spectral region depends on the inclination of the base planes from perpendicular to the helix axis (Wada, 1972; Norden, 1978). This method has been applied in our laboratory to natural DNA (Dougherty et al., 1983; Edmondson & Johnson, 1985a) and to various synthetic polynucleotides containing one or two types of bases, such as poly[r(A)] and poly[r(C)] (Causley & Johnson, 1982), poly[d(A)•d(T)] and poly[d(AT)]•poly[d(AT)] (Edmondson & Johnson, 1985b), and poly[d(G)•d(C)] and poly[d(GC)]•poly[d(GC)] (Edmondson & Johnson, 1986). The results obtained from these experiments indicate that the bases of B-form polynucleotides in solution are more inclined than those found in fibers or crystals, and that the DNA structure in solution is not same as that in crystals.

In this report we extend LD measurements to the synthetic polynucleotides containing four different bases, poly[d(AC)]•poly[d(GT)] and poly[d(AG)]•poly[d(CT)]. Measurements are made in 10 mM sodium phosphate buffer for the B-form and 80% 2,2,2-trifluoroethanol (TFE) for the A-form. Poly[d(AC)]•poly[d(GT)] is an alternating purine-pyrimidine sequence that is found quite frequently in eukaryotic DNA sequences (Hamada & Kakunaga, 1982; Pardue et al., 1987; Braaten et al., 1988). Poly[d(AG)]•poly[d(CT)] is one of the polypurine-polypyrimidine sequences that occurs frequently in transcribed eukaryotic genes, and has been found to be hypersensitive to DNase I and single-strand-specific nuclease (Pulleyblank et al., 1985; Christophe et al., 1985; Lyamichev et al., 1985). The presence of such repeat motifs in genomic sequence of higher eukaryotes suggests special biological roles in various cellular processes, such as nucleosome organization, recombination, and other gene expression. The structural information about the polymers in solution reported here will provide important conformational characteristics needed to understand the roles of these sequences in living cells.

## MATERIALS AND METHODS

**Sample Preparation :** Poly[d(AC)]•poly[d(GT)] and poly[d(AG)]•poly[d(CT)] were purchased from Pharmacia, and dissolved in 10 mM sodium phosphate buffer at concentrations of 3-6 optical density units/mL. Poly[d(AC)]•poly[d(GT)] was at pH 7.0, but poly[d(AG)]•poly[d(CT)] was maintained at pH 8.0 to avoid disproportionation to the triple-stranded structure, which requires a proton for each C•G•C<sup>+</sup> base pair (Antao et al., 1988). To ensure that our results were not influenced by contaminating ions, an aliquot of poly[d(AC)]•poly[d(GT)] and poly[d(AG)]•poly[d(CT)] solution was dialyzed using Spectra/Por tubing (6000-8000 molecular weight cutoff) against 0.5 M NaCl, 10 mM EDTA (pH 8.0) for 24 hr to remove divalents (Devarajan & Shafer, 1986), and then twice against 10 mM sodium phosphate buffer. The CD and LD spectra did not change with dialysis. The A-form of these polymers was produced by slowly adding TFE with continuous mixing to form an 80% (v/v) solvent, with the pH of the buffer maintained. The extinction coefficients of poly[d(AC)]•poly[d(GT)] and poly[d(AG)]•poly[d(CT)] in buffer at 260 nm were taken to be 6500 and 5700 M<sup>-1</sup> cm<sup>-1</sup>, respectively (Allen et al., 1984). The extinction coefficients of these polymers in 80% TFE were determined spectrometrically at 260 nm to be 6100 M<sup>-1</sup> cm<sup>-1</sup> for poly[d(AC)]•poly[d(GT)] and 5400 M<sup>-1</sup> cm<sup>-1</sup> for poly[d(AG)]•poly[d(CT)].

**Spectroscopic Measurements :** Isotropic absorption (A) spectra were measured on a Cary 15 spectrometer flushed with nitrogen. CD and flow LD spectra were measured on a modified McPherson 225 vacuum uv spectrometer as previously described (Causley & Johnson, 1982; Edmondson & Johnson, 1985b). For LD measurement, calibration of the spectrometer was checked by using a quartz window as a reference. The quartz window was tilted 15° from perpendicular to the light path, and the LD was measured from 300 to 200 nm at 20 nm intervals. Then the LD scale factor was determined from the known

LD of a quartz window (Norden & Seth, 1985) divided by voltage measured. The scale factor was stable with respect to wavelength and time to within  $\pm 2\%$ .

All measurements were performed at 20 °C. For each experiment, the A and LD spectra were measured three to five times and averaged. Previous work shows that our results are independent of shear (Causley & Johnson, 1982), and here the flow LD spectra were obtained with shear rates of about  $11000 \text{ s}^{-1}$ . The relatively high flow rate (3-4 mL/min) of sample solution through flow cell was obtained using a Masterflex pump (Cole-Parmer), yielding a relatively larger LD signal compared to previous reports (Causley & Johnson, 1982; Edmondson & Johnson, 1985b, 1986). The spectra were smoothed with a cubic spline algorithm. To facilitate graphic comparison, the A and LD spectra were normalized to an area of 100, since we do not require absolute values for our analysis.

#### **Data Analysis : In flow experiments**

$$LD = A_{\parallel} - A_{\perp} \quad (1)$$

for linearly polarized light incident parallel( $\parallel$ ) and perpendicular( $\perp$ ) to the helix axis. For a helical array of chromophores, this can be expressed in terms of the orientation of the bases as

$$LD(\lambda) = 3S A(\lambda) (3 \sin^2\alpha \sin^2\beta - 1) / 2 \quad (2)$$

where S is an orientation parameter ( $0 < S < 1$ ),  $\alpha$  is the inclination of base normal with respect to helical axis, and  $\beta$  is the angle within the plane of the base between the transition dipole and the axis about which the base is inclining. For DNA, the LD at wavelength  $\lambda$  is the sum of the contributions from each transition dipole i of base j weighted by its extinction coefficient,  $\epsilon$ , for isotropic absorption

$$LD(\lambda) = 3S \sum \epsilon_{ij}(\lambda) [ 3 \sin^2 \alpha_j \sin^2 (\chi_j - \delta_{ij}) - 1 ] / 2 \quad (3)$$

where relative to an origin (the vector N3-C6 for purine and N1-C4 for pyrimidine),  $\delta$  is the direction of the transition dipole, and angle  $\chi$  defines the inclination axis of base  $j$ . The directions of the transition dipoles are known. Furthermore, we do not have to approximate  $S$  or extrapolate our data to  $S = 1$ . Our A and LD spectra contain enough information to solve directly for  $S$  (or  $S$  combined with the normalization of A and LD spectra). We use the shape of A and LD spectra to solve for all of the unknowns. Thus any tertiary structure formed by the polymer does not affect our analysis.

In the earlier reports we assumed that the energies and bandwidths for the transitions of each base in polynucleotide were identical to those resolved in the absorption of the corresponding monomers, and only the intensities of the bands change due to exciton interaction in the polynucleotide studied. We then fit the normalized reduced linear dichroism,  $R(\lambda) = LD(\lambda) / A(\lambda)$ . We plot  $R(\lambda)$  here for its pedagogical value, but in this work we fit the A and LD spectra individually, using a much more sophisticated method recently developed in our laboratory (Chou and Johnson, 1993). To briefly describe this method: the bands are represented by log-normal functions (Siano & Metzler, 1969; Siano, 1972). We determine the parameters for all bands (position,  $\mu$ ; width,  $\zeta$ ; integrated intensity,  $\sigma$ ; and skewness,  $\rho$ ) and the  $\alpha$  and  $\chi$  angles for the bases in polynucleotide through the Levenberg-Marquardt algorithm (Brown & Dennis, 1972) by fitting simultaneously the individual A and LD spectra with Eq. (3). From an initial guess of parameters for all bands and the  $\alpha$  and  $\chi$  angles, the algorithm iteratively generates a sequence of approximations towards the minimum for the sum of squares error fit to the A and LD spectra. Iteration for the best fit to A and LD spectra is not stable, presumably because we are overfitting data that contain error. Instead we monitor the variance of all parameters with each iteration and choose the bottom of the multidirectional valley of these variances, which is very stable to error in A and LD.

## RESULTS

The directions of the transition dipoles for each base are taken from Clark and coworkers (Clark, 1977, 1989, 1990; Zaloudek, 1985; Novros, 1986), and listed in Table 2.1. Initial values of parameters for all bands are from the fitting of poly[d(A)•d(T)] and poly[d(G)•d(C)] (Jin and Johnson, to be published). Initial  $\alpha$  and  $\chi$  angles for the polynucleotides are from earlier reports (Edmondson & Johnson, 1985b, 1986).

**Poly[d(AC)]•poly[d(GT)]** : The CD, A, LD , and R spectra of poly[d(AC)]•poly[d(GT)] in 10 mM sodium phosphate buffer (pH 7.0) and in 80% TFE (pH 7) are shown in Figures 2.1 and 2.2, respectively. The CD spectrum in buffer is similar to that reported in the literature (Riazance et al., 1987; Antao et al., 1990; Gray et al., 1990). The CD spectrum observed for this polymer in 80 % TFE with its negative band at about 210 nm is indicative of the A form. An intense positive band is also observed in the vacuum uv at 180 nm in buffer and 183 nm in 80 % TFE. No significant changes were observed in the CD spectrum after the LD measurements, demonstrating that the structure of polynucleotide was not altered by the shear gradients.

The normalized reduced dichroism spectrum of poly[d(AC)]•poly[d(GT)] in buffer shown in Figure 2.1 has a fairly constant negative magnitude at long wavelengths, and is most negative at 265 nm. A small bump is observed at 226 nm, and the magnitude of R decreases in the short wavelength region. This variation of the reduced dichroism with wavelength demonstrates that the bases are not perpendicular to the helix axis. The R spectrum of poly[d(AC)]•poly[d(GT)] in 80% TFE is considerably different from the spectrum in buffer (Figure 2.2). It has a large bump at 222 nm, is most negative at about 256 nm, and varies considerably in the region between 220 and 180 nm.

The poly[d(AC)]•poly[d(GT)] A and LD spectra were fit simultaneously yielding band parameters and the  $\alpha$  and  $\chi$  angles. The fits are within the line

widths in the figures. The position, intensity, width, and skewness of each log-normal band are listed in Tables 2.2 and 2.3. The results indicate that the band positions are very similar in both buffer and in 80 % TFE, but the intensity or width are different. One striking feature of the results of decomposition is that the second band of thymine has a positive LD in the A-form. From the fitting, we see that dA is inclined  $29.2^\circ$ , T is inclined  $36.2^\circ$ , dG is inclined  $25.0^\circ$ , and dC is inclined  $28.1^\circ$  for B-form poly[d(AC)]•poly[d(GT)] in buffer. These inclinations are about same as those found earlier for the simpler polynucleotides, poly[d(A)•d(T)] and poly[d(G)•d(C)] (Edmondson & Johnson, 1985b, 1986).

The inclinations of bases for the A-form in 80 % TFE are greater than those in buffer (Table 2.3):  $31.1^\circ$ ,  $38.1^\circ$ ,  $30.0^\circ$ , and  $36.4^\circ$  for dA, T, dG, and dC, respectively, but the inclination axes of all bases are comparable with their counterparts in buffer.

**Poly[d(AG)]•poly[d(CT)]** : Figures 2.3 and 2.4 show the CD, A, LD, and R spectra of poly[d(AG)]•poly[d(CT)] in 10 mM sodium phosphate buffer (pH 8.0) and in 80 % TFE (pH 8), respectively. The CD spectrum in buffer is similar to that reported in the literature (Antao et al, 1988; Gray et al, 1990). The CD spectrum in 80% TFE has a negative band at about 210 nm, indicating A form. An intense positive band is observed in the vacuum uv at 191 nm in buffer and 188 nm in 80% TFE.

The R spectrum of poly[d(AG)]•poly[d(CT)] in buffer (Figure 2.3) has a fairly constant negative magnitude at long wavelengths, and is most negative at 250 nm. It has a small bump at 225 nm, and a less negative flat region between 200 and 215 nm. The R spectrum of this polymer in 80 % TFE is more varied than the spectrum in buffer (Figure 2.4). It is most negative at 255 nm, has a bump at 228 nm, and varies in the region between 220 and 180 nm.

Simultaneous fits to the A and LD spectra for poly[d(AG)]•poly[d(CT)] in buffer and 80 % TFE are summarized in Tables 2.4 and 2.5. The fits are within the linewidths in the figures. The results indicate that the band position and

width are very similar for the polymer in both environments, but the intensities differ. For the B-form in buffer dA is inclined  $19.0^\circ$ , T is inclined  $31.9^\circ$ , dG is inclined  $18.1^\circ$ , and dC is inclined  $31.2^\circ$ . These inclination angles are slightly smaller than those found in poly[d(AC)]•poly[d(GT)] in buffer.

The inclination of bases for the A form in 80 % TFE are greater than the inclination in buffer (Table 2.5):  $27.6^\circ$ ,  $36.1^\circ$ ,  $22.0^\circ$ , and  $32.4^\circ$  for dA, T, dG, and dC, respectively. These inclination angles also are slightly smaller than those found in A-form of poly[d(AC)]•poly[d(GT)] in 80% TFE. The inclination axes of all bases are comparable with their counterparts in buffer.



Table 2.1. Transition Dipole Directions

Base	Band	Direction	Reference
Adenine	I	83	Clark (1989, 1990)
	II	25	
	III	-45	
	IV	15	
	V	72	
	VI	-45	
Thymine	I	-9	Novros & Clark (1986)
	II	-53	
	III	-26	
Guanine	I	-4	Clark (1977)
	II	-75	
	III	-71	
	IV	41	
Cytosine	I	6	Zaloudek et al.(1985)
	II	-35	
	III	76	
	IV	86	
	V	0	

Table 2.2. Simultaneous Fitting of Absorption and LD Spectra for Poly[d(AC)]•Poly[d(GT)] in 10 mM Sodium Phosphate Buffer, pH 7.0.

Base	$\mu$ (nm)	$\zeta \times 10^{-3}$	$\sigma$ (nm)	$\rho$	$\alpha$ (deg)	$\chi$ (deg)
d(A)	279.5 $\pm$ 0.5	14.3 $\pm$ 0.7	13.3 $\pm$ 0.7	1.47 $\pm$ 0.13	29.2 $\pm$ 0.6	-5.5 $\pm$ 2.0
	255.5 $\pm$ 0.1	58.2 $\pm$ 0.5	13.9 $\pm$ 0.1	1.13 $\pm$ 0.01		
	206.9 $\pm$ 0.1	83.1 $\pm$ 0.8	12.4 $\pm$ 0.1	1.13 $\pm$ 0.01		
	193.3 $\pm$ 0.1	16.2 $\pm$ 0.4	5.9 $\pm$ 0.1	1.15 $\pm$ 0.04		
	184.2 $\pm$ 0.1	65.9 $\pm$ 0.4	7.0 $\pm$ 0.1	1.19 $\pm$ 0.02		
	175.9 $\pm$ 0.1	28.1 $\pm$ 1.8	3.7 $\pm$ 0.1	1.06 $\pm$ 0.02		
d(T)	261.5 $\pm$ 0.7	49.0 $\pm$ 1.3	20.7 $\pm$ 0.8	1.29 $\pm$ 0.05	36.2 $\pm$ 0.5	45.9 $\pm$ 2.0
	197.0 $\pm$ 1.4	77.2 $\pm$ 2.5	22.6 $\pm$ 0.9	1.50 $\pm$ 0.00		
	177.9 $\pm$ 0.1	74.1 $\pm$ 1.3	4.7 $\pm$ 0.1	1.01 $\pm$ 0.01		
d(G)	275.6 $\pm$ 0.2	55.8 $\pm$ 0.8	16.6 $\pm$ 0.2	1.28 $\pm$ 0.01	25.0 $\pm$ 0.5	-26.4 $\pm$ 1.8
	249.4 $\pm$ 0.1	34.6 $\pm$ 0.3	12.6 $\pm$ 0.1	1.40 $\pm$ 0.03		
	197.3 $\pm$ 0.1	87.8 $\pm$ 0.7	12.2 $\pm$ 0.1	1.20 $\pm$ 0.01		
	183.2 $\pm$ 0.1	100.7 $\pm$ 0.3	10.6 $\pm$ 0.1	1.44 $\pm$ 0.01		
d(C)	261.1 $\pm$ 0.2	56.9 $\pm$ 0.7	14.8 $\pm$ 0.2	1.01 $\pm$ 0.01	28.1 $\pm$ 0.9	21.2 $\pm$ 2.3
	224.9 $\pm$ 0.2	52.2 $\pm$ 0.5	21.5 $\pm$ 0.2	1.44 $\pm$ 0.02		
	217.8 $\pm$ 0.4	12.3 $\pm$ 0.4	9.0 $\pm$ 0.2	1.06 $\pm$ 0.04		
	192.6 $\pm$ 0.1	75.1 $\pm$ 0.3	11.4 $\pm$ 0.1	1.43 $\pm$ 0.01		
	174.5 $\pm$ 0.3	29.7 $\pm$ 1.1	11.4 $\pm$ 0.5	1.03 $\pm$ 0.03		

Table 2.3. Simultaneous Fitting of Absorption and LD Spectra for Poly[d(AC)]•Poly[d(GT)] in 80 % TFE, pH 7

Base	$\mu$ (nm)	$\zeta \times 10^{-3}$	$\sigma$ (nm)	$\rho$	$\alpha$ (deg)	$\chi$ (deg)
d(A)	277.7 $\pm$ 1.2	28.1 $\pm$ 1.1	22.9 $\pm$ 1.6	1.40 $\pm$ 0.01	31.1 $\pm$ 0.5	-4.4 $\pm$ 1.7
	256.2 $\pm$ 0.1	36.3 $\pm$ 0.4	9.7 $\pm$ 0.1	1.09 $\pm$ 0.02		
	207.3 $\pm$ 0.2	81.3 $\pm$ 0.9	12.4 $\pm$ 0.1	1.49 $\pm$ 0.03		
	199.3 $\pm$ 0.5	20.4 $\pm$ 0.8	9.2 $\pm$ 0.4	1.50 $\pm$ 0.00		
	187.2 $\pm$ 0.1	60.3 $\pm$ 0.5	7.2 $\pm$ 0.1	1.07 $\pm$ 0.02		
	176.2 $\pm$ 0.1	57.7 $\pm$ 2.5	5.1 $\pm$ 0.1	1.26 $\pm$ 0.02		
d(T)	269.5 $\pm$ 0.6	36.8 $\pm$ 0.7	17.2 $\pm$ 0.6	1.50 $\pm$ 0.00	38.1 $\pm$ 0.6	39.9 $\pm$ 2.5
	196.0 $\pm$ 1.4	143.1 $\pm$ 3.0	30.4 $\pm$ 1.0	1.20 $\pm$ 0.05		
	176.1 $\pm$ 0.1	73.1 $\pm$ 3.5	6.9 $\pm$ 0.2	1.35 $\pm$ 0.02		
d(G)	275.0 $\pm$ 0.4	75.4 $\pm$ 1.5	19.2 $\pm$ 0.2	1.50 $\pm$ 0.00	30.0 $\pm$ 1.1	-21.8 $\pm$ 1.4
	237.9 $\pm$ 0.5	34.9 $\pm$ 1.2	16.3 $\pm$ 0.5	1.02 $\pm$ 0.02		
	194.3 $\pm$ 0.1	81.6 $\pm$ 0.6	11.9 $\pm$ 0.1	1.27 $\pm$ 0.02		
	170.8 $\pm$ 0.2	66.6 $\pm$ 1.5	16.9 $\pm$ 0.5	1.18 $\pm$ 0.01		
d(C)	259.1 $\pm$ 0.2	79.4 $\pm$ 1.1	17.1 $\pm$ 0.3	1.43 $\pm$ 0.02	36.4 $\pm$ 0.7	23.1 $\pm$ 1.9
	218.2 $\pm$ 0.2	62.0 $\pm$ 0.7	12.3 $\pm$ 0.2	1.31 $\pm$ 0.01		
	209.2 $\pm$ 0.1	10.4 $\pm$ 0.9	5.1 $\pm$ 0.3	1.17 $\pm$ 0.07		
	191.8 $\pm$ 0.1	55.6 $\pm$ 0.8	9.1 $\pm$ 0.2	1.23 $\pm$ 0.04		
	182.4 $\pm$ 0.3	109.0 $\pm$ 1.7	20.5 $\pm$ 0.3	1.31 $\pm$ 0.04		

Table 2.4. Simultaneous Fitting of Absorption and LD Spectra for Poly[d(AG)]•Poly[d(CT)] in 10 mM Sodium Phosphate Buffer, pH 8.0.

Base	$\mu$ (nm)	$\zeta \times 10^{-3}$	$\sigma$ (nm)	$\rho$	$\alpha$ (deg)	$\chi$ (deg)
d(A)	279.2 $\pm$ 0.1	15.2 $\pm$ 0.1	12.5 $\pm$ 0.1	1.45 $\pm$ 0.00	19.0 $\pm$ 0.6	-1.4 $\pm$ 1.8
	253.2 $\pm$ 0.1	50.3 $\pm$ 0.1	14.1 $\pm$ 0.1	1.01 $\pm$ 0.01		
	207.9 $\pm$ 0.1	64.3 $\pm$ 0.2	12.9 $\pm$ 0.1	1.45 $\pm$ 0.01		
	196.3 $\pm$ 0.1	10.8 $\pm$ 0.1	6.7 $\pm$ 0.1	1.03 $\pm$ 0.01		
	178.0 $\pm$ 0.1	48.3 $\pm$ 0.1	7.6 $\pm$ 0.1	1.01 $\pm$ 0.01		
	176.2 $\pm$ 0.1	22.9 $\pm$ 0.2	7.3 $\pm$ 0.1	1.01 $\pm$ 0.01		
d(T)	266.9 $\pm$ 0.2	54.6 $\pm$ 0.5	20.9 $\pm$ 0.2	1.45 $\pm$ 0.00	31.9 $\pm$ 0.3	62.3 $\pm$ 1.3
	200.9 $\pm$ 0.2	57.2 $\pm$ 0.3	23.6 $\pm$ 0.1	1.23 $\pm$ 0.03		
	175.8 $\pm$ 0.1	32.5 $\pm$ 0.6	7.4 $\pm$ 0.1	1.29 $\pm$ 0.01		
d(G)	276.0 $\pm$ 0.1	43.8 $\pm$ 0.2	19.0 $\pm$ 0.1	1.32 $\pm$ 0.01	18.1 $\pm$ 0.5	-1.7 $\pm$ 1.9
	251.1 $\pm$ 0.1	34.1 $\pm$ 0.1	11.6 $\pm$ 0.1	1.01 $\pm$ 0.01		
	197.0 $\pm$ 0.1	66.9 $\pm$ 0.1	12.6 $\pm$ 0.1	1.05 $\pm$ 0.01		
	183.1 $\pm$ 0.1	76.5 $\pm$ 0.2	11.2 $\pm$ 0.1	1.29 $\pm$ 0.01		
d(C)	264.5 $\pm$ 0.1	46.3 $\pm$ 0.2	15.7 $\pm$ 0.1	1.38 $\pm$ 0.01	31.2 $\pm$ 0.4	13.0 $\pm$ 1.7
	226.4 $\pm$ 0.1	41.8 $\pm$ 0.2	16.3 $\pm$ 0.1	1.45 $\pm$ 0.00		
	216.0 $\pm$ 0.2	11.6 $\pm$ 0.2	9.9 $\pm$ 0.1	1.45 $\pm$ 0.00		
	194.6 $\pm$ 0.1	62.4 $\pm$ 0.2	11.6 $\pm$ 0.1	1.01 $\pm$ 0.01		
	175.6 $\pm$ 0.1	34.1 $\pm$ 0.3	8.6 $\pm$ 0.1	1.01 $\pm$ 0.01		

Table 2.5. Simultaneous Fitting of Absorption and LD Spectra for Poly[d(AG)]•Poly[d(CT)] in 80 % TFE, pH 8.

Base	$\mu$ (nm)	$\zeta \times 10^{-3}$	$\sigma$ (nm)	$\rho$	$\alpha$ (deg)	$\chi$ (deg)
d(A)	280.3 $\pm$ 0.2	16.3 $\pm$ 0.1	21.7 $\pm$ 0.3	1.45 $\pm$ 0.00	27.6 $\pm$ 0.4	-4.6 $\pm$ 1.7
	255.4 $\pm$ 0.1	47.1 $\pm$ 0.3	14.1 $\pm$ 0.1	1.18 $\pm$ 0.01		
	208.3 $\pm$ 0.1	60.8 $\pm$ 0.5	13.3 $\pm$ 0.1	1.19 $\pm$ 0.01		
	196.8 $\pm$ 0.1	10.4 $\pm$ 0.3	6.5 $\pm$ 0.1	1.02 $\pm$ 0.01		
	185.4 $\pm$ 0.1	43.0 $\pm$ 0.1	7.8 $\pm$ 0.1	1.04 $\pm$ 0.01		
	176.5 $\pm$ 0.1	20.2 $\pm$ 0.4	6.7 $\pm$ 0.1	1.01 $\pm$ 0.01		
d(T)	268.2 $\pm$ 0.5	53.8 $\pm$ 1.1	22.5 $\pm$ 0.6	1.02 $\pm$ 0.02	36.1 $\pm$ 0.6	66.6 $\pm$ 1.6
	205.6 $\pm$ 0.5	56.5 $\pm$ 0.6	20.9 $\pm$ 0.3	1.34 $\pm$ 0.04		
	178.7 $\pm$ 0.4	22.8 $\pm$ 1.2	9.8 $\pm$ 0.4	1.02 $\pm$ 0.01		
d(G)	277.5 $\pm$ 0.1	43.5 $\pm$ 0.4	16.8 $\pm$ 0.1	1.33 $\pm$ 0.01	22.0 $\pm$ 0.6	-10.7 $\pm$ 1.8
	250.6 $\pm$ 0.1	30.4 $\pm$ 0.1	13.7 $\pm$ 0.1	1.01 $\pm$ 0.01		
	197.9 $\pm$ 0.1	61.8 $\pm$ 0.3	12.7 $\pm$ 0.1	1.02 $\pm$ 0.01		
	182.7 $\pm$ 0.1	68.0 $\pm$ 0.3	11.2 $\pm$ 0.1	1.33 $\pm$ 0.01		
d(C)	265.1 $\pm$ 0.1	45.0 $\pm$ 0.3	15.3 $\pm$ 0.1	1.14 $\pm$ 0.01	32.4 $\pm$ 0.7	18.7 $\pm$ 1.7
	226.5 $\pm$ 0.1	42.6 $\pm$ 0.3	18.8 $\pm$ 0.1	1.37 $\pm$ 0.01		
	215.9 $\pm$ 0.2	12.5 $\pm$ 0.1	12.9 $\pm$ 0.2	1.45 $\pm$ 0.00		
	197.6 $\pm$ 0.1	53.8 $\pm$ 0.2	13.8 $\pm$ 0.1	1.29 $\pm$ 0.02		
	174.6 $\pm$ 0.1	31.3 $\pm$ 0.7	7.1 $\pm$ 0.1	1.01 $\pm$ 0.01		

Figure 2.1. Poly[d(AC)]•poly[d(GT)] in 10 mM sodium phosphate buffer, pH 7.0:  
(a) CD, (b) normalized LD ( — ), A ( --- ), and reduced dichroism (....). The extinction coefficient at 260 nm is  $6500 \text{ M}^{-1}\text{cm}^{-1}$  for A.

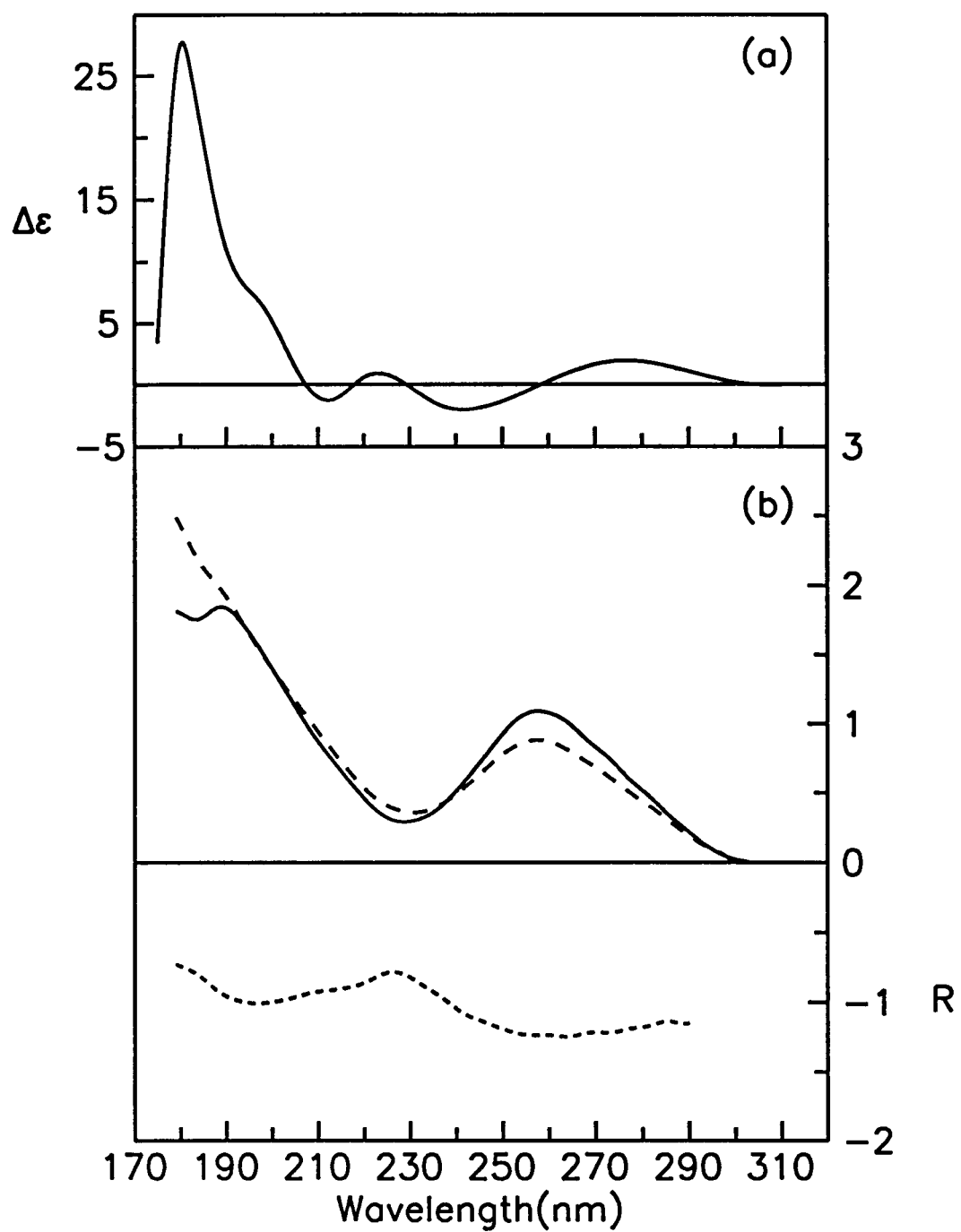


Figure 2.1

Figure 2.2. Poly[d(AC)]•poly[d(GT)] in 80 % trifluoroethanol, pH 7 : (a) CD, (b) normalized LD ( — ), A ( --- ), and reduced dichroism (····). The extinction coefficient at 260 nm is  $6100 \text{ M}^{-1}\text{cm}^{-1}$  for A.



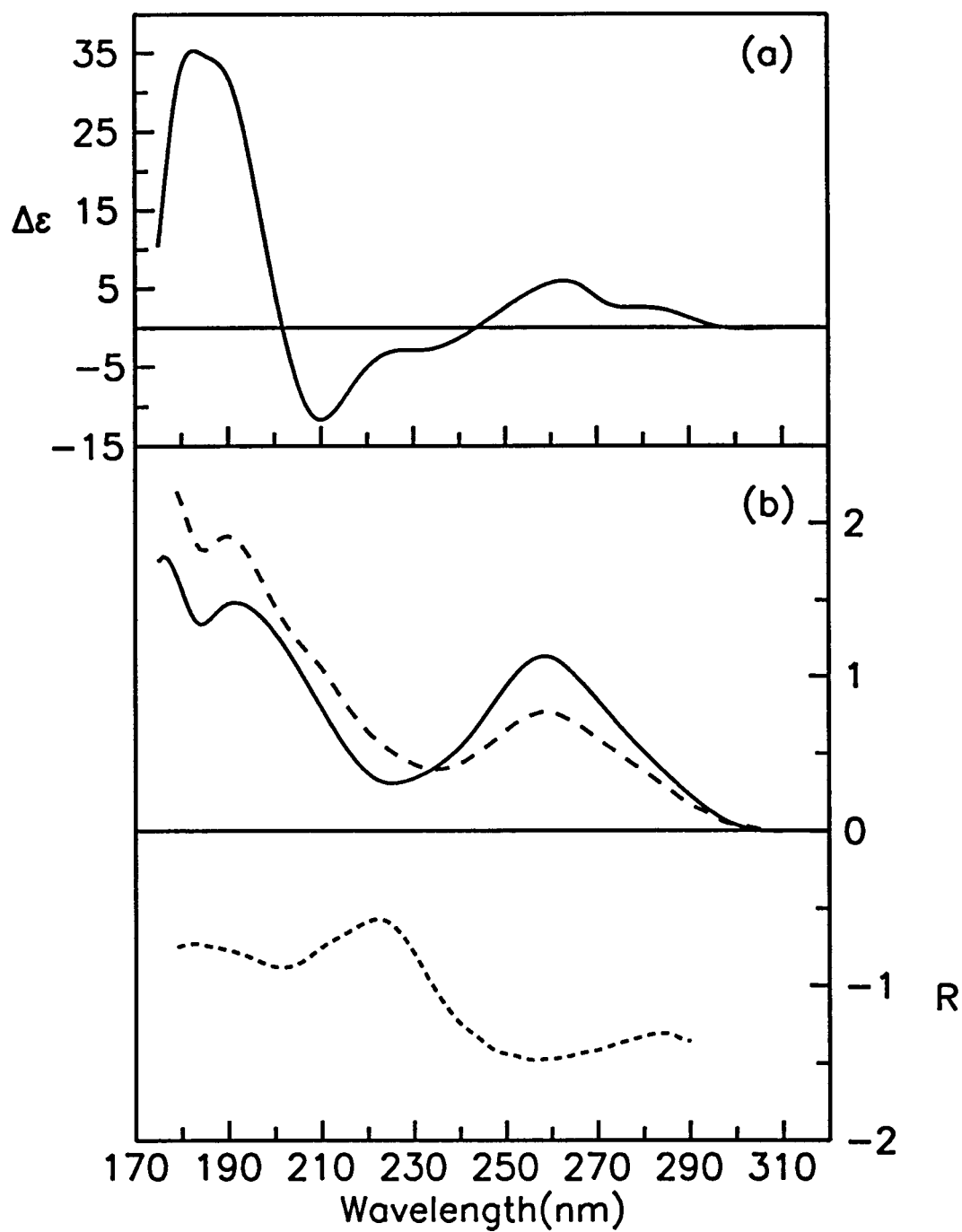


Figure 2.2

Figure 2.3. Poly[d(AG)]•poly[d(CT)] in 10 mM sodium phosphate buffer, pH 8.0:  
(a) CD, (b) normalized LD ( — ), A ( --- ), and reduced dichroism (....). The extinction coefficient at 260 nm is  $5700 \text{ M}^{-1}\text{cm}^{-1}$  for A.

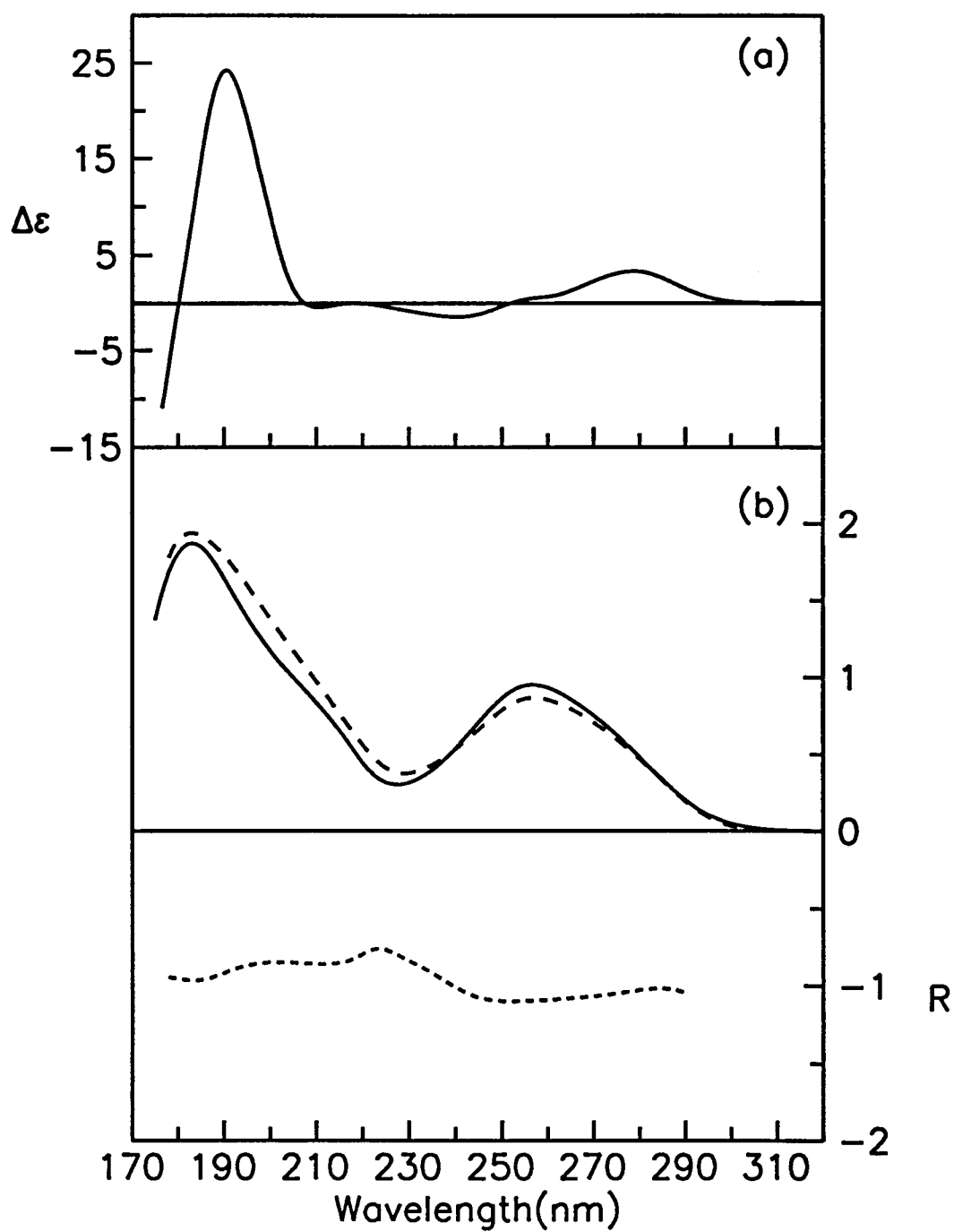


Figure 2.3

Figure 2.4. Poly[d(AG)]•poly[d(CT)] in 80 % trifluoroethanol, pH 8 : (a) CD, (b) normalized LD ( ——— ), A ( ——— ), and reduced dichroism (····). The extinction coefficient at 260 nm is  $5400 \text{ M}^{-1}\text{cm}^{-1}$  for A.

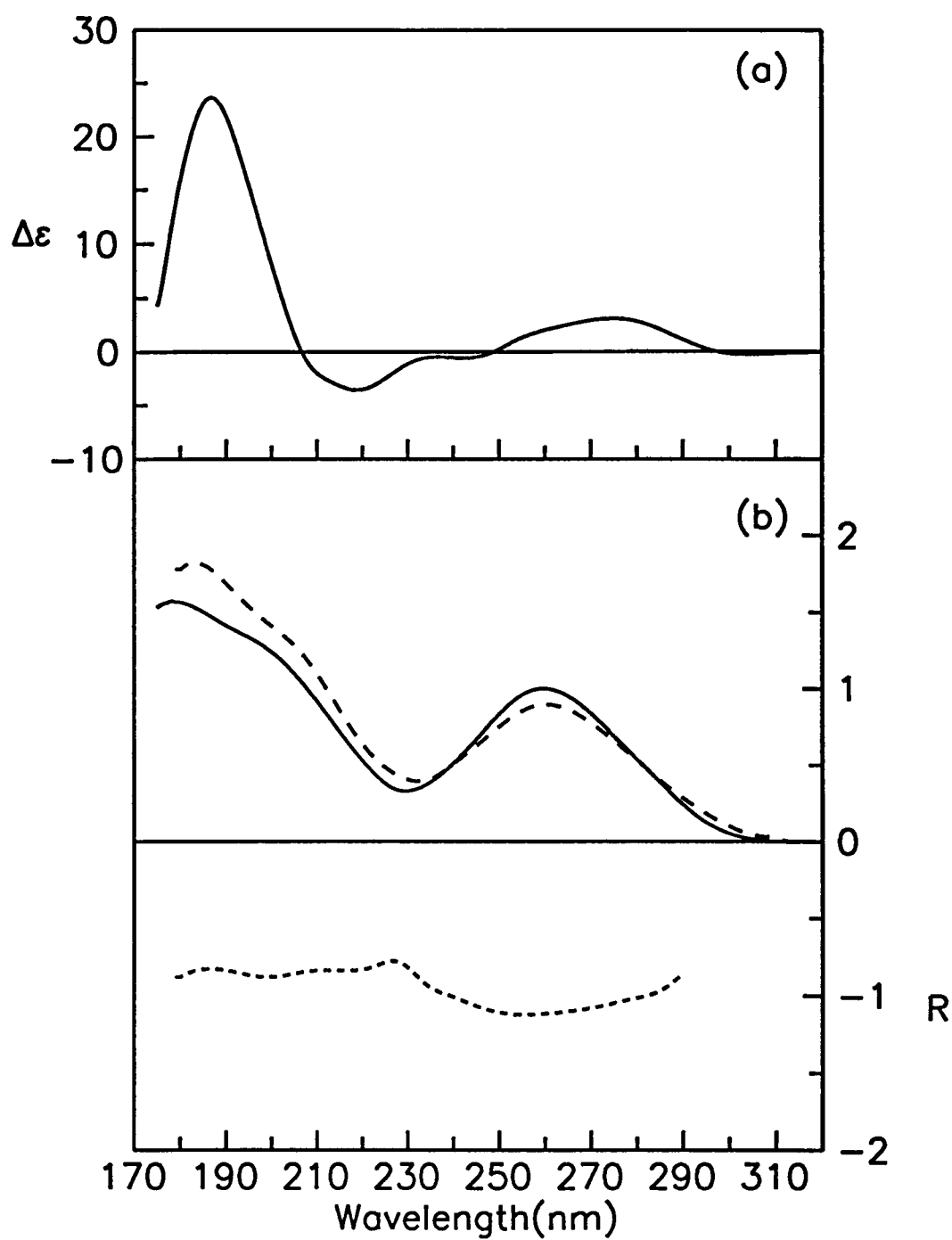


Figure 2.4

## DISCUSSION

Several improvements in the method for fitting and analyzing the spectra were used in this work. First, the transition dipole directions are different, especially for dA, which has six different transitions instead of four used in previous studies (Causley & Johnson, 1982; Edmondson & Johnson, 1985b). Second, our algorithm for calculating inclination and axis of inclination has several advantages over the simplex algorithm used for previous analyses in our laboratory. One of the most important improvements is that the position of a band for a given base can be different for each polynucleotide, and a skewness parameter is added to vary the shape of each absorption band. This has resulted in a more reasonable band decomposition, and more reliable calculation of inclination and axis of inclination.

Basically, our results are based on several assumptions. First, we assume that the electronic transitions with out-of-plane directions are negligible, because the intensity of  $n \rightarrow \pi^*$  transitions is about two orders of magnitude less than  $\pi \rightarrow \pi^*$  transitions, and there is no direct experimental evidence for  $n \rightarrow \pi^*$  transitions in nucleic acids. Further, earlier fitting of reduced dichroism spectra for synthetic double-stranded polynucleotides required only  $\pi \rightarrow \pi^*$  transitions to fit the bumps around 220 nm; this is strong evidence that  $n \rightarrow \pi^*$  transitions do not contribute significantly. Second,  $\pi \rightarrow \pi^*$  transitions may have out-of-plane components due to the internal vibrations of the bases, but these so-called forbidden components are expected to be small (Kwiatkowski, 1968; Hug & Tinoco, 1973), and will be absorbed into S in our analysis if the out-of-plane component is constant over the wavelength range studied. Thus we neglect these forbidden components. Third, the directions of the transition dipoles in the double-stranded polymers are assumed to be identical to the experimental directions found for single crystals of the monomers.

To determine if our results are sensitive to small changes in the transition dipole directions, we repeated each fitting 100 times, with the transition dipole

randomly varying  $\pm 10^\circ$  about the values listed in Table 2.1. The average and standard deviation is calculated from the 100 independently fitted results for each variable, and these results are presented in Tables 2.2 - 2.5. The standard deviation for the base inclination are only  $1^\circ - 2^\circ$ , indicating that our results are not sensitive to reasonable errors in the transition dipole directions.

CD spectra of poly[d(AC)]•poly[d(GT)] in two different environments (Figures 2.1 and 2.2) indicate that the polynucleotide assumes B-form structure in buffer and A-form structure in 80 % TFE. Larger base inclinations for this polymer in 80 % TFE (Tables 2.2 and 2.3) also indicate that poly[d(AC)]•poly[d(GT)] undergoes a B- to A-form transition by adding TFE to 80 % (v/v). Poly[d(AG)]•poly[d(CT)] is a polypurine-polypyrimidine sequence that has a potential to form triple helical structure under conditions of high superhelical density or low pH (Pulleyblank et al., 1985; Christophe et al., 1985; Antao et al., 1988). Recent studies demonstrate that this sequence can exist as triplex even in normal buffer solution at neutral pH (Antao et al., 1988; Kan et al., 1991). Our CD spectrum of this polymer in 10 mM sodium phosphate buffer at pH 7.0 shows a negative band at about 220 nm, indicating the existence of some triplex (data not shown). Thus we followed Antao et al. (1988), and dissolved poly[d(AG)]•poly[d(CT)] in 10 mM sodium phosphate buffer, pH 8.0, to get the double-stranded B-form structure. CD spectra of poly[d(AG)]•poly[d(CT)] in two different environments (Figures 2.3 and 2.4) indicate that the polynucleotide assumes B- and A-form structure at pH 8 in buffer and in 80% TFE, respectively. This B- to A-form transition on adding TFE to 80 % (v/v) resulted in larger base inclination, as expected (Tables 2.4 and 2.5). It is interesting to note that the bases in poly[d(AC)]•poly[d(GT)] are more inclined than those in poly[d(AG)]•poly[d(CT)] for both B and A forms.

The inclination angles reported here in solution are considerably larger than those determined by X-ray diffraction studies either on DNA fibers (Arnott et al., 1980; Leslie et al., 1980; Arnott et al., 1983) or oligonucleotide crystals (Wang et al., 1979; Drew et al., 1980; Dickerson & Drew, 1981; Drew & Dickerson,

1981b). Similar results were found earlier for (A + T) polymer and (G + C) polymer, and the B form of *E.coli*. DNA (Dougherty et al., 1983; Edmondson & Johnson, 1985b, 1986). In addition, results from infrared LD (Baret et al., 1978; Flemming et al., 1988) for synthetic polynucleotides also show larger inclinations than those observed in DNA fibers and crystals. It appears that in the freedom of solution, base pairs incline to maximize charge interactions (Sarai et al., 1988) for polymorphic DNA.



## **ACKNOWLEDGEMENTS**

We wish to thank Ping-Jung Chou for the use of his program to analyze LD data. This research was supported by PHS grant number GM43133 from the Institute of General Sciences.

## REFERENCES

- Allen, F. S., Gray, D. M., & Ratliff, R. L. (1984) *Biopolymers* **23**, 2639-2659.
- Antao, V. P., Gray, D. M., & Ratliff, R. L. (1988) *Nucleic Acids Res.* **16**, 719-738.
- Antao, V. P., Ratliff, R. L., & Gray, D. M. (1990) *Nucleic Acids Res.* **18**, 4111-4122.
- Arnott, S., Chandrasekaran, R., Birdsall, D. L., Leslie, A.G. W., & Ratliff, R. L. (1980) *Nature* **283**, 743-745.
- Arnott, S., Chandrasekaran, R., Puijjaner, L. C., Walker, J. K., Hall, I. H., & Birdsall, D. L. (1983) *Nucleic Acids Res.* **11**, 1457-1474.
- Baret, J.F., Carbone, G. P., & Penon, P. (1978) *Biopolymers* **17**, 2319-2339.
- Braaten, D. C., Thomas, J. R., Little, R. D., Dickson, K. R., Goldberg, I., Schlessinger, D., Ciccodicola, A., & D'Urso, M. (1988) *Nucleic Acids Res.* **16**, 865-881.
- Bram, S. & Tougaard, P. (1972) *Nature New Biol.* **239**, 128-131.
- Brown, K. M. & Dennis, J. E., Jr. (1972) *Numer. Math.* **18**, 289-297.
- Causley, G. C. & Johnson, W. C., Jr. (1982) *Biopolymers* **21**, 1763-1780.
- Chou, P. J. & Johnson, W. C., Jr. (1993) *J. Am. Chem. Soc.* **115**, 1205-1214.
- Christophe, D., Cabrer, B., Bacolla, A., Targovnik, H., Pohl, V., & Vassart, G. (1985) *Nucleic Acids Res.* **13**, 5127-5144.
- Clark, L. B. (1977) *J. Am. Chem. Soc.* **99**, 3934-3938.
- Clark, L. B. (1989) *J. Phys. Chem.* **93**, 5345-5347.
- Clark, L. B. (1990) *J. Phys. Chem.* **94**, 2873-2879.
- Devarajan, S. & Shafer, R. (1986) *Nucleic Acids Res.* **14**, 5099-5109.
- Dickerson, R. E. & Drew, H. (1981) *J. Mol. Biol.* **149**, 761-786.

- Dougherty, A. M., Causley, G. C., & Johnson, W. C., Jr. (1983) *Proc. Natl. Acad. Sci. USA* **80**, 2193-2195.
- Drew, H. & Dickerson, R. E. (1981b) *J. Mol. Biol.* **152**, 723-736.
- Drew, H., Takano, T., Tanaka, S., Itakura, K., & Dickerson, R. E. (1980) *Nature* **286**, 567-573.
- Edmondson, S. P. & Johnson, W. C., Jr. (1985a) *Biochemistry* **24**, 4802-4806.
- Edmondson, S. P. & Johnson, W. C., Jr. (1985b) *Biopolymers* **24**, 825-841.
- Edmondson, S. P. & Johnson, W. C., Jr. (1986) *Biopolymers* **25**, 2335-2348.
- Flemming, J., Pohle, W., & Weller, K. (1988) *Int. J. Biol. Macromol.* **10**, 248-254.
- Fratini, A. V., Kopka, M. L., Drew, H. R., & Dickerson, R. E. (1982) *J. Biol. Chem.* **257**, 14686-14707.
- Fuller, W. & Wilkins, M. H. F. (1965) *J. Mol. Biol.* **12**, 60-80.
- Girod, J. C., Johnson, W. C., Jr., Huntington, S. K., & Maestre, M. F. (1973) *Biochemistry* **12**, 5092-5096.
- Gray, D. M., Johnson, K. H., Vaughan, M. R., Morris, P. A., Sutherland, J. C., & Ratliff, R. L. (1990) *Biopolymers* **29**, 317-323.
- Hamada, H. & Kakunaga, T. (1982) *Nature* **298**, 396-398.
- Heinemann, U. & Alings, C. (1989) *J. Mol. Biol.* **210**, 369-381.
- Hug, W. & Tinoco, I., Jr. (1973) *J. Am. Chem. Soc.* **95**, 2803-2813.
- Ivanov, V. I., Minchenkova, L. E., Schyolkina, A. K., & Poletayev, A. I. (1973) *Biopolymers* **12**, 89-110.
- Jain, S., Zon, G., & Sundaralingam, M. (1991) *Biochemistry* **30**, 3567-3576.
- Kan, L. S., Callahan, D. E., Trapane, T. L., Miller, P. S., Ts'o, P. O. P., & Huang, D. H. (1991) *J. Biomol. Struct. Dynam.* **8**, 911-933.
- Kwiatkowski, J. S. (1968) *Ther. Chim. Acta* **10**, 47-64.

- Leslie, A. G. W., Arnott, S., Chandrasekaran, R., & Ratliff, R. L. (1980) *J. Mol. Biol.* **143**, 49-72.
- Lyamichev, V. I., Mirkin, S. M., & Frank-Kamenetskii, M. D. (1985) *J. Biomol. Struct. Dyn.* **3**, 327-338.
- Narayana, N., Ginell, S. L., Russu, I. M., & Berman, H. M. (1991) *Biochemistry* **30**, 4449-4455.
- Norden, B. (1978) *Appl. Spectrosc. Rev.* **14**, 157-248.
- Norden, B. & Seth, S. (1985) *Appl. Spectrosc.* **39**, 647-655.
- Novros, J. S. & Clark, L. B. (1986) *J. Phys. Chem.* **90**, 5666-5668.
- Pardue, M. L., Lowenhaupt, K., Rich, A., & Nordheim, A. (1987) *EMBO J.* **6**, 1781-1789.
- Pohl, F. M. (1976) *Nature* **260**, 365-366.
- Pulleyblank, D. E., Haniford, D. B., & Morgan, A. R. (1985) *Cell* **42**, 271-280.
- Riazance, J. H., Johnson, W. C., Jr., McIntosh, L. P., & Jovin, T. M. (1987) *Nucleic Acids Res.* **15**, 7627-7636.
- Sarai, A., Mazur, J., Nussinov, R., & Jernigan, R. L. (1988) *Biochemistry* **27**, 8498-8502.
- Siano, D. B. (1972) *J. Chem. Educ.* **49**, 755-757.
- Siano, D. B. & Metzler, D. E. (1969) *J. Chem. Phys.* **51**, 1856-1861.
- Wada, A. (1972) *Appl. Spectrosc. Rev.* **6**, 1-30.
- Wang, A. H. J., Quigley, G. J., Kolpak, F. J., Crawford, J. L., van Boom, J. H., van der Marcel, G., & Rich, A. (1979) *Nature* **282**, 680-686.
- Zaloudek, F., Novros, J. S., & Clark, L. B. (1985) *J. Am. Chem. Soc.* **107**, 7377-7351.

### **SECTION III**

**Infrared Linear Dichroism Reveals that A-, B-, and C-DNA in Films  
Have Bases Highly Inclined from Perpendicular to the  
Helix Axis.**

**Hunseung Kang and W. Curtis Johnson, Jr.**

Department of Biochemistry and Biophysics  
Oregon State University  
Corvallis, OR 97331-6503

Submitted for publication

## ABSTRACT

Infrared linear dichroism has been employed to investigate the inclination of the bases in films of poly[d(AC)]•poly[d(GT)], poly[d(AG)]•poly[d(CT)], and natural DNAs (from *E. coli* and calf thymus). All DNAs investigated assume the B-form at high (>94%) relative humidity. Poly[d(AC)]•poly[d(GT)], *E. coli* DNA, and calf thymus DNA assume the A-form at low (75%) relative humidity, where as poly[d(AG)]•poly[d(CT)] assumes the C-form at low (66%) relative humidity. Infrared linear dichroism demonstrates that the bases for DNA in films are inclined from perpendicular to the helix axis, even in the B-DNA. C-DNA has almost same inclinations as in the B-DNA, and the inclinations are slightly increased in the A-DNA. These inclination angles confirm our earlier UV linear dichroism results for the orientations of the bases for DNA in solution. Infrared linear dichroism has also been used to obtain conformational angles for the phosphodiester backbone geometry of A-, B-, and C-forms of DNA.

## INTRODUCTION

The recent development of techniques for analyzing solution structures of biopolymers, such as optical spectroscopy, FTIR, and NMR spectroscopy, reveals the structural details of nucleic acids in aqueous solution, which resembles the real environment in the interior of living cells. But despite progress in studying nucleic acid structure in the solution state as well as in solid state, there is still uncertainty about the molecular structure of DNA. This is due mainly to the polymorphic nature of DNA, since the structure depends on the sequence (Bram & Tougaard, 1972; Leslie et al., 1980; Dickerson & Drew, 1981; Sarai et al., 1988), solvent (Girod et al., 1973; Ivanov et al., 1973; Pohl, 1976), and salt (Fuller & Wilkins, 1965; Bram & Tougaard, 1972; Ivanov et al., 1973; Leslie et al., 1980). One feature of the molecular structure of a nucleic acid is the inclination of the base pairs in the double helical structure of DNA. This knowledge about base orientation in DNA is required to understand many biological processes such as DNA-protein, DNA-ligand, or DNA-drug interactions.

Linear dichroism (LD) is a useful technique to get information about the inclination of chromophores in biopolymers. Many groups have used electric or flow linear dichroism in the ultraviolet (UV) to measure the inclination angle of the bases in free DNA with respect to the helix axis (Charney & Milstien, 1978; Hogan et al., 1978; Charney & Yamaoka, 1982; Charney et al., 1986; Clack & Gray, 1992). A more detailed review of this work can be found in Chou and Johnson (1993). Measurements have also been made on DNA complexed with ligands or drugs (Sen et al., 1986; Hard, 1987; Schurr & Fujimoto, 1988; van Amerongen et al., 1990; Norden et al., 1992b). Our laboratory has used vacuum UV flow LD (UV LD) to extract inclination angles for individual bases in the A-, B-, and Z-forms of synthetic polynucleotides (Causley & Johnson, 1982; Edmondson & Johnson, 1985a, 1986), and natural DNAs (Dougherty et al., 1983; Edmondson & Johnson, 1985b) in solution. Specific inclinations have

been determined for the bases in natural and synthetic polynucleotides containing four different types of bases using a sophisticated algorithm recently developed in our laboratory (Chou & Johnson, 1993; Kang & Johnson, 1993). Recently Cheng et al. (1992) and Nibedita et al. (1993) have reported B-DNA structures with bases rather highly tilted from the helical axis using NMR measurements and distance geometry methods. The results obtained from all these studies indicate that the bases are more highly inclined from perpendicular to the helical axis in solution than found in fibers or crystals, especially for B-DNA. In addition to these experimental reports, many workers (Levitt, 1978; Zhurkin et al., 1978; Singh et al., 1985; Rao et al., 1986; Edmondson, 1987; Ansevin & Wang, 1990; Srinivasan et al., 1990; Swaminathan et al., 1991) have used energy minimization, molecular mechanics, or molecular dynamics for modeling DNA structures, and have reported energetically favorable B-DNA models with base pairs highly inclined from perpendicular to the helical axis.

With the development of Fourier transform interferometers and special software that enables rapid and accurate data collection and management, infrared spectroscopy is becoming one of the most useful techniques to probe the molecular structure of nucleic acids in aqueous solution, as well as in gels or in films. Various synthetic polynucleotides and natural DNAs have been investigated to obtain specific marker bands for A-, B-, C-, D-, and Z-forms of DNA (Taillandier & Liquier, 1992 and references therein). By using oriented samples and polarized light, it is also possible to get information about the orientation of the transition dipoles for carbonyl bond stretching and ring stretching vibrational modes in the base plane, which, in turn, is related to the inclination of the bases. Baret et al. (1978) and Flemming et al. (1988) have used infrared linear dichroism (IR LD) to extract inclination angles for bases in natural DNA and poly[d(AT)]•poly[d(AT)] in films, and reported high inclination angles for both A- and B-DNA.



In this study we apply IR LD measurements to synthetic polynucleotides poly[d(AC)]•poly[d(GT)] and poly[d(AG)]•poly[d(CT)], and natural DNAs (from *E. coli* and calf thymus) in oriented films to extract inclination angles for the bases in the B-, C-, and A-forms. We compare the IR LD results with our earlier UV LD results about base inclinations for DNA in aqueous solution (Chou & Johnson, 1993; Kang & Johnson, 1993). In addition, since infrared spectroscopy is a very sensitive tool for monitoring the phosphodiester backbone geometry of nucleic acids, we also use IR LD to extract conformational angles of the phosphodiester backbone for A-, B-, and C-forms of these DNAs. The inclination of the bases in these DNAs using the LD of vibrational transitions reported here supports our earlier reports using ultraviolet transitions, and gives a more solid basis for understanding base inclinations for DNA in the interior of living cells.

## MATERIALS AND METHODS

**Sample Preparation:** Poly[d(AC)]•poly[d(GT)] and poly[d(AG)]•poly[d(CT)] were purchased from Pharmacia and used without further purification. Natural DNAs (calf thymus DNA from Pharmacia, and *E. coli* DNA from Sigma Co.) were treated with phenol/chloroform to remove residual protein, and were ethanol-precipitated. About 1 mg of each DNA was dissolved in doubly distilled water. After 24 hr at 4°C to ensure the formation of a homogeneous solution, the sample was washed several times with doubly distilled water using a centricon-10 microconcentrator (Amicon Co.), lyophilized, and redissolved in a small amount of doubly distilled water to yield a viscous gel of DNA. Poly[d(AG)]•poly[d(CT)] was treated similarly, except 1 mM sodium phosphate buffer, pH 8.0, was used to avoid the formation of a triple helix.

Gels of the DNA samples were then oriented on a calcium fluoride or a KRS-5 window by manual unidirectional stroking with the rounded bottom of a plastic microcentrifuge tube until dry, as described previously (Bradbury et al., 1961; Pilet & Brahms, 1973; Pilet et al., 1975; Kursar & Holzwarth, 1976; Baret et al., 1978). The salt content of the sample was controlled by previously described methods (Rupprecht & Forslind, 1970; Pilet & Brahms, 1973; Pilet et al., 1975) that equilibrate an oriented film in a 73 % ethanol-water solution containing 0.1 M NaCl for 2-3 days at 4 °C. This procedure gives samples with a salt content ranging from 3 to 4 % NaCl (w/w).

**Infrared Measurements :** The windows were placed in a sealed chamber under controlled relative humidity (r.h.), which was governed by a saturated salt solution in either H<sub>2</sub>O or D<sub>2</sub>O (Bradbury et al., 1961; Pilet & Brahms, 1973; Pilet et al., 1975; Kursar & Holzwarth, 1976; Baret et al., 1978). The sealed chamber (Figure 3.1) was constructed using plastic with second window, and attached on the cell mount which was inserted into standard cell holder in IR spectrophotometer. Saturated salt solution was placed in the bottom of this

sealed chamber. All salts used were reagent grade, and D<sub>2</sub>O (99.9 %) was from Aldrich. The hydration of the film was determined by monitoring the 3420 cm<sup>-1</sup> band, which is due to the water in the film. To ensure that each film is equilibrated for sufficient time at each hydration level required to cause the desired transition, a slow, stepwise dehydration-rehydration protocol was used as described by Keller & Hartman (1986). Each r.h. value was equilibrated for 24 hr before spectra were recorded. The B-, A-, and C-forms of DNA were obtained at 94% r.h. (K<sub>2</sub>SO<sub>4</sub>), 75% r.h. (NaCl), and 66% r.h. (NaNO<sub>2</sub>), respectively. Sometimes heating the film at 45 °C for 3 hr with the humidity controlled by a saturated NaCl solution was required to induce the B- to A-form transition. This treatment introduces no denaturation as measured by the intensity of the 1710 cm<sup>-1</sup> band.

Infrared spectra were measured on a Nicolet 510P Fourier transform infrared spectrometer equipped with a triglycine sulfate (TGS) detector. About 100-200 scans were collected at a 4 cm<sup>-1</sup> sensitivity (with 2 cm<sup>-1</sup> interval), and the resulting interferogram was Fourier transformed using a Happ-Genzel apodization function. The dichroic spectra were recorded for the oriented samples with the electric vector of light polarized parallel and perpendicular to orientation axis, which was achieved by rotating a wire-grid silver bromide polarizer (Cambridge Physical Sci.) through 90 degrees. Orienting films at various angles in the spectrometer showed that we were not measuring artifacts. Absence of the dichroic ratios over the wavenumber measured for the non-oriented samples also showed that we were not measuring artifacts.

**Theoretical :** For a partially oriented sample, which may be regarded as containing a fraction *S* of perfectly oriented material and a fraction (1-*S*) of randomly oriented material, the dichroic ratio (*R*) of each vibrational band is related by Fraser's formula (Fraser, 1953)

$$R = A_{\perp} / A_{\parallel} = \frac{(1/2) S \sin^2\theta + (1/3) (1 - S)}{S \cos^2\theta + (1/3) (1 - S)} \quad (1)$$

where  $A_{\perp}$  and  $A_{\parallel}$  are the absorption of polarized radiation with the electric vector perpendicular and parallel to the orientation axis, and  $\theta$  is the angle between the transition dipole of the vibrational mode and the orientation axis of the sample. This  $\theta$  angle depends both on the direction of transition dipole within the base plane and the angle of inclination for the base with respect to the helix axis (designated as  $\alpha$ ) (Flemming et al., 1988). We will determine  $S$  from the data in such a way that the effect of any tertiary structure will reside in  $S$ .

In order to determine  $\theta$  from the measured  $R$  value, the orientation parameter of the sample,  $S$ , has to be estimated. It is generally assumed that the  $\theta$  of the vibrational band that has the largest dichroic ratio is  $90^\circ$ , and  $S$  is then estimated from the measured  $R$  value of that vibrational band. If the  $\theta$  of that band is less than  $90^\circ$ , then the  $\alpha$  values will be underestimated. The band at about  $1710$  or the band at about  $1526 \text{ cm}^{-1}$  for the films hydrated with  $\text{H}_2\text{O}$  (Pilet & Brahms, 1973; Pilet et al., 1975; Flemming et al., 1988), and the band at about  $1696$  or  $1672 \text{ cm}^{-1}$  for the films hydrated with  $\text{D}_2\text{O}$  (Bradbury et al., 1961; Baret et al., 1978) were used to estimate  $S$ . Once  $S$  is known for a particular sample, we can calculate  $\theta$  for other absorption bands using eq. (1). If the bases are inclined,  $\theta$  will be  $90^\circ$  only if the transition dipole of the most dichroic band is lying on the axis around which the base is inclined. Here, we consider systematically the direction of the transition dipole (designated as  $\delta$ ) relative to the axis of inclination (designated as  $\chi$ ) in the base plane, deduced from our earlier vacuum-UV LD measurements, to estimate a more reasonable  $\theta$  angle for the most dichroic band, and then calculate a more accurate  $S$ . From the relationship discussed in Results and Discussion section, we find that the most dichroic band for B-DNA has  $\theta=82^\circ$ , and for A-DNA has  $\theta=79^\circ$ . These

values were used to calculate  $S$ . Since the C-form is so similar to the B-form, we assumed  $\theta=82^\circ$  for C-DNA.

**Data Analysis :** Measured spectra were smoothed using a Savitzky-Golay algorithm with 9 points, and the baseline due to the calcium fluoride or KRS-5 windows was subtracted. All numerical manipulations and data treatment used the software developed by Nicolet Inst. Co. For the phosphodiester backbone orientation, the absorbances of the antisymmetric and symmetric stretching bands of the phosphate ( $\text{PO}_2^-$ ) group at about  $1230$  and  $1090\text{ cm}^{-1}$ , respectively, are well separated, and their strength was simply determined by integrating each band.

The in-plane stretching bands of the DNA bases in the range of  $1750$  to  $1500\text{ cm}^{-1}$  exhibit a rather complex band contour, especially around  $1650\text{ cm}^{-1}$ , which includes the water absorption. Therefore, we collected the spectra of the DNA samples under the  $\text{D}_2\text{O}$  vapor saturated with the appropriate salt to avoid the interference of the water absorption. These overlapping bands should be separated into individual bands to get a reasonable band intensity and a reliable dichroic ratio for each band. Several band-narrowing procedures, such as the Fourier self-deconvolution (FSD), the derivative method, and curve fitting, can be used to enhance the resolution of the observed spectrum. For quantitative results, curve fitting of the original band contour has been suggested by many workers (Maddams, 1980; Arrondo et al., 1993; Lamba et al., 1993; Surewicz et al., 1993). Here, we decomposed the overlapping bands by means of a least-square curve fitting program based on the Levenberg-Marquardt algorithm (Brown & Dennis, 1972). We used a sum of the Lorentzian and the Gaussian band shapes to represent the observed spectrum. The fitting program was written to vary the fraction of both band shapes to give the best fit. To get the number of bands and their positions for the initial input into the fitting program, the second derivative and FSD algorithms (Nicolet Inst. Co.) with a halfwidth of  $18\text{ cm}^{-1}$  and  $k$  values between  $1.2$  and  $1.5$  were applied to the original

spectrum. The fraction of the two band shapes was set to 0.5, and the width and the intensity of each band were estimated visually from the Fourier self-deconvoluted spectra for the initial input parameters. From these initial estimates for band parameters, the fitting algorithm iteratively generates a sequence of approximations toward the minimum sum of square error. The fitting was stopped at the point where the variances of each parameter were stable, and the resulting integrated intensity was used to calculate the dichroic ratio ( $R$ ) of individual vibrational bands. This curve fitting procedure was repeated several times with the slightly modified initial input parameters to make sure our band decomposition was reproducible.

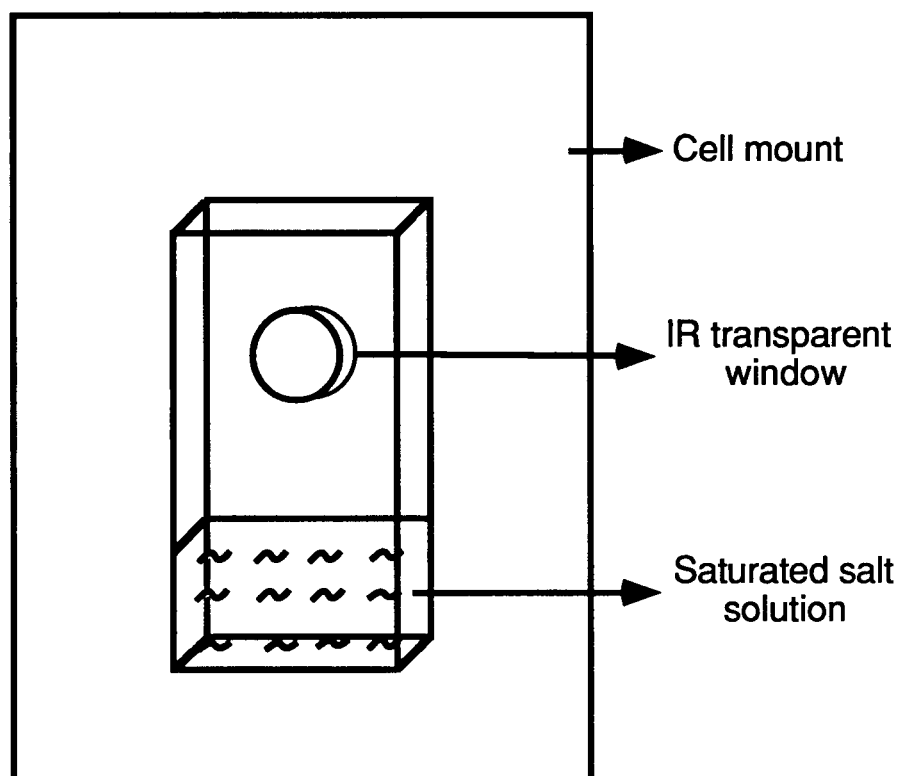


Figure 3.1. Diagram showing sealed chamber.

## RESULTS AND DISCUSSION

**Characterization of the A-, B-, and C-Forms :** Figure 3.2 gives representative FTIR spectra of poly[d(AC)]•poly[d(GT)] and poly[d(AG)]•poly[d(CT)] in films hydrated with H<sub>2</sub>O at high and low relative humidity (r.h.). The characteristic marker bands for each form of DNA are indicated in the figure, and are summarized in Table 3.1 with their proposed assignments. The spectra of *E.coli* and calf thymus DNA (Figure 3.3) are quite similar as those of natural DNA reported previously (Tsuboi, 1969; Taillandier et al., 1985; Keller & Hartman, 1986; Liquier et al., 1990), and the characteristic marker bands are summarized in Table 3.1. The spectra of poly[d(AC)]•poly[d(GT)] at high and low r.h. are quite similar as those reported previously (Taillandier et al., 1984b; Taboury & Taillandier, 1985). The spectra of all polynucleotides tested at high ( >94 % ) r.h. have absorption bands at 1422, 1329, and 1281 cm<sup>-1</sup>, characteristic of C2'-endo sugar pucker of B-DNA (Taillandier et al., 1984b; Adam et al., 1986; Taillandier & Liquier, 1992). Several marker bands for B-DNA are also observed at 968, 893, and 833 cm<sup>-1</sup>. The position of strong absorption bands at 1223 cm<sup>-1</sup> due to the antisymmetric stretching mode of the phosphate (PO<sub>2</sub><sup>-</sup>) groups also suggests these DNAs assume B-form at high (>94%) r.h.

A slow, stepwise dehydration - rehydration protocol was used to induce the B- to A-form transition for each DNA, as suggested by Keller & Hartman (1986). For this purpose, K<sub>2</sub>SO<sub>4</sub>, KCl, (NH<sub>4</sub>)<sub>2</sub>SO<sub>4</sub>, NaCl, NaNO<sub>2</sub>, and NaBr were used to achieve 94, 86, 80, 75, 66, and 56% r.h., respectively. It is evident from Figures 3.2 and 3.3 or Table 3.1 that poly[d(AC)]•poly[d(GT)], *E.coli* DNA, and calf thymus DNA equilibrated at low (75%) r.h. have several A-DNA marker bands at 1489, 1335, and 1274 cm<sup>-1</sup>, characteristic of C3'-endo sugar pucker (Taillandier et al., 1984b; Adam et al., 1986; Taillandier & Liquier, 1992). Several A-DNA marker bands are also observed at 966, 897, 881, 862, and 806 cm<sup>-1</sup>. The shift of the strong absorption band due to the antisymmetric



stretching mode of the  $\text{PO}_2^-$  groups from 1223 to 1239  $\text{cm}^{-1}$  and the appearance of a new band at 1185  $\text{cm}^{-1}$  also indicate that these DNAs assume the A-form at low (75%) r.h. In the spectral region due to in-plane double bond stretching of the bases, characteristic bands for the B- and A-forms are observed at 1714 and 1710  $\text{cm}^{-1}$ , respectively, for all DNAs hydrated with  $\text{H}_2\text{O}$ .

In addition to these specific marker bands for each form of DNA, the B- and A-forms of DNA can be characterized by measuring dichroic spectra of an oriented sample. B-DNA is characterized by an almost zero dichroic ratio for the band at 1223  $\text{cm}^{-1}$  and a highly perpendicular dichroic ratio for the band at 1087  $\text{cm}^{-1}$ . In contrast, A-DNA shows a perpendicular dichroic ratio at 1239  $\text{cm}^{-1}$ , and a parallel dichroic ratio at 1086  $\text{cm}^{-1}$  (Bradbury et al., 1961; Pilet & Brahms, 1973; Pilet et al., 1975; Kursar & Holzwarth, 1976; Baret et al., 1978). Figure 3.4 shows the dichroic spectra of oriented DNA samples hydrated with  $\text{H}_2\text{O}$  in the spectral region of the  $\text{PO}_2^-$  vibration. Poly[d(AC)]•poly[d(GT)], poly[d(AG)]•poly[d(CT)], and natural DNAs at high (94%) r.h. show an almost zero dichroic ratio for the antisymmetric stretching band of  $\text{PO}_2^-$  at 1223  $\text{cm}^{-1}$  and a strong perpendicular dichroic ratio for the symmetric stretching band of  $\text{PO}_2^-$  at 1087  $\text{cm}^{-1}$ . These dichroic ratios are reversed for poly[d(AC)]•poly[d(GT)] and natural DNAs at low (75%) r.h., but the spectrum of poly[d(AG)]•poly[d(CT)] at low r.h. has a parallel dichroic ratio for the 1223  $\text{cm}^{-1}$  band and a strong perpendicular dichroic ratio for the 1087  $\text{cm}^{-1}$  band of the  $\text{PO}_2^-$  groups.

Spectra of oriented DNA with a parallel dichroic ratio for the antisymmetric stretching band and a strong perpendicular dichroic ratio for the symmetric stretching band for  $\text{PO}_2^-$  groups are believed to characterize C-DNA (Brahms et al., 1973; Fritzsche et al., 1976; Taillandier & Liquier, 1992). Usually, the C-form of DNA is produced under specific conditions such as high  $\text{Li}^+$  salt and low relative humidity (Marvin et al., 1961; Brahms et al., 1973; Loprete & Hartman, 1989). To decide whether our parallel dichroic ratio observed for the antisymmetric phosphate stretching band in the oriented spectrum of

poly[d(AG)]•poly[d(CT)] at low (<66%) r.h. indicates the C-form, we carefully investigated other regions of the infrared spectra. Our FTIR spectrum for poly[d(AC)]•poly[d(GT)] and natural DNA hydrated with D<sub>2</sub>O vapor at high and low r.h. have a peak at 1675 and 1682 cm<sup>-1</sup>, respectively, characteristic of B- and A-DNA, but do not have a band at 1660 cm<sup>-1</sup> characteristic of C-DNA (Loprete & Hartman, 1989). In contrast, for poly[d(AG)]•poly[d(CT)] hydrated with D<sub>2</sub>O the peak at 1673 cm<sup>-1</sup> is shifted to 1663 cm<sup>-1</sup> by lowering the r.h., indicating a B to C transition. The shifts of bands at 1714 to 1709 cm<sup>-1</sup>, 1222 to 1220 cm<sup>-1</sup>, 971 to 968 cm<sup>-1</sup>, 893 to 891 cm<sup>-1</sup>, and 835 to 833 cm<sup>-1</sup> for poly[d(AG)]•poly[d(CT)] hydrated with H<sub>2</sub>O (Figure 3.2), also indicate that this polynucleotide undergoes B→C transition by decreasing r.h. (Loprete & Hartman, 1989). We also observed the shape of the band due to the symmetric phosphate stretching that represents the C-form; that is, it does not show a weak shoulder at 1071 cm<sup>-1</sup> but has a sharp, well-separated band at 1069 cm<sup>-1</sup> indicative of C-DNA (Loprete & Hartman, 1989). We tried extensively to produce A-form of poly[d(AG)]•poly[d(CT)] by adjusting salt and r.h., but failed. Leslie et al. (1980) also have reported that poly[d(AG)]•poly[d(CT)] in fibers can not undergo a B to A transition, but instead undergoes a B to C transition by lowering the r.h.

Clearly, poly[d(AC)]•poly[d(GT)], *E. coli* DNA, and calf thymus DNA assume the B- and A-forms at high (>94 %) and low (75 %) r.h., respectively, and poly[d(AG)]•poly[d(CT)] assumes the B- and C-forms at high (>94%) and low (66%) r.h., respectively. All of these transitions were fully reversible upon rehydration.

Table 3.1. IR Absorption Bands Observed for Different DNA Conformations\*  
in H<sub>2</sub>O

poly[d(AC)]• poly[d(GT)]		poly[d(AG)]• poly[d(CT)]		natural DNA		assignment
B form	A form	B form	C form	B form	A form	
1714	1710	1714	1709	1714	1710	in-plane
1493	1489	1493	1493	1493	1490	
1456	1455	1458	1458	1457	1457	
1422		1423	1423	1422		C2' endo/anti
	1419				1419	C3' endo/anti
1375	1373	1374	1374	1374	1374	purine/anti
	1335				1335	dA,dT C3 endo/anti
1329		1329	1329	1329		dT C2' endo/anti
1298	1296	1298	1298	1298	1296	
1281		1281		1281		dT C2' endo/anti
	1274				1274	dT C3' endo/anti
1224	1240	1221	1220	1224	1238	antisymmetric PO <sub>2</sub> <sup>-</sup>
	1185				1185	
1088	1088	1087	1088	1086	1086	symmetric PO <sub>2</sub> <sup>-</sup>
			1069			
1052	1053	1052	1053	1053	1053	
968	966	971	968	968	966	deoxyribose
893	897	893	891	893	897	deoxyribose
	881				881	
862	862	862		862		deoxyribose, backbone
833		835	833	837		backbone
	806				805	backbone

\* B-, C-, and A-DNA were obtained at high(>94%), low(66%), and low(75%) r.h., respectively

Figure 3.2. Infrared spectra of (a) poly[d(AC)]•poly[d(GT)] in the B form at 94% r.h., (b) poly[d(AC)]•poly[d(GT)] in the A form at 75% r.h., (c) poly[d(AG)]•poly[d(CT)] in the B form at 94% r.h., and (d) poly[d(AG)]•poly[d(CT)] in the C form at 66% r.h. Characteristic marker bands are indicated by their wavenumbers.

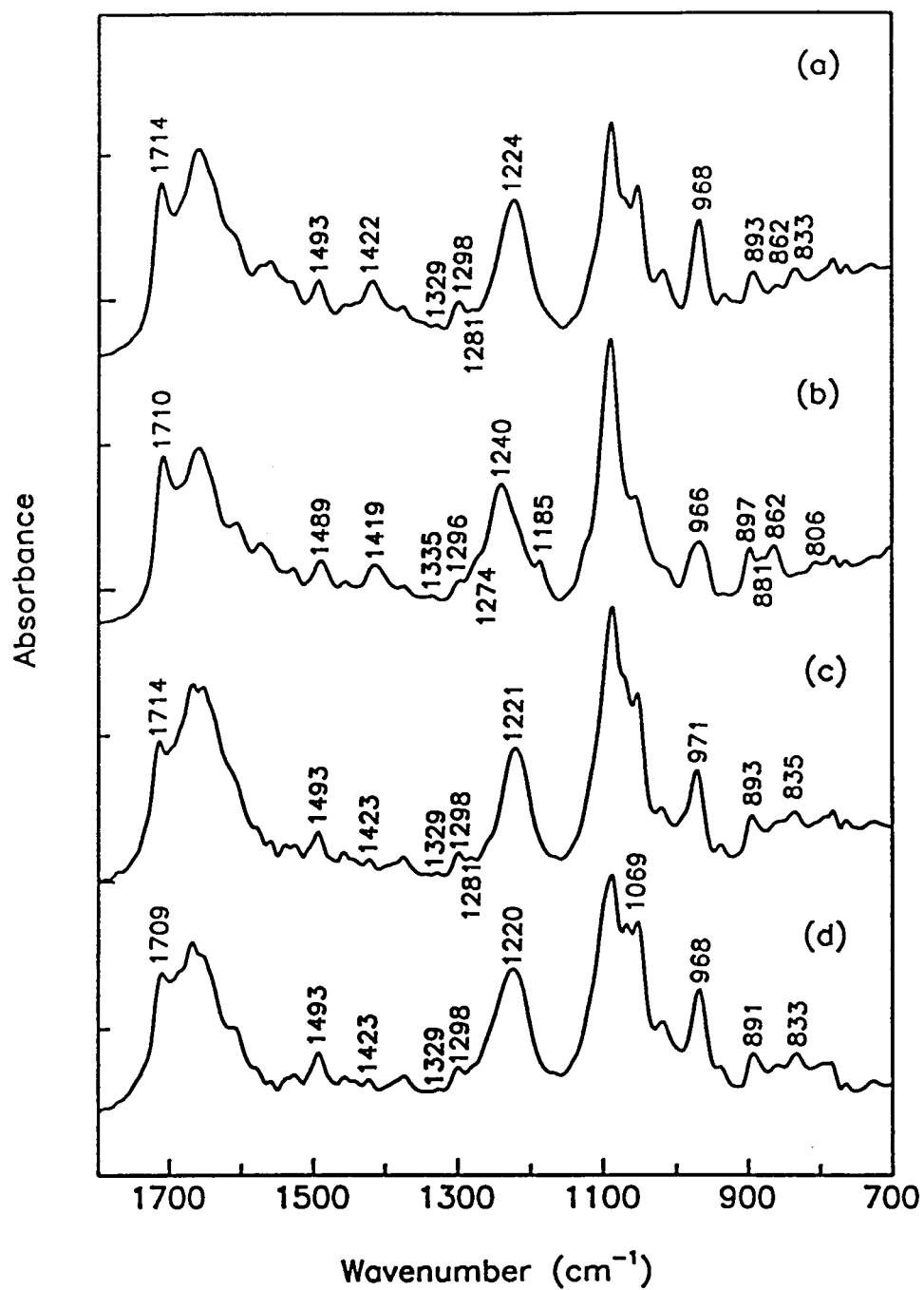


Figure 3.2

Figure 3.3. Infrared spectra of (a) calf thymus DNA in the B form at 94% r.h.,  
(b) calf thymus DNA in the A form at 75% r.h.,  
(c) *E. coli* DNA in the B form at 94% r.h., and  
(d) *E. coli* DNA in the A form at 75% r.h.  
Characteristic marker bands are indicated by their wavenumbers.

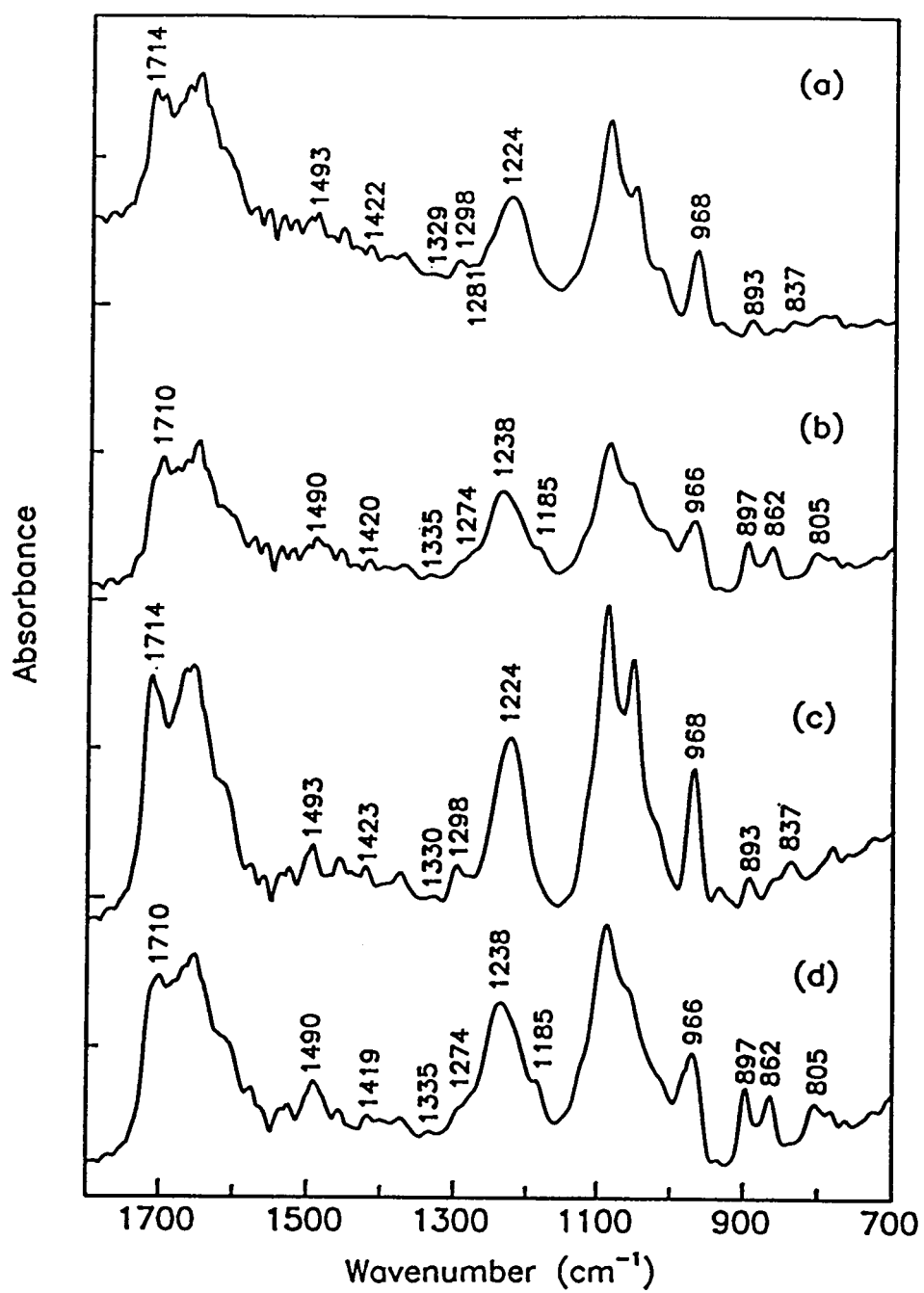
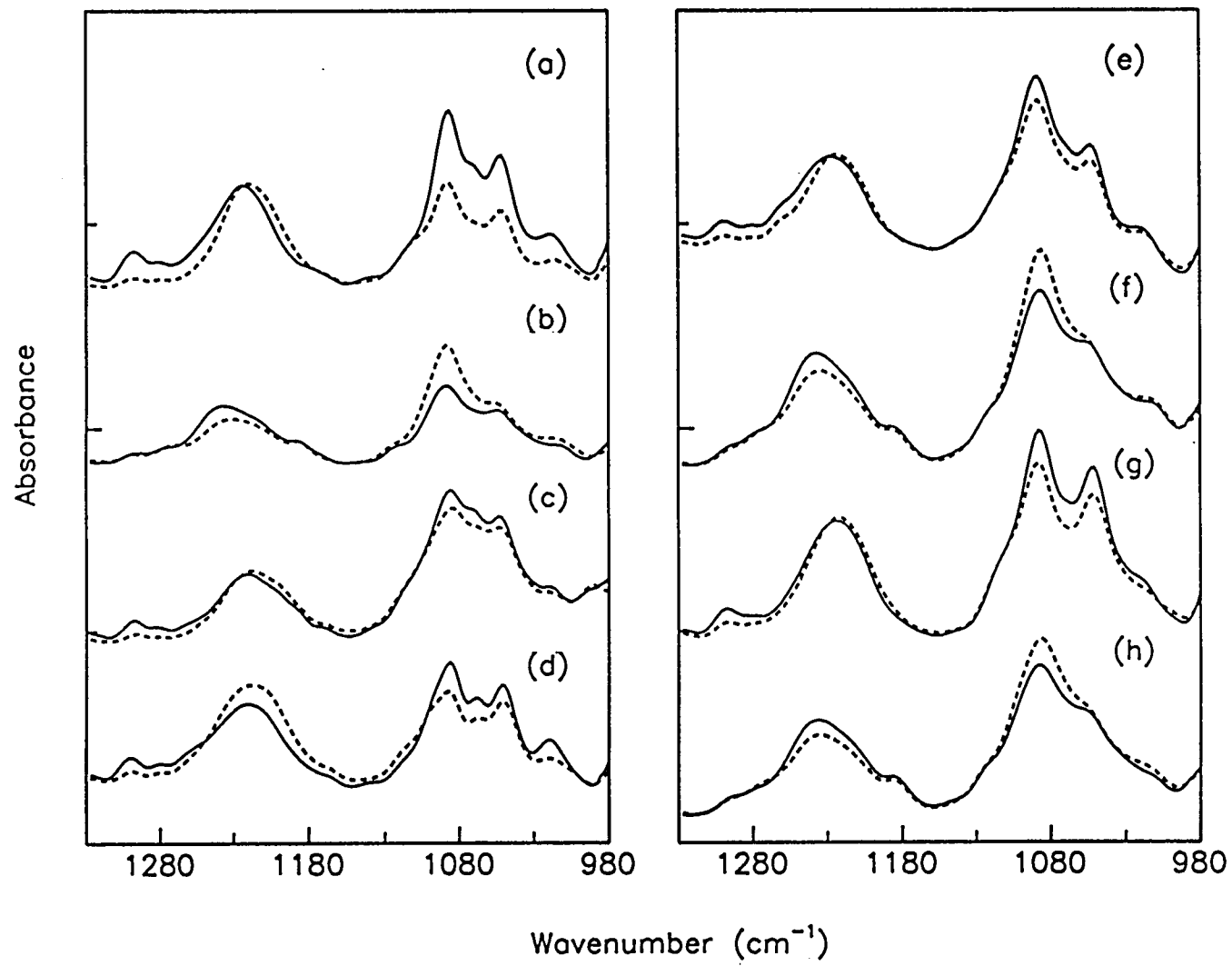


Figure 3.3

Figure 3.4. Dichroic spectra in the  $\text{PO}_2^-$  stretching vibration region for the oriented DNA samples measured with the electric vector of the polarized light perpendicular (—) and parallel (....) to the helix axis. (a) B form of poly[d(AC)]•poly[d(GT)], (b) A form of poly[d(AC)]•poly[d(GT)], (c) B form of poly[d(AG)]•poly[d(CT)], (d) C form of poly[d(AG)]•poly[d(CT)], (e) B form of calf thymus DNA, (f) A form of calf thymus DNA, (g) B form of *E. coli* DNA, and (h) A form of *E. coli* DNA. B-, C-, and A-DNA are obtained at 94%, 66%, and 75% r.h., respectively.



Figure 3.4



**Estimation of the Orientation Parameter :** In the equation (1) there are two unknowns,  $\theta$  and  $S$ . In order to determine  $\theta$ , it is necessary to estimate  $S$ . This is possible by using an appropriate intense and well-separated band for which the direction of the transition dipole of that vibrational mode is known from the results of other methods. The in-plane stretching bands of the DNA bases are spread over the wavenumber range of 1750 to 1500  $\text{cm}^{-1}$ . Thus, the band with maximum value of dichroic ratio ( $R$ ) is usually taken to estimate  $S$ . For this purpose, a band at about 1710 or 1526  $\text{cm}^{-1}$ , and in the deuterated form, at about 1696 or 1672  $\text{cm}^{-1}$ , are chosen (Bradbury et al., 1961; Pilet & Brahms, 1973; Pilet et al., 1975; Baret et al., 1978; Flemming et al., 1988).

In dichroic spectra for our oriented DNA samples, the most dichroic band was observed at about 1710  $\text{cm}^{-1}$  in  $\text{H}_2\text{O}$  and at about 1696  $\text{cm}^{-1}$  in  $\text{D}_2\text{O}$ . We assign this band to the  $\text{C4=O}$  bond stretching of thymine. The band at about 1710  $\text{cm}^{-1}$  in  $\text{H}_2\text{O}$  or at about 1696  $\text{cm}^{-1}$  in  $\text{D}_2\text{O}$  was previously assigned to the  $\text{C2=O}$  bond stretching vibration of thymine (Tsuboi et al., 1973; Kursar & Holzwarth, 1976; Baret et al., 1978). However, Ovaska et al. (1984) used a fixed partial charge model to calculate the transition dipole directions for the double-bond region vibrations of pyrimidine bases, and reported that the band at about 1670  $\text{cm}^{-1}$  is mainly the  $\text{C2=O}$  stretching, and the band at about 1710  $\text{cm}^{-1}$  is mainly due to  $\text{C4=O}$  stretching of thymine. In addition, our earlier UV LD results (Kang & Johnson, 1993; Chou & Johnson, 1993) showed that the axis of inclination for the thymine base lies in the same direction as the transition dipole of the  $\text{C4=O}$  bond stretching vibration. Since the most dichroic ratio is observed for a band that has the transition dipole is in the same direction as the axis of inclination, we assign the band at about 1710  $\text{cm}^{-1}$  to the  $\text{C4=O}$  bond stretching rather than  $\text{C2=O}$  bond stretching of thymine.

Many authors have assumed the  $\theta$  angle for the most dichroic IR band to be  $90^\circ$  when estimating the orientation parameter  $S$ . However, since  $\theta$  depends on both the inclination of base and the direction of transition dipole in the base plane (Flemming et al., 1988), this assumption is really valid only if the

transition dipole direction of the most dichroic band is collinear with the axis around which the bases are inclining. Figure 3.5 represents the dependence of  $\theta$  on the inclination of base,  $\alpha$ , and direction of transition dipole relative to the axis of inclination in the base plane,  $\beta$ . The directions of vibrational transition dipoles for the pyrimidine bases were calculated by Ovaska et al. (1984), and the axes of inclination for each base are known from our UV LD measurements (Kang & Johnson, 1993; Chou & Johnson, 1993). It is obvious from Figure 3.5 that  $\theta$  is more affected by the relative direction of the transition dipole with respect to axis of inclination for more highly inclined bases. Our UV LD results indicate that the average angles of inclination for thymine bases are about  $29 \pm 4^\circ$  and  $37 \pm 2^\circ$  for B- and A-form, respectively, of synthetic polynucleotides and natural DNAs in solution, and the inclination axis relative to the vector N1-C4 are about  $41 \pm 10^\circ$  for both the B- and A-forms of DNA. Since the direction of the transition dipole for the thymine C4=O bond stretching at about  $1710 \text{ cm}^{-1}$  was estimated to be about  $245^\circ$ , based on the fixed partial charge model approximation (Ovaska et al., 1984), the relative angle  $\beta$  between these two vectors is about  $24^\circ$ . This corresponds to a  $\theta$  of  $82$  and  $79^\circ$  for B- and A-form of DNA, respectively (Figure 3.5).

From these considerations, we use  $82$  and  $79^\circ$  for the  $\theta$  of the most dichroic band in B- and A-DNA, respectively, to estimate  $S$ . It is interesting to note that the  $\theta$  for the most dichroic band used to estimate  $S$  are comparable with those values,  $84^\circ$  for B-DNA and  $76^\circ$  for A-DNA, calculated from the energetically favored tilt and propeller twist angles in the several conformations of DNA for the  $\theta$  of transition dipole of the C2=O bond stretching of thymine (Pohle et al., 1984). However, these small differences of  $\theta$  do not affect significantly the final inclination angles, since only  $1$  to  $2^\circ$  changes in the final inclination angles result from the variation of  $90$  to  $80^\circ$  for the  $\theta$  of the most dichroic band.

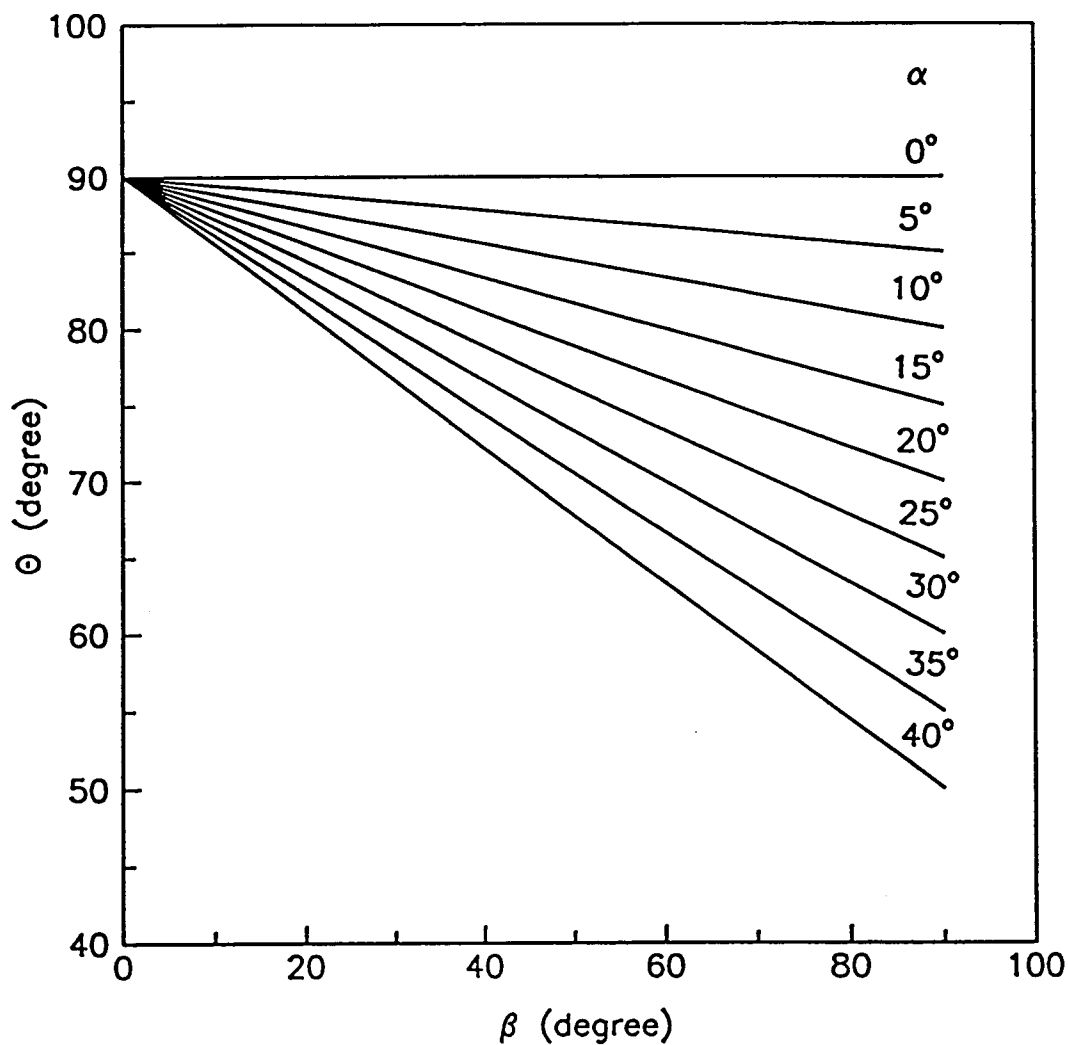


Figure 3.5. Dependence of the  $\theta$  angle on both the base inclination ( $\alpha$ ) and the relative angle between the transition dipole and the axis of inclination ( $\beta$ ).

**Decomposition of Overlapping Bands :** The infrared spectrum of a DNA film in the range of 1750 to 1500  $\text{cm}^{-1}$  contains several overlapping bands due to in-plane stretching of carbonyl bonds and ring stretching of the bases, and the transition dipole direction for each vibrational mode is directly related to the inclination angle of bases. These overlapping bands should be decomposed into individual bands to obtain quantitative intensities and reliable dichroic ratios for each band. Figures 3.6 and 3.7 represent the dichroic spectra in the base stretching region of the oriented films for the synthetic polynucleotides and natural DNAs hydrated with  $\text{D}_2\text{O}$  at different r.h. Figures 3.8 and 3.9 represent the examples of band decomposition for a poly[d(AC)]•poly[d(GT)] film hydrated with  $\text{D}_2\text{O}$  at high (94%) r.h., and poly[d(AG)]•poly[d(CT)] film hydrated with  $\text{D}_2\text{O}$  at low (66%) r.h. in the range of 1750 to 1500  $\text{cm}^{-1}$ . We used a sum of the Lorentzian and the Gaussian band shape to represent each band. Usually, either the Lorentzian or the Gaussian band shape has been used to decompose the overlapping bands of infrared spectrum (Maddams, 1980; Arrondo et al., 1993; Lamba et al., 1993; Surewicz et al., 1993). However, reports by Maddams (1980), and Pitha & Jones (1966, 1967) showed that combined use of the Lorentzian and the Gaussian band shape gave better results to curve fitting of infrared data. Therefore, we tried to decompose the observed spectra using either the Lorentzian or the Gaussian band shape, or using both band shapes. We confirmed that combined use of both band shapes resulted in better fit to the observed spectrum (data not shown).

To estimate the most important values for the input parameters to the curve fitting routine (the number of bands and their positions) second derivative and FSD algorithms with a halfwidth of 18  $\text{cm}^{-1}$  and the k values between 1.2 and 1.5 were applied to the measured spectrum. The horizontal baseline was set with the lowest absorption value at the highest wavenumber. None of the input parameters (position, width, intensity, and fraction of band shape) were kept constant during the curve fitting procedure.

As shown in Figures 3.8 and 3.9, the infrared spectra in the range of 1750 to 1500  $\text{cm}^{-1}$  for DNA samples hydrated with  $\text{D}_2\text{O}$  are decomposed with 9 bands, each of which shows a definite inflection in the measured spectrum. The positions of each band after curve fitting were almost same as the values of the parameters estimated from the original spectra using the second derivative and FSD algorithms with the fraction of each band shape varied randomly between 0 and 1. In all cases, the fittings were extremely good as judged by the very low sum of square error.

Although it is not necessary to assign each vibrational mode to the specific transition dipoles, we try to assign the decomposed bands of IR spectra for synthetic polynucleotides and natural DNAs to known vibrational modes in the base plane. However, because of the proximity of the peak positions for the in-plane stretching modes of DNA bases in the DNA samples with four different types of bases, it is not easy to assign individual absorption bands to specific C=O bond stretching or ring stretching vibrations. We used the reported assignments of vibrational modes for purine and pyrimidine bases (Tsuboi et al., 1962; Howard & Miles, 1965; Kyogoku et al., 1967; Ovaska et al., 1984), and for simpler polynucleotides such as poly[d(A)], poly[d(G)], poly[d(A)]•poly[d(T)], and poly[d(G)]•poly[d(C)] (Miles, 1964; Miles & Frazier, 1964; Howard et al., 1969; Baret et al., 1978). We tentatively assign the 1696  $\text{cm}^{-1}$  band to the C4=O thymine stretching mode, and the band at 1671  $\text{cm}^{-1}$  to both the C2=O thymine and C6=O guanine stretching mode. The band at 1644  $\text{cm}^{-1}$  is assigned to both the C2=O cytosine and C=C thymine stretching modes, and the band at 1622  $\text{cm}^{-1}$  to the C=C and C=N double bond stretching modes for adenine and cytosine. Finally, the bands at 1575 and 1561  $\text{cm}^{-1}$  are assigned to the ring stretching vibration of adenine, guanine, and cytosine. Assignments of the bands below 1550  $\text{cm}^{-1}$  are very difficult as it is believed that the base and sugar units give rise to many bands here; the peaks arise from the superposition of many bands (Bradbury et al., 1961).

Figure 3.6. Dichroic spectra for the in-plane double bond stretching region for the oriented DNA films hydrated with  $D_2O$ . The electric vector of the light polarized is perpendicular (—) and parallel (....) to the helix axis. (a) B form of poly[d(AC)]•poly[d(GT)], (b) A form of poly[d(AC)]•poly[d(GT)], (c) B form of poly[d(AG)]•poly[d(CT)], and (d) C form of poly[d(AG)]•poly[d(CT)]. B-, C-, and A-DNA are obtained at 94%, 66%, and 75% r.h., respectively.

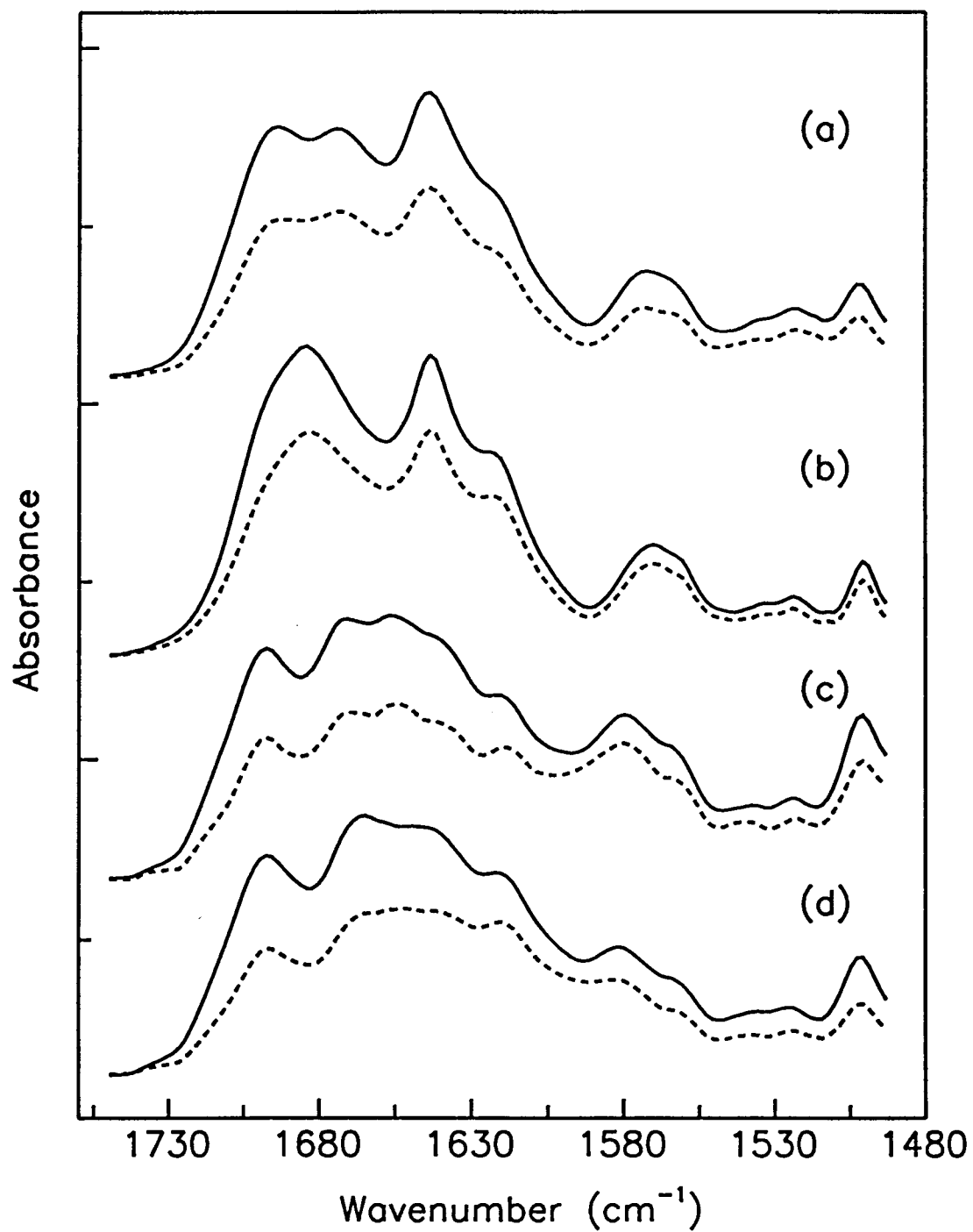


Figure 3.6



Figure 3.7. Dichroic spectra for the in-plane double bond stretching region for the oriented DNA films hydrated with D<sub>2</sub>O. The electric vector of the light polarized is perpendicular (—) and parallel (....) to the helix axis. (a) B form of calf thymus DNA, (b) A form of calf thymus DNA, (c) B form of *E. coli* DNA, and (d) A form of *E. coli* DNA. B- and A-DNA are obtained at 94% and 75% r.h., respectively.

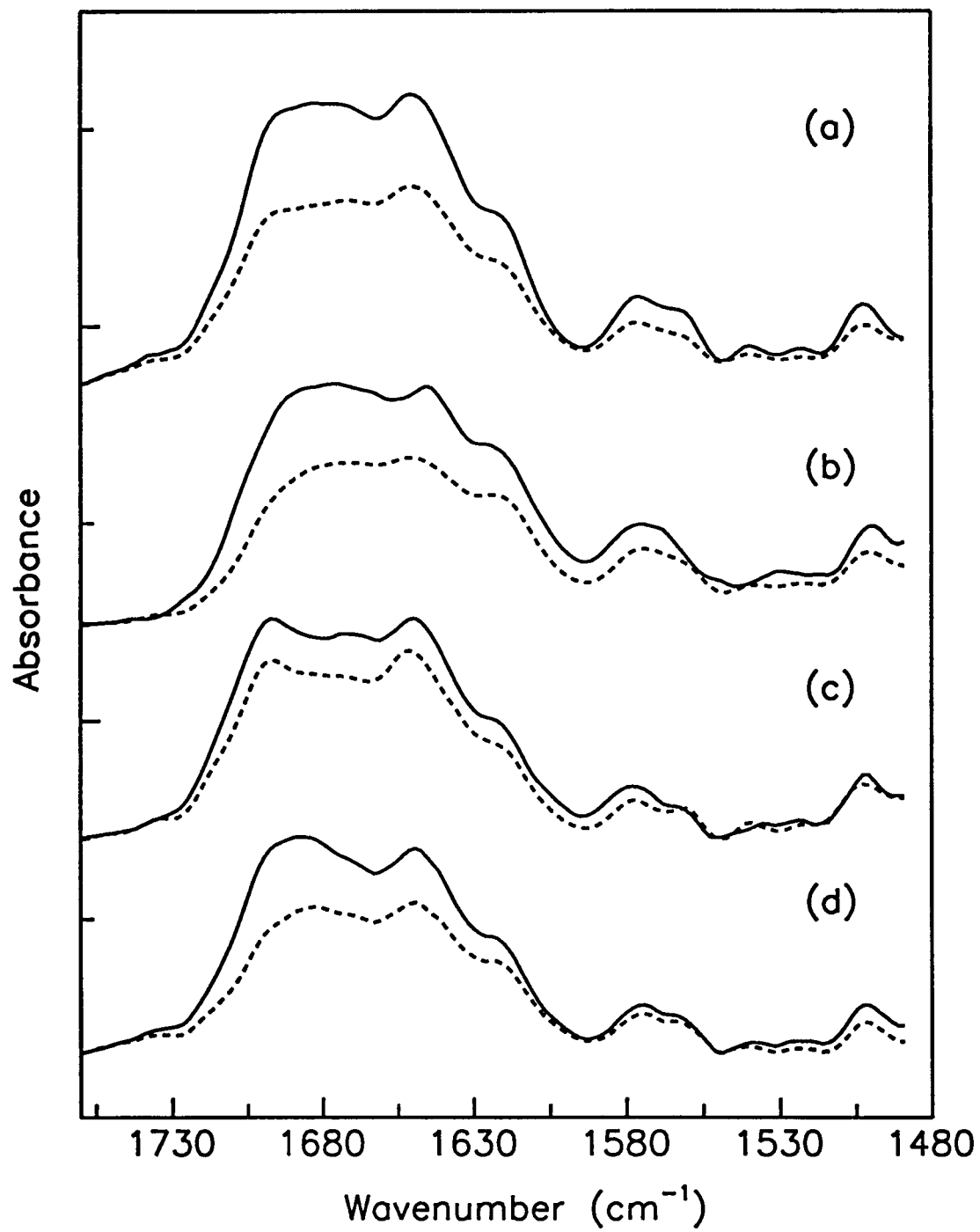


Figure 3.7

Figure 3.8. (a) Dichroic spectra for the in-plane double bond stretching region for an oriented poly[d(AC)]•poly[d(GT)] film hydrated with D<sub>2</sub>O at 94% r.h. The electric vector of the light polarized is perpendicular (—) and parallel (---) to the helical axis. (b) Decomposition of overlapping absorption bands (—) with sum of individual bands (---). A sum of the Lorentzian and the Gaussian band contour is used to represent the observed band shape.

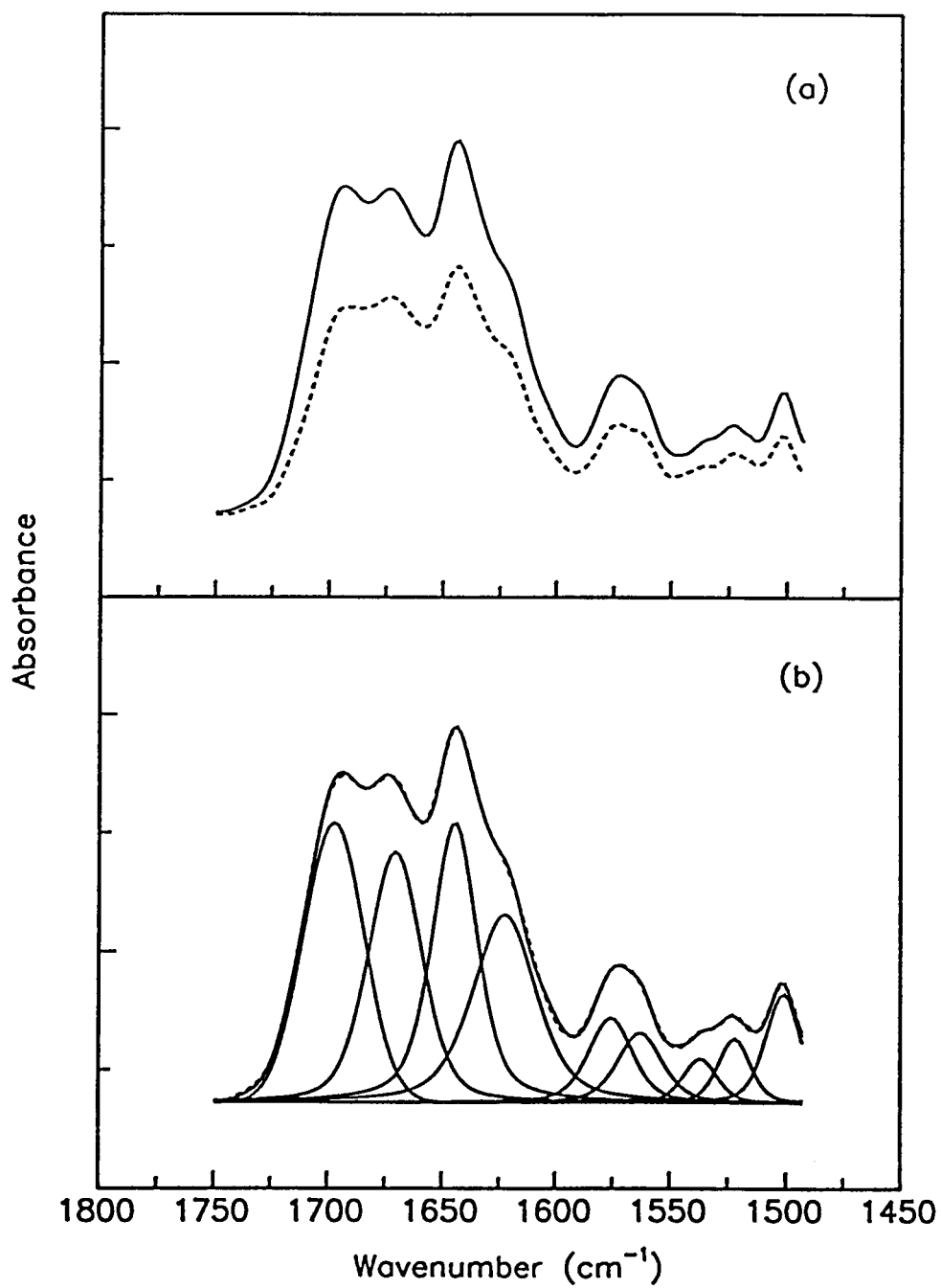
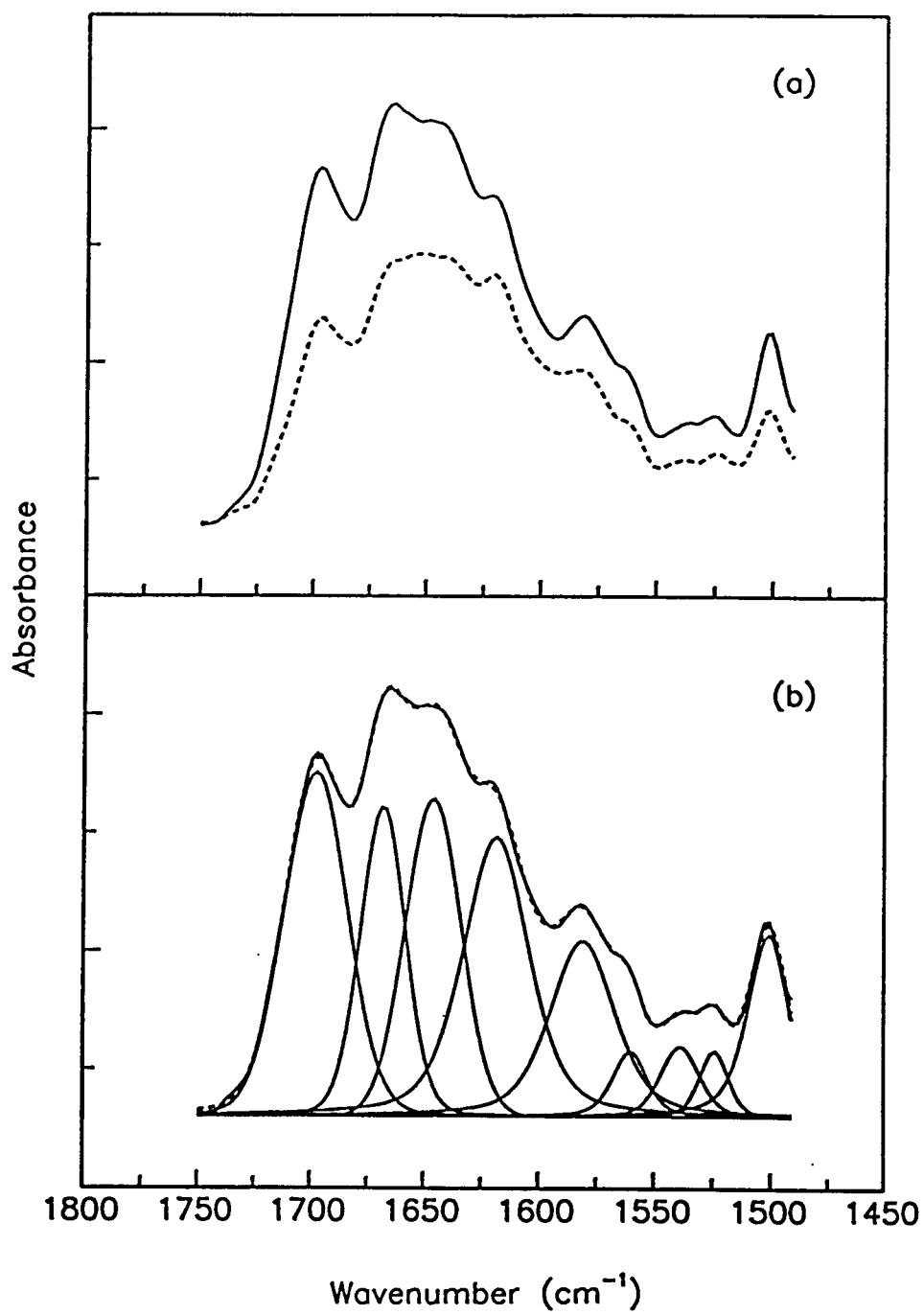


Figure 3.8

Figure 3.9. (a) Dichroic spectra and (b) decomposition of overlapping bands for an oriented poly[d(AG)]•poly[d(CT)] film hydrated with D<sub>2</sub>O at 66% r.h. The conditions of measurements and decomposition are same as those in Figure 3.8.

**Figure 3.9**

**Inclination of the Bases :** The  $\theta$  angle depends on both the direction of transition dipole of the vibrational mode within the base plane and the inclination angle of base. If the transition dipole is perpendicular to the axis around which the base is inclined, then  $\theta = 90^\circ - \alpha$ , where  $\alpha$  represents the inclination of base normal with respect to the helical axis. Otherwise,  $\theta > 90^\circ - \alpha$ , and determines the minimum  $\alpha$ . However, we do not have enough information to determine both the specific angles of inclination for individual bases and their axes from IR LD measurements. Thus the  $\theta$  angle calculated from eq. (1) will correspond to minimum angle of base inclination.

The infrared spectra used to determine the inclination of the bases were measured in a  $D_2O$  atmosphere, because the deuteration of DNA films not only frees the  $1750$  to  $1500\text{ cm}^{-1}$  region from interfering  $H_2O$  absorption but also replaces N-H in the bases with N-D, which simplifies the vibrational modes of the DNA bases in this spectral region. We use the absorption band showing the largest dichroic ratio at about  $1695\text{ cm}^{-1}$  as a reference to estimate orientation parameter,  $S$ . The dichroic ratios and their corresponding  $\theta$  angles for the other in-plane stretching vibrational bands of DNA films with different degrees of orientation are calculated and summarized in Tables 3.2-3.5 for poly[d(AC)]•poly[d(GT)], poly[d(AG)]•poly[d(CT)], and natural DNAs (from *E.coli* and calf thymus). Since the bands below  $1550\text{ cm}^{-1}$  arise from a combination of the base and sugar units, we consider only 6 bands in the range of  $1750$  to  $1550\text{ cm}^{-1}$  to deduce the inclination of bases. To compensate for any possible errors in estimating orientation parameter,  $S$ , DNA films with different degrees of orientation were investigated, and the average  $\theta$  angles were calculated for each vibrational mode. A glance at the Tables 3.2-3.5 tells us that the dichroic ratios and the corresponding  $\theta$  angles vary according to the wavenumber. This wavenumber dependence of  $\theta$  demonstrates that the bases are not perpendicular to the helix axis. These Tables also show that for all synthetic polynucleotides and natural DNAs investigated, the bases in the B- and C-form

are inclined at least 15 to 25° from perpendicular to the helical axis. The inclinations increase slightly for the A-form of the same DNA samples.

The  $\theta$  angles obtained by IR LD represent a minimum inclination of the bases and assume that the vibrational modes for C=O stretching and ring stretching are located in the base plane. If there is some out-of-plane portion of the in-plane vibrational modes, the differences in the corresponding  $\theta$  angles of the bases can no longer be explained simply by base inclination. This so-called protrusion angle, the angle between the transition moment of the vibrational mode and the base plane, is believed to due to the out-of-plane portions of the in-plane vibrational modes created by electronic interaction of overlapping bases or by interaction of the dipoles with the surrounding electrostatic environment (Baret et al., 1978). However, there is no direct evidence that such effects exist. In addition, out-of-plane vibrations generally take place far away from the 1750-1500  $\text{cm}^{-1}$  region, where the in-plane stretching vibrations of C=O groups and ring stretching vibrations take place. Flemming et al. (1988) have estimated the protrusion angle for the transition moment of a C=O vibrational band at 1710  $\text{cm}^{-1}$  by using tilt and twist angles obtained from X-ray diffraction analysis, and discussed why the calculated high protrusion angle could not explain the large inclination angle of DNA bases in films compared with fiber diffraction data. All evidence indicates that protrusion angles are not large, and  $\theta$  angles deduced from IR LD measurements are due to the inclination of bases in the double helical structure of DNA.

Although our IR LD results do not have the information content to give specific inclination angles for individual bases, the  $\theta$  angles do provide other important information about base orientation in the double helical DNA structure. We have already reported quite high base inclinations for the B- and A-form of poly[d(AC)]•poly[d(GT)], poly[d(AG)]•poly[d(CT)], and several natural DNAs in aqueous solution using flow UV LD measurements (20-25° for purines and 30-35° for pyrimidines in B-DNA) (Kang & Johnson, 1993; Chou & Johnson, 1993). We also reported that A-DNA has slightly increased inclinations for both



the purine and the pyrimidine bases. However, the differences of the inclination angles between B- and A-DNA in solution are not as large as the values deduced from fiber or crystal diffraction data ( $6^\circ$  for B-DNA vs.  $20^\circ$  for A-DNA). IR LD confirms a substantial inclination for the bases of the B- and A-form of synthetic polynucleotides and natural DNAs in films. The inclination angles for the bases of natural DNA in films reported here are quite similar as those published elsewhere (Flemming et al., 1988). Poly[d(AC)]•poly[d(GT)] and poly[d(AG)]•poly[d(CT)] show inclinations comparable with those for poly(dA)•poly(dT) and poly[d(AT)]•poly[d(AT)] in films (Baret et al., 1978). Tables 3.2-3.5 also show that A-DNA has a slightly increased base inclination compared with B-DNA, but the difference in the base inclination is not large enough to discriminate between B- and A-DNA in films. These findings are consistent with Flemming et al. (1988), who point out that base inclination is not a good criterion to discriminate between B- and A-DNA. In addition to A- and B-DNA, we report for the first time the base inclination for the C-form of poly[d(AG)]•poly[d(CT)] in a film.

Our results about base inclinations of DNA in films deduced from IR LD measurements using vibrational transitions support our earlier UV LD results using electronic transitions, that the bases are highly inclined, even in the B-form. The information about the molecular structure of DNAs in gel or hydrated film provides valuable structural parameters to connect the molecular structure of DNA in solid state (e.g. crystal) with those in solution state. Considering the relatively high condensed environment of nuclei where the DNA molecules are occupied, the structural information about DNA molecules in film or gel provides important clues to understand the real nature of molecular structure of DNA in living cells.

**Conformation of Phosphodiester Backbone Geometry :** The torsional angles for the sugar-phosphodiester backbone and glycosidic bond of DNA are a determining factor in the relative stability of specific forms of DNA. X-ray fiber

Table 3.2. Dichroic Ratios from Various Experiments and Corresponding  $\theta$  Angles for Poly[d(AC)]•Poly[d(GT)] in Films Hydrated with D<sub>2</sub>O.

		1696	1671	1644	1622	1575	1561
B form at high r.h.(>94%)	R	2.47	2.38	2.04	1.96	2.21	1.72
		2.61	2.61	2.15	1.99	2.40	2.20
		1.62	1.50	1.41	1.61	1.51	1.48
		1.60	1.50	1.54	1.50	1.40	1.50
		1.35	1.31	1.28	1.17	1.28	1.28
		1.40	1.28	1.28	1.21	1.20	1.28
	$\theta$	82.0*	80.1	74.3	73.0	77.1	69.1
		82.0	82.0	74.6	72.3	78.4	75.4
		82.0	75.2	71.3	81.3	75.7	74.3
		82.0	76.0	78.1	76.0	71.4	76.0
		82.0	77.2	74.4	66.1	74.4	74.4
		82.0	71.7	71.7	67.2	66.6	71.7
	avg.	82.0	77.0±3.3	74.1±2.2	72.7±5.1	73.9±3.9	73.5±2.4
A form at low r.h.(75%)	R	3.20	3.00	2.25	2.48	2.25	1.81
		1.78	1.67	1.48	1.51	1.30	1.50
		1.44	1.34	1.34	1.20	1.15	1.24
		1.46	1.21	1.17	1.19	1.24	1.29
	$\theta$	79.0*	77.4	70.9	73.0	70.9	66.6
		79.0	75.2	69.5	70.3	64.3	70.1
		79.0	72.4	72.4	64.9	62.4	67.0
		79.0	65.1	63.1	64.1	66.5	69.0
	avg.	79.0	72.5±4.6	68.9±3.5	68.1±3.7	66.0±3.2	68.1±1.4

\* The  $\theta$  angles were set at this value to calculate orientation parameter(S).

Table 3.3. Dichroic Ratios from Various Experiments and Corresponding  $\theta$  Angles for Poly[d(AG)]•Poly[d(CT)] in Film Hydrated with D<sub>2</sub>O.

		1699	1673	1650	1630	1581	1561
B form at high r.h.(>94%)	R	1.90	1.62	1.49	1.30	1.26	1.52
		1.90	1.64	1.54	1.17	1.26	1.59
		2.10	1.80	1.75	1.60	1.65	1.55
		1.24	1.18	1.20	1.14	1.11	1.20
		1.24	1.20	1.20	1.18	1.19	1.21
	$\theta$	82.0*	72.7	69.1	63.9	62.3	69.9
		82.0	73.3	70.5	60.1	62.8	71.9
		82.0	75.9	74.6	70.8	72.0	69.6
		82.0	72.6	75.2	68.1	65.1	75.2
		82.0	75.2	75.2	72.6	73.8	76.6
	avg.	82.0	73.9±1.4	72.8±2.6	67.1±4.2	67.2±4.4	72.5±2.8
C form at low r.h.(66%)	R	1.89	1.79	1.63	1.50	1.33	1.32
		1.80	1.62	1.53	1.37	1.25	1.30
		1.50	1.40	1.35	1.25	1.20	1.22
	$\theta$	82.0*	78.1	73.2	69.5	64.8	64.5
		82.0	74.7	71.8	66.8	63.1	64.7
		82.0	74.8	72.0	66.9	64.5	65.4
	avg.	82.0	75.9±1.6	72.3±0.6	67.7±1.2	64.1±0.7	64.9±0.4

\* The  $\theta$  angles were set at this value to calculate orientation parameter(S).

Table 3.4. Dichroic Ratios from Various Experiments and Corresponding  $\theta$  Angles for *E. coli* DNA in Film Hydrated with D<sub>2</sub>O.

		1695	1671	1647	1620	1577	1561
B form at high r.h.(>94%)	R	1.34	1.32	1.19	1.27	1.30	1.15
		1.28	1.17	1.11	1.18	1.10	1.10
		1.31	1.25	1.15	1.23	1.20	1.13
	$\theta$	82.0°	79.3	67.8	74.2	68.6	65.0
		82.0	68.9	63.7	69.8	62.8	62.8
		82.0	74.5	65.9	72.6	69.9	64.4
	avg.	82.0	74.2±4.2	65.8±1.7	72.2±1.8	67.1±3.1	64.1±0.9
	R	1.22	1.21	1.09	1.07	1.06	1.04
		1.31	1.15	1.09	1.10	1.11	1.11
		1.19	1.09	1.03	1.12	1.10	1.13
A form at low r.h.(75%)	$\theta$	79.0°	77.3	63.3	61.4	60.4	58.5
		79.0	65.2	61.0	61.7	62.4	62.4
		79.0	64.6	58.0	68.2	65.8	69.5
	avg.	79.0	69.0±5.9	60.8±2.2	63.7±3.1	62.9±2.2	63.5±4.6

\* The  $\theta$  angle were set at this vaule to calculate orientation parameter (S).

Table 3.5. Dichroic Ratios from Various Experiments and Corresponding  $\theta$  Angles for Calf Thymus DNA in Film Hydrated with  $D_2O$ .

		1695	1671	1647	1620	1577	1561
B form at high r.h.(>94%)	R	2.01	1.71	1.20	1.75	1.27	1.60
		1.60	1.59	1.48	1.32	1.50	1.47
		1.80	1.65	1.34	1.51	1.38	1.53
	$\theta$	82.0*	73.3	60.6	74.3	62.4	70.6
		82.0	81.3	75.0	68.0	76.0	74.5
		82.0	75.8	65.9	71.2	67.1	71.8
	avg.	82.0	76.8 $\pm$ 3.3	67.2 $\pm$ 5.9	71.2 $\pm$ 2.6	68.5 $\pm$ 5.6	72.3 $\pm$ 1.6
	R	1.78	1.53	1.22	1.25	1.41	1.30
		1.33	1.27	1.13	1.12	1.16	1.21
		1.54	1.40	1.17	1.18	1.30	1.26
A form at low r.h.(75%)	$\theta$	79.0*	70.9	61.9	62.8	67.5	64.3
		79.0	73.3	63.3	62.6	65.3	68.8
		79.0	71.8	62.1	62.5	67.5	65.8
	avg.	79.0	72.0 $\pm$ 0.9	62.4 $\pm$ 0.6	62.6 $\pm$ 0.1	66.8 $\pm$ 1.0	66.3 $\pm$ 1.9

\* The  $\theta$  angles were set at this value to calculate orientation parameter(S).

or crystal diffraction analysis, NMR measurements, and theoretical calculations provide useful information about such torsional angles (Pohle et al., 1986, and references therein). IR LD spectroscopy is another useful technique to yield quantitative information about the geometrical arrangement of the phosphate groups in the backbone of DNA in solution, condensed gel, or hydrated film. Many workers have measured the conformational angles of the phosphate groups in A-, B-, C-, and D-forms of synthetic polynucleotides and natural DNAs by IR LD (Brahms et al., 1973; Pilet & Brahms, 1973; Pilet et al., 1975; Fritzsche et al., 1976; Kursar & Holzwarth, 1976; Baret et al., 1978; Flemming et al., 1988). The phosphate arrangement is determined by the two angles,  $\theta_{oo}$  and  $\theta_{opo}$ , which are formed between the O---O line and the bisector of the OPO and the DNA helix axis, respectively. As discussed in the papers by Pohle et al. (1984, 1986), the conformational angles of the  $PO_2^-$  groups for the A- and B-form of DNA obtained by different methods show a broad range of the angles rather than have one specific value. For example, the angles for O---O line and OPO bisector obtained from NMR, IR LD, or theoretical calculations are in the range of 52-56° and 62-70°, respectively, in the B-DNA, and in the range of 59-64° and 46-50°, respectively, in the A-DNA. In contrast, these angles deduced from fiber diffraction data spread over wider range than those presented above (48-66° and 49-71° for  $\theta_{oo}$  and  $\theta_{opo}$ , respectively, in the B-DNA, and 65-79° and 15-49° for  $\theta_{oo}$  and  $\theta_{opo}$ , respectively, in the A-DNA). Pohle et al. (1984) have compared the angles deduced from IR LD with those from X-ray data, and showed that the discrepancies in the conformational angles originated from inaccurate modeling of DNA structure to fit fiber diffraction data, causing these angles to spread over a wide range of  $\theta$  values, depending on the model used to fit the X-ray data. However, by selecting proper modelling for the X-ray data, values fairly close to IR LD results were obtained for the A-, B-, and Z-forms of DNA.

We measured the dichroic spectra of oriented films of DNA samples hydrated with  $H_2O$  under different r.h. for A-, B- and C-form (Figure 3.4). The

orientation parameter of the sample,  $S$ , which must be known to calculate  $\theta$  in Eq. (1), was determined from the largest dichroic ratio of a band near  $1710\text{ cm}^{-1}$  assigned to the  $\text{C4=O}$  stretching band for the thymine base (see above). The integrated intensity of individual bands arising from the antisymmetric and symmetric stretching vibrations of the  $\text{PO}_2^-$  group at about  $1230\text{ cm}^{-1}$  and  $1085\text{ cm}^{-1}$  were calculated, and the orientation angles of the  $\text{O---O}$  line and the OPO bisector relative to the helix axis were determined from the measured dichroic ratio of corresponding bands (Table 3.6). The dichroic ratios were also checked by measuring the peak intensity of each band from the baseline as described by Pohle et al. (1984), and the differences resulting from these two methods were within the experimental error. For B-DNA, the angle for the OPO bisector ( $\theta_{\text{opo}}$ ) is about  $67^\circ$  for  $\text{poly}[\text{d(AC)}]\cdot\text{poly}[\text{d(GT)}]$  and  $\text{poly}[\text{d(AG)}]\cdot\text{poly}[\text{d(CT)}]$ , and is about  $63^\circ$  for natural DNAs. The angle for the  $\text{O---O}$  line ( $\theta_{\text{oo}}$ ) is about  $54^\circ$  for both synthetic polynucleotides and natural DNAs from different sources. For the A-form of natural DNA and  $\text{poly}[\text{d(AC)}]\cdot\text{poly}[\text{d(GT)}]$ , the  $\theta_{\text{opo}}$  and  $\theta_{\text{oo}}$  are about  $46^\circ$  and  $64^\circ$ , respectively. These conformational angles are comparable to angles reported by other workers (Pohle et al., 1986, and references therein). The orientation angles of  $\text{PO}_2^-$  group for the C-form of  $\text{poly}[\text{d(AG)}]\cdot\text{poly}[\text{d(CT)}]$  are about  $64^\circ$  and  $48^\circ$  for  $\theta_{\text{opo}}$  and  $\theta_{\text{oo}}$ , respectively. These angles are comparable with those reported values for C-DNA (Brahms et al., 1973; Pohle et al., 1984). The agreement of these conformational angles for  $\text{PO}_2^-$  groups with values reported by other groups indicates that we indeed observed  $\text{B}\rightarrow\text{A}$  or  $\text{B}\rightarrow\text{C}$  transitions for our synthetic polynucleotides and natural DNAs by decreasing the r.h.

Table 3.6. Conformational angles for Phosphodiester Backbone of DNA in Film Hydrated with H<sub>2</sub>O<sup>+</sup>.

DNA <sup>+</sup>	$\theta_{\infty}$ (deg)	$\theta_{\text{opo}}$ (deg)
poly[d(AC)]•poly[d(GT)] as B form	53.7±0.8	68.9±2.3
poly[d(AG)]•poly[d(CT)] as B form	54.5±1.6	63.2±1.7
<i>E. coli</i> DNA as B form	54.5±1.5	64.1±1.1
calf thymus DNA as B form	54.9±1.8	60.0±1.6
poly[d(AG)]•poly[d(CT)] as C form	47.9±0.7	65.5±2.9
poly[d(AC)]•poly[d(GT)] as A form	63.2±2.8	45.2±2.6
<i>E. coli</i> DNA as A form	64.5±2.1	44.6±3.5
calf thymus DNA as A form	64.2±1.7	48.2±0.5

\* The angles are averaged values calculated from dichroic ratio of ir bands from various experiments for DNA films with different degrees of orientation.

+ The B-, C-, and A-forms of DNA were obtained at 94%, 66%, and 75% r.h., respectively.



## **ACKNOWLEDGEMENTS**

We wish to thank Ping-Jung Chou for the use of his program to decompose IR data. We also wish to thank Dr. Christine Pastorek for her help to use FT-IR spectrophotometer. This research was supported by PHS grant number GM43133 from the Institute of General Medical Sciences.

## REFERENCES

- Adam, S., Liquier, J., Taboury, J. A., & Taillandier, E. (1986) *Biochemistry* **25**, 3220-3225.
- Ansevin, A. T. & Wang, A. H. (1990) *Nucleic Acids Res.* **18**, 6119-6126.
- Arrondo, J. L. R., Muga, A., Castresana, J., & Goni, F. M. (1993) *Prog. Biophys. Mol. Biol.* **59**, 23-56.
- Baret, J. F., Carbone, G. P., & Penon, P. (1978) *Biopolymers* **17**, 2319-2339.
- Bradbury, E. M., Price, W. C., & Wilkinson, G. R. (1961) *J. Mol. Biol.* **3**, 301-317.
- Brahms, J., Pilet, J., Lan, T. T. P., & Hill, L. R. (1973) *Proc. Natl. Acad. Sci. USA* **70**, 3352-3355.
- Bram, S. & Tougard, P. (1972) *Nature New Biol.* **239**, 128-131.
- Brown, K. M. & Dennis, J. E., Jr. (1972) *Numer. Math.* **18**, 289-297.
- Causley, G. C. & Johnson, W. C., Jr. (1982) *Biopolymers* **21**, 1763-1780.
- Charney, E., Chen, H. H., Henry, E. R., & Rau, D. C. (1986) *Biopolymers* **25**, 885-904.
- Charney, E. & Milstien, J. B. (1978) *Biopolymers* **17**, 1629-1655.
- Charney, E. & Yamaoka, K. (1982) *Biochemistry* **21**, 834-842.
- Cheng, J. W., Chou, S. H., Salazar, M., & Reid, B. R. (1992) *J. Mol. Biol.* **228**, 118-137.
- Chou, P. J. & Johnson, W. C., Jr. (1993) *J. Am. Chem. Soc.* **115**, 1205-1214.
- Clack, B. A. & Gray, D. M. (1992) *Biopolymers* **32**, 795-810.
- Dickerson, R. E. & Drew, H. (1981) *J. Mol. Biol.* **149**, 761-786.
- Dougherty, A. M., Causley, G. C., & Johnson, W. C., Jr. (1983) *Proc. Natl. Acad. Sci. USA* **80**, 2193-2195.
- Edmondson, S. P. (1987) *Biopolymers* **26**, 1941-1956.

- Edmondson, S. P. & Johnson, W. C., Jr. (1985a) *Biopolymers* **24**, 825-841.
- Edmondson, S. P. & Johnson, W. C., Jr. (1985b) *Biochemistry* **24**, 4802-4806.
- Edmondson, S. P. & Johnson, W. C., Jr. (1986) *Biopolymers* **25**, 2335-2348.
- Flemming, J., Pohle, W., & Weller, K. (1988) *Int. J. Biol. Macromol.* **10**, 248-254.
- Fraser, R. D. B. (1953) *J. Chem. Phys.* **21**, 1511-1515.
- Fritzsche, H., Lang, H., & Pohle, W. (1976) *Biochim. Biophys. Acta* **432**, 409-412.
- Fuller, W. & Wilkins, M. H. F. (1965) *J. Mol. Biol.* **12**, 60-80.
- Girod, J. C., Johnson, W. C., Jr., Huntington, S. K., & Maestre, M. F. (1973) *Biochemistry* **12**, 5092-5096.
- Hard, T. (1987) *Biopolymers* **26**, 613-618.
- Hogan, M., Dattagupta, N., & Crothers, D. M. (1978) *Proc. Natl. Acad. Sci. USA* **75**, 195-199.
- Howard, F. B., Frazier, J., & Miles, H. T. (1969) *Proc. Natl. Acad. Sci. USA* **64**, 451-458.
- Howard, F. B. & Miles, H. T. (1965) *J. Biol. Chem.* **240**, 801-805.
- Ivanov, V. I., Minchenkova, L. E., Schyolkina, A. K., & Poletayev, A. I. (1973) *Biopolymers* **12**, 89-110.
- Kang, H & Johnson, W. C., Jr. (1993) *Biopolymers* **33**, 245-253.
- Keller, P. B. & Hartman, K. A. (1986) *Spectrochim. Acta* **42A**, 299-306.
- Kursar, T. & Holzwarth, G. (1976) *Biochemistry* **15**, 3352-3357.
- Kyogoku, Y., Higuchi, S., & Tsuboi, M. (1967) *Spectrochim. Acta* **23A**, 969-983.
- Lamba, O. P., Borchman, D., Sinha, S. K., Shah, J., Renugopalakrishnan, V., & Yappert, M. C. (1993) *Biochim. Biophys. Acta* **1163**, 113-123.
- Leslie, A. G. W., Arnott, S., Chandrasekaran, R. & Ratliff, R. L. (1980)

- J. Mol. Biol.* **143**, 49-72.
- Levitt, M. (1978) *Proc. Natl. Acad. Sci. USA* **75**, 640-644.
- Liquier, J., Taillandier, E., Peticolas, W. L., & Thomas, G. A. (1990) *J. Biomol. Struct. Dyn.* **8**, 295-302.
- Loprete, D. M. & Hartman, K. A. (1989) *J. Biomol. Str. Dyn.* **7**, 347-362.
- Maddams, W. F. (1980) *Appl. Spectrosc.* **34**, 245-267.
- Marvin, D. A., Spencer, M., Wilkins, M. H. F., & Hamilton, L. D. (1961) *J. Mol. Biol.* **3**, 547-565.
- Miles, H. T. (1964) *Proc. Natl. Acad. Sci. U.S.A.* **51**, 1104-1109.
- Miles, H. T. & Frazier, J. (1964) *Biochem. Biophys. Res. Commun.* **14**, 21-28.
- Nibedita, R., Kumar, R. A., Majumdar, A., Hosur, R. V., & Govil, G. (1993) *Biochemistry* **32**, 9053-9064.
- Norden, B., Elvingson, C., Kubista, M., Sjogerg, B., Ryberg, H., Ryberg, M., Mortensen, K., & Takahashi, M. (1992) *J. Mol. Biol.* **226**, 1175-1191.
- Ovaska, M., Norden, B., & Matsuoka, Y. (1984) *Chem. Phys.Lett.* **109**, 412-415.
- Pilet, J., Blicharski, J., & Brahms, J. (1975) *Biochemistry* **14**, 1869-1876.
- Pilet, J. & Brahms, J. (1973) *Biopolymers* **12**, 387-403.
- Pitha, J. & Jones, R. N. (1966) *Can. J. Chem.* **44**, 3031-3050.
- Pitha, J. & Jones, R. N. (1967) *Can. J. Chem.* **45**, 2347-2352.
- Pohl, F. M. (1976) *Nature* **260**, 365-366.
- Pohle, W., Fritzsche, H., & Zhurkin, V. B. (1986) *Comments Mol. Cell. Biophys.* **3**, 179-194.
- Pohle, W., Zhurkin, V. B., & Fritzsche, H. (1984) *Biopolymers* **23**, 2603-2622.
- Rao, S. N., Singh, U. C., & Kollman, P. A. (1986) *Israel J. Chem.* **27**, 189-197.
- Rupprecht, A. & Forslind, B. (1970) *Biochim. Biophys. Acta.* **204**, 304-316.

- Sarai, A., Mazur, J., Nussinov, R., & Jernigan, R. L. (1988) *Biochemistry* **27**, 8498-8502.
- Schurr, J. M. & Fujimoto, B. S. (1988) *Biopolymers* **27**, 1543-1569.
- Sen, D., Mitra, S., & Crothers, D. M. (1986) *Biochemistry* **25**, 3441-3447.
- Singh, U. C., Weiner, S. J., & Kollman, P. (1985) *Proc. Natl. Acad. Sci. USA* **82**, 755-759.
- Srinivasan, J., Withka, J. M., & Beveridge, D. L. (1990) *Biophys. J.* **58**, 533-547.
- Surewicz, W. K., Mantsch, H. H., & Chapman, D. (1993) *Biochemistry* **32**, 389-394.
- Swaminathan, S., Ravishanker, G., & Beveridge, D. L. (1991) *J. Am. Chem. Soc.* **113**, 5027-5040.
- Taboury, J. A. & Taillandier, E. (1985) *Nucleic Acids Res.* **13**, 4469-4483.
- Taillandier, E. & Liquier, J. (1992) in *Methods in Enzymol.* vol. 211 (edited by Lilley, D. M. J. & Dahlberg, J. E.), pp. 307-335, Academic Press.
- Taillandier, E., Liquier, J., & Taboury, J. A. (1985) in *Adv. in Infrared and Raman Spectrosc.* vol. **12** (edited by Clark, R. J. H. & Hester, R. E.), pp. 65-114, Wiley Heyden.
- Taillandier, E., Taboury, J. A., Adam, S., & Liquier, J. (1984b) *Biochemistry* **23**, 5703-5706.
- Tsuboi, M. (1969) *Appl. Spectrosc. Rev.* **3**, 45-90.
- Tsuboi, M., Kyogoku, Y., & Shimanouchi, T. (1962) *Biochim. Biophys. Acta* **55**, 1-12.
- Tsuboi, M., Takahasi, S., & Harada, I. (1973) in *Physico-Chemical Properties of Nucleic Acids*, vol. 2 (edited by Duchesne, J.), pp. 92-145, Academic Press, New York, N.Y.
- van Amerongen, H., Kwa, S. L. S., & van Grondelle, R. (1990) *J. Mol. Biol.* **216**, 717-727.
- Zhurkin, V. B., Lysov, Y. P., & Ivanov, V. I. (1978) *Biopolymers* **17**, 377-412.

## SECTION IV

### CONCLUSIONS

1. Vacuum UV flow LD and a sophisticated algorithm, recently developed in our laboratory, provide specific inclination angles and axes of inclination for the four individual bases in the A- and B-forms of DNA in solution.

2. Flow LD demonstrates that the bases for poly[d(AC)]•poly[d(GT)] and poly[d(AG)]•poly[d(CT)] are inclined from perpendicular to the helix axis. The inclination angles are 20-25° for purines and 30-35° for pyrimidines in the B-form.

3. The inclinations are increased in the A-form, as expected. For the poly[d(AC)]•poly[d(GT)] and poly[d(AG)]•poly[d(CT)] the inclination angles are 25-30° for purines and 33-38° for pyrimidines.

4. For the films used in infrared LD measurements, B- and A-forms of poly[d(AC)]•poly[d(GT)], *E. coli* DNA, and calf thymus DNA are obtained at high (>94%) and low (75%) r.h., respectively. In contrast, for poly[d(AG)]•poly[d(CT)], B- and C-forms are obtained at high (>94%) and low (66%) r.h., respectively.

5. Infrared LD shows that the bases for B-DNA in films have sizable inclinations, which are comparable with those found in solution from UV LD. Poly[d(AG)]•poly[d(CT)] in the C-form has almost same inclinations as in B-DNA, and the inclinations are increased slightly for the A-form. The average minimum inclinations for B- and A-form of DNA in film are, respectively, 15-20° and 20-25°.

6. Conformational angles for the phosphodiester backbone geometry are determined by infrared LD measurements. The  $\theta_{\infty}$  angles for the A- and B-forms of synthetic polynucleotides and natural DNAs are  $64^{\circ}$  and  $55^{\circ}$ , respectively. The  $\theta_{\text{opo}}$  angles for A- and B-form are, respectively,  $45\text{--}48^{\circ}$  and  $61\text{--}68^{\circ}$ . For the C-DNA, the  $\theta_{\infty}$  and  $\theta_{\text{opo}}$  angles are about  $48^{\circ}$  and  $66^{\circ}$ .

## SECTION V

### BIBLIOGRAPHY

- Adam, S., Liquier, J., Taboury, J. A., & Taillandier, E. (1986) *Biochemistry* **25**, 3220-3225.
- Adnet, F., Liquier, J., Taillandier, E., Singh, M. P., Rao, K. E., & Lown, J. W. (1992) *J. Biomol. Struct. Dyn.* **10**, 565-575.
- Akhebat, A., Dagneaux, C., Liquier, J., & Taillandier, E. (1992) *J. Biomol. Struct. Dyn.* **10**, 577-588.
- Allen, F. S., Gray, D. M., & Ratliff, R. L. (1984) *Biopolymers* **23**, 2639-2659.
- Ansevin, A. T. & Wang, A. H. (1990) *Nucleic Acids Res.* **18**, 6119-6126.
- Antao, V. P., Gray, D. M., & Ratliff, R. L. (1988) *Nucleic Acids Res.* **16**, 719-738.
- Antao, V. P., Ratliff, R. L., & Gray, D. M. (1990) *Nucleic Acids Res.* **18**, 4111-4122.
- Arnott, S., Chandrasekaran, R., Birdsall, D. L., Leslie, A. G. W., & Ratliff, R. L. (1980) *Nature* **283**, 743-745.
- Arnott, S., Chandrasekaran, R., Hukins, D. W. L., Smith, P. J. C., & Watts, L. (1974) *J. Mol. Biol.* **88**, 523-533.
- Arnott, S., Chandrasekaran, R., Puijianer, L. C., Walker, J. K., Hall, I. H., & Birdsall, D. L. (1983) *Nucleic Acids Res.* **11**, 1457-1474.
- Arnott, S. & Hukins, D. W. L. (1972) *Biochem. Biophys. Res. Commun* **47**, 1504-1509.
- Arnott, S. & Hukins, D. W. L. (1973) *J. Mol. Biol.* **81**, 93-105.
- Arnott, S. & Selsing, E. (1974) *J. Mol. Biol.* **88**, 509-521.
- Arrondo, J. L. R., Muga, A., Castresana, J., & Goni, F. M. (1993) *Prog. Biophys. Mol. Biol.* **59**, 23-56.
- Baase, W. A. & Johnson, W. C., Jr. (1976) *Nucleic Acids Res.* **3**, 3123-3131.
- Baase, W. A. & Johnson, W. C., Jr. (1979) *Nucleic Acids Res.* **6**, 797-814.



- Baret, J. F., Carbone, G. P., & Penon, P. (1978) *Biopolymers* **17**, 2319-2339.
- Behling, R. W. & Kearns, D. R. (1986) *Biochemistry* **25**, 3335-3346.
- Bingman, C. A., Zon, G., & Sundaralingam, M. (1992) *J. Mol. Biol.* **227**, 738-756.
- Bokma, J. T., Johnson, W. C., Jr., & Blok, J. (1987) *Biopolymers* **26**, 893-909.
- Braaten, D. C., Thomas, J. R., Little, R. D., Dickson, K. R., Goldberg, I., Schlessinger, D., Ciccodicola, A., & D'Urso, M. (1988) *Nucleic Acids Res.* **16**, 865-881.
- Bradbury, E. M., Price, W. C., & Wilkinson, G. R. (1961) *J. Mol. Biol.* **3**, 301-317.
- Brahms, J., Maurizot, J. C. & Michelson, A. M. (1967) *J. Mol. Biol.* **25**, 481-495.
- Brahms, J., Pilet, J., Lan, T. T. P., & Hill, L. R. (1973) *Proc. Natl. Acad. Sci. USA* **70**, 3352-3355.
- Bram, S. & Tougaard, P. (1972) *Nature New Biol.* **239**, 128-131.
- Brown, K. M. & Dennis, J. E., Jr. (1972) *Numer. Math.* **18**, 289-297.
- Cantor, C. R. & Tinoco, I., Jr. (1965) *J. Mol. Biol.* **13**, 65-77.
- Catlin, J. T. & Guschlbauer, W. (1975) *Biopolymers* **14**, 51-72.
- Causley, G. C. & Johnson, W. C., Jr. (1982) *Biopolymers* **21**, 1763-1780.
- Causley, G. C., Staskus, P. W., & Johnson, W. C., Jr. (1983) *Biopolymers* **22**, 945-967.
- Chandrasekaran, R., Wang, M., He, R. G., Puigjaner, L. C., Byler, M. A., Millane, R. P., & Arnott, S. (1989) *J. Biomol. Struct. Dyn.* **6**, 1189-1202.
- Charney, E. & Chen, H. H. (1987) *Proc. Natl. Acad. Sci. USA* **84**, 1546-1549.
- Charney, E., Chen, H. H., Henry, E. R., & Rau, D. C. (1986) *Biopolymers* **25**, 885-904.
- Charney, E. & Milstien, J. B. (1978) *Biopolymers* **17**, 1629-1655.
- Charney, E. & Yamaoka, K. (1982) *Biochemistry* **21**, 834-842.

- Chen, H. H. & Clark, L. B. (1969) *J. Chem. Phys.* **51**, 1862-1871.
- Chen, H. H. & Clark, L. B. (1973) *J. Chem. Phys.* **58**, 2593-2603.
- Cheng, J. W., Chou, S. H., Salazar, M., & Reid, B. R. (1992) *J. Mol. Biol.* **228**, 118-137.
- Chou, P. J. & Johnson, W. C., Jr. (1993) *J. Am. Chem. Soc.* **115**, 1205-1214.
- Christophe, D., Cabrer, B., Bacolla, A., Targovnik, H., Pohl, V., & Vassart, G. (1985) *Nucleic Acids Res.* **13**, 5127-5144.
- Clark, L. B. (1977) *J. Am. Chem. Soc.* **99**, 3934-3938.
- Clark, L. B. (1986) *J. Am. Chem. Soc.* **108**, 5109-5113.
- Clark, L. B. (1989) *J. Phys. Chem.* **93**, 5345-5347.
- Clark, L. B. (1990) *J. Phys. Chem.* **94**, 2873-2879.
- Clark, B. A. & Gray, D. M. (1992) *Biopolymers* **32**, 795-810.
- Clore, G. M., Gronenborn, A. M., Moss, D. S., & Tickle, I. J. (1985) *J. Mol. Biol.* **185**, 219-226.
- Coll, M., Fita, I., Lloveras, J., Subirana, J. A, Bardella, F., Dinh, T. H., & Igolen, J. (1988) *Nucleic Acids Res.* **16**, 8695-8705.
- Dev, S. B. & Walters, L. (1990) *Biopolymers* **29**, 289-299.
- Devarajan, S. & Shafer, R. (1986) *Nucleic Acids Res.* **14**, 5099-5109.
- Dewey, T. G. & Turner, D. H. (1979) *Biochemistry* **18**, 5757-5762.
- Dewey, T. G. & Turner, D. H. (1980) *Biochemistry* **19**, 1681-1685.
- Dickerson, R. E. & Drew, H. (1981) *J. Mol. Biol.* **149**, 761-786.
- Dickerson, R. E., Drew, H. R., Conner, B. N., Wing, R. M., Fratini, A. V., & Kopka, M. L. (1982) *Science* **216**, 475-485.
- Digabriele, A. D., Sanderson, M. R., & Steitz, T. A. (1989) *Proc. Natl. Acad. Sci. USA* **86**, 1816-1820.

- Ding, D. W., Rill, R., & van Holde, K. E. (1972) *Biopolymers* **11**, 2109-2124.
- Dougherty, A. M., Causley, G. C. & Johnson, W. C., Jr. (1983) *Proc. Natl. Acad. Sci. USA* **80**, 2193-2195.
- Drew, H. R. & Dickerson, R. E. (1981a) *J. Mol. Biol.* **151**, 535-556.
- Drew, H. R. & Dickerson, R. E. (1981b) *J. Mol. Biol.* **152**, 723-736.
- Drew, H. R., Takano, T., Tanaka, S., Itakura, K., & Dickerson, R. E. (1980) *Nature* **286**, 567-573.
- Edmondson, S. P. (1987) *Biopolymers* **26**, 1941-1956.
- Edmondson, S. P. & Johnson, W. C., Jr. (1985a) *Biochemistry* **24**, 4802-4806.
- Edmondson, S. P. & Johnson, W. C., Jr. (1985b) *Biopolymers* **24**, 825-841.
- Edmondson, S. P. & Johnson, W. C., Jr. (1986) *Biopolymers* **25**, 2335-2348.
- Eriksson, M., Norden, B., & Eriksson, S. (1988) *Biochemistry* **27**, 8144-8151.
- Ezra, F. S., Lee, C. H., Kondo, N. S., Danyluk, S. S., & Sarma, R. H. (1977) *Biochemistry* **16**, 1977-1987.
- Falk, M., Hartman, K. A., & Lord, R. C. (1963) *J. Am. Chem. Soc.* **85**, 391-394.
- Flemming, J., Pohle, W., & Weller, K. (1988) *Int. J. Biol. Macromol.* **10**, 248-254.
- Forni, A., Moretti, I., Marconi, G., Mongelli, N., & Samori, B. (1989b) *Biopolymers* **28**, 2177-2194.
- Forni, A., Moretti, I., Torre, G., Marconi, G., & Samori, B. (1989a) *Biopolymers* **28**, 2161-2176.
- Fraser, R. D. B. (1953) *J. Chem. Phys.* **21**, 1511-1515.
- Fratini, A. V., Kopka, M. L., Drew, H. R., & Dickerson, R. E. (1982) *J. Biol. Chem.* **257**, 14686-14707.
- Frechet, D., Ehrlich, R., & Remy, P. (1979) *Nucleic Acids Res.* **7**, 1981-2001.
- Freier, S. M., Hill, K. O., Dewey, T. G., Marky, L. A., Breslauer, K. J. &

- Turner, D. H. (1981) *Biochemistry* **20**, 1419-1426.
- Fritzsche, H., Lang, H., & Pohle, W. (1976) *Biochim. Biophys. Acta* **432**, 409-412.
- Fuller, W. & Wilkins, M. H. F. (1965) *J. Mol. Biol.* **12**, 60-80.
- Geacintov, N. E., Ibanez, V., Rougee, M., & Bensasson, R. V. (1987) *Biochemistry* **26**, 3087-3092.
- Gessner, R. V., Frederick, C. A., Quigley, G. J., Rich, A., & Wang, A. H. J. (1989) *J. Biol. Chem.* **264**, 7921-7935.
- Girod, J. C., Johnson, W. C., Jr., Huntington, S. K., & Maestre, M. F. (1973) *Biochemistry* **12**, 5092-5096.
- Gray, D. M., Johnson, K. H., Vaughan, M. R., Morris, P. A., Sutherland, J. C., & Ratliff, R. L. (1990) *Biopolymers* **29**, 317-323.
- Gray, D. M., Ratliff, R. L., & Vaughan, M. R. (1992) in *Methods in Enzymol.* vol. **211** (edited by Lilley, D. M. J. & Dahlberg, J. E.), pp. 389-406, Academic Press.
- Gronenborn, A. M. & Clore, G. M. (1989) *Biochemistry* **28**, 5978-5984.
- Hamada, H. & Kakunaga, T. (1982) *Nature* **298**, 396-398.
- Hard, T. (1987) *Biopolymers* **26**, 613-618.
- Hare, D. R. & Reid, B. R. (1986) *Biochemistry* **25**, 5341-5350.
- Heinemann, U. & Alings, C. (1989) *J. Mol. Biol.* **210**, 369-381.
- Hogan, M., Dattagupta, N., & Crothers, D. M. (1978) *Proc. Natl. Acad. Sci. USA* **75**, 195-199.
- Howard, F. B., Frazier, J., & Miles, H. T. (1969) *Proc. Natl. Acad. Sci. USA* **64**, 451-458.
- Howard, F. B. & Miles, H. T. (1965) *J. Biol. Chem.* **240**, 801-805.
- Howard, F. B., Miles, H. T., Liu, K., Frazier, J., Raghunathan, G., & Sasisekharan, V. (1992) *Biochemistry* **31**, 10671-10677.

- Hug, W. & Tinoco, I., Jr. (1973) *J. Am. Chem. Soc.* **95**, 2803-2813.
- Ivanov, V. I., Minchenkova, L. E., Schyolkina, A. K., & Poletayev, A. I. (1973) *Biopolymers* **12**, 89-110.
- Jain, S., Zon, G., & Sundaralingam, M. (1991) *Biochemistry* **30**, 3567-3576.
- Johnson, W. C., Jr. (1988) in *Polarized Spectroscopy of Ordered Systems* vol. (edited by Samori, B. & Thulstrup, E. W.), pp. 167-183, Kluwer Academic Publishers.
- Johnston, B. H. (1992) in *Methods in Enzymol.* vol. **211** (edited by Lilley, D. M. J. & Dahlberg, J. E.), pp. 127-158, Academic Press, New York.
- Kan, L. S., Callahan, D. E., Trapane, T. L., Miller, P. S., Ts'o, P. O. P., & Huang, D. H. (1991) *J. Biomol. Struct. Dynam.* **8**, 911-933.
- Kang, H & Johnson, W. C., Jr. (1993) *Biopolymers* **33**, 245-253.
- Keller, P. B. & Hartman, K. A. (1986) *Spectrochim. Acta* **42A**, 299-306.
- Kondo, N. S. & Danyluk, S. S. (1976) *Biochemistry* **15**, 756-768.
- Kursar, T. & Holzwarth, G. (1976) *Biochemistry* **15**, 3352-3357.
- Kwiatkowski, J. S. (1968) *Ther. Chim. Acta* **10**, 47-64.
- Kyogoku, Y., Higuchi, S., & Tsuboi, M. (1967) *Spectrochim. Acta* **23A**, 969-983.
- Lamba, O. P., Borchman, D., Sinha, S. K., Shah, J., RenuGOPalakrishnan, V., & Yappert, M. C. (1993) *Biochim. Biophys. Acta* **1163**, 113-123.
- Larsen, T. A., Kopka, M. L., & Dickerson, R. E. (1991) *Biochemistry* **30**, 4443-4449.
- Lee, C. H. & Charney, E. (1982) *J. Mol. Biol.* **161**, 289-303.
- Lee, C. H., Ezra, F. S., Kondo, N. S., Sarma, R. H., & Danyluk, S. S. (1976) *Biochemistry* **15**, 3627-3639.
- Leslie, A. G. W., Arnott, S., Chandrasekaran, R., & Ratliff, R. L. (1980) *J. Mol. Biol.* **143**, 49-72.
- Levitt, M. (1978) *Proc. Natl. Acad. Sci. USA* **75**, 640-644.

- Liquier, J., Coffinier, P., Firon, M., & Taillandier, E. (1991) *J. Biomol. Struct. Dyn.* **9**, 437-445.
- Liquier, J., Gadenne, M. C., Taillandier, E., Defer, N., Favatier, F., & Kruh, J. (1979) *Nucleic Acids Res.* **6**, 1479-1493.
- Liquier, J., Lafaix, M. P., Taillandier, E., & Brahms, J. (1975) *Biochemistry* **14**, 4191-4197.
- Liquier, J., Mchami, A., & Taillandier, E. (1989) *J. Biomol. Struct. Dyn.* **7**, 119-126.
- Liquier, J., Taillandier, E., Peticolas, W. L., & Thomas, G. A. (1990) *J. Biomol. Struct. Dyn.* **8**, 295-302.
- Loprete, D. M. & Hartman, K. A. (1989) *J. Biomol. Str. Dyn.* **7**, 347-362.
- Lowe, M. J. & Schellman, J. A. (1972) *J. Mol. Biol.* **65**, 91-109.
- Lyamichev, V. I., Mirkin, S. M., & Frank-Kamenetskii, M. D. (1985) *J. Biomol. Struct. Dyn.* **3**, 327-338.
- Maddams, W. F. (1980) *Appl. Spectrosc.* **34**, 245-267.
- Marvin, D. A., Spencer, M., Wilkins, M. H. F., & Hamilton, L. D. (1961) *J. Mol. Biol.* **3**, 547-565.
- Matsuoka, Y. & Norden, B. (1982a) *J. Phys. Chem.* **86**, 1378-1386.
- Matsuoka, Y. & Norden, B. (1982b) *Biopolymers* **21**, 2433-2452.
- Matsuoka, Y. & Norden, B. (1983) *Biopolymers* **22**, 1731-1746.
- Miles, H. T. (1964) *Proc. Natl. Acad. Sci. USA* **51**, 1104-1109.
- Miles, H. T. & Frazier, J. (1964) *Biochem. Biophys. Res. Commun.* **14**, 21-28.
- Mirau, P. A., Behling, R. W., & Kearns, D. R. (1985) *Biochemistry* **24**, 6200-6211.
- Mirau, P. A. & Kearns, D. R. (1984) *Biochemistry* **23**, 5439-5446.
- Mohr, S. C., Sokolov, N. V. H. A., He, C., & Setlow, P. (1991) *Proc. Natl. Acad. Sci. USA* **88**, 77-81.

- Munt, N. A., Granot, J., Behling, R. W., & Kearns, D. R. (1984) *Biochemistry* **23**, 944-955.
- Narayana, N., Ginell, S. L., Russu, I. M., & Berman, H. M. (1991) *Biochemistry* **30**, 4449-4455.
- Nerdal, W., Hare, D. R., & Reid, B. R. (1988) *J. Mol. Biol.* **201**, 717-739.
- Nibedita, R., Kumar, R. A., Majumdar, A., Hosur, R. V., Govil, G., Majumder, K., & Chauhan, V. S. (1993) *Biochemistry* **32**, 9053-9064.
- Nilges, M., Clore, G. M., Gronenborn, A. M., Piel, N., & McLaughlin, L. W. (1987) *Biochemistry* **26**, 3734-3744.
- Nilsson, L., Clore, G. M., Gronenborn, A. M., Brunger, A. T., & Karplus, M. (1986) *J. Mol. Biol.* **188**, 455-475.
- Noble, B. & Daniel, J. W. (1977) *Applied Linear Algebra*, Prentice-Hall, Englewood Cliffs, NJ.
- Norden, B. (1978) *Appl. Spectrosc. Rev.* **14**, 157-248.
- Norden, B., Elvingson, C., Eriksson, T., Kubista, M., Sjoberg, B., Takahashi, M., & Mortensen, K. (1990) *J. Mol. Biol.* **216**, 223-228.
- Norden, B., Elvingson, C., Kubista, M., Sjoberg, B., Ryberg, H., Ryberg, M., Mortensen, K., & Takahashi, M. (1992b) *J. Mol. Biol.* **226**, 1175-1191.
- Norden, B., Kubista, M., & Kurucsev, T. (1992a) *Quart. Rev. Biophys.* **25**, 51-170.
- Norden, B. & Seth, S. (1985) *Appl. Spectrosc.* **39**, 647-655.
- Novros, J. S. & Clark, L. B. (1986) *J. Phys. Chem.* **90**, 5666-5668.
- Olsthorn, C. S. M., Bostelaar, L. J., de Rooij, J. F. M., van Boom, J. H., & Altona, C. (1981) *Eur. J. Biochem.* **115**, 309-321.
- Olsthorn, C. S. M., Doornbos, J., de Leeuw, H. P. M., & Altona, C. (1982) *Eur. J. Biochem.* **125**, 367-382.
- Olsthorn, C. S. M., Haasnoot, C. A. G., & Altona, C. (1980) *Eur. J. Biochem.* **106**, 85-95.
- Ovaska, M., Norden, B., & Matsuoka, Y. (1984) *Chem. Phys. Lett.* **109**, 412-415.

- Pardue, M. L., Lowenhaupt, K., Rich, A., & Nordheim, A. (1987) *EMBO J.* **6**, 1781-1789.
- Pilet, J., Blicharski, J., & Brahms, J. (1975) *Biochemistry* **14**, 1869-1876.
- Pilet, J. & Brahms, J. (1973) *Biopolymers* **12**, 387-403.
- Pitha, J. & Jones, R. N. (1966) *Can. J. Chem.* **44**, 3031-3050.
- Pitha, J. & Jones, R. N. (1967) *Can. J. Chem.* **45**, 2347-2352.
- Pohl, F. M. (1976) *Nature* **260**, 365-366.
- Pohle, W., Bohl, M., Flemming, J., & Bohlig, H. (1990) *Biophys. Chem.* **35**, 213-226.
- Pohle, W. & Fritzsche, H. (1990) *J. Mol. Struct.* **219**, 341-346.
- Pohle, W., Fritzsche, H., & Zhurkin, V. B. (1986) *Comments Mol. Cell. Biophys.* **3**, 179-194.
- Pohle, W., Zhurkin, V. B., & Fritzsche, H. (1984) *Biopolymers* **23**, 2603-2622.
- Powell, J. T., Richards, E. G., & Gratzer, W. B. (1972) *Biopolymers* **11**, 235-250.
- Premilat, S. & Albiser, G. (1983) *Nucleic Acids Res.* **11**, 1897-1908.
- Pulleyblank, D. E., Haniford, D. B., & Morgan, A. R. (1985) *Cell* **42**, 271-280.
- Rao, S. N., Singh, U. C., & Kollman, P. A. (1986) *Israel J. Chem.* **27**, 189-197.
- Riazance, J. H., Johnson, W. C., Jr., McIntosh, L. P., & Jovin, T. M. (1987) *Nucleic Acids Res.* **15**, 7627-7636.
- Rill, R. L. (1972) *Biopolymers* **11**, 1929-1941.
- Rupprecht, A. & Forslind, B. (1970) *Biochim. Biophys. Acta.* **204**, 304-316.
- Saenger, W., Hunter, W. N., & Kennard, O. (1986) *Nature* **324**, 385-388.
- Sarai, A., Mazur, J., Nussinov, R., & Jernigan, R. L. (1988) *Biochemistry* **27**, 8498-8502.
- Schneider, B., Ginell, S. L., Jones, R., Gaffney, B., & Berman, H. M. (1992)



*Biochemistry* **31**, 9622-9628.

Schurr, J. M. & Fujimoto, B. S. (1988) *Biopolymers* **27**, 1543-1569.

Sen, D., Mitra, S., & Crothers, D. M. (1986) *Biochemistry* **25**, 3441-3447.

Siano, D. B. (1972) *J. Chem. Educ.* **49**, 755-757.

Siano, D. B. & Metzler, D. E. (1969) *J. Chem. Phys.* **51**, 1856-1861.

Singh, U. C., Weiner, S. J., & Kollman, P. A. (1985) *Proc. Natl. Acad. Sci. USA* **82**, 755-759.

Sprecher, C. A., Baase, W. A., & Johnson, W. C., Jr. (1979) *Biopolymers* **18**, 1009-1019.

Srinivasan, J., Withka, J. M., & Beveridge, D. L. (1990) *Biophys. J.* **58**, 533-547.

Surewicz, W. K., Mantsch, H. H., & Chapman, D. (1993) *Biochemistry* **32**, 389-394.

Swaminathan, S., Ravishanker, G., & Beveridge, D. L. (1991) *J. Am. Chem. Soc.* **113**, 5027-5040.

Swenberg, C. E., Carberry, S. E., & Geacintov, N. E. (1990) *Biopolymers* **29**, 1735-1744.

Taboury, J. A. & Taillandier, E. (1985) *Nucleic Acids Res.* **13**, 4469-4483.

Taillandier, E., Fort, L., Liquier, J., Couppez, M., & Sautiere, P. (1984a) *Biochemistry* **23**, 2644-2650.

Taillandier, E. & Liquier, J. (1992) in *Methods in Enzymol.* vol. **211** (edited by Lilley, D. M. & Dahlberg, J. E.), pp. 307-335, Academic Press, New York.

Taillandier, E., Liquier, J., & Taboury, J. A. (1985) in *Adv. in Infrared and Raman Spectrosc.* vol. **12** (edited by Clark, R. J. H. & Hester, R. E.), pp. 65-114, Wiley Heyden.

Taillandier, E., Taboury, J. A., Adam, S., & Liquier, J. (1984b) *Biochemistry* **23**, 5703-5706.

Tsuboi, M. (1969) *Appl. Spectrosc. Rev.* **3**, 45-90.

- Tsuboi, M., Kyogoku, Y., & Shimanouchi, T. (1962) *Biochim. Biophys. Acta* **55**, 1-12.
- Tsuboi, M., Takahasi, S., & Harada, I. (1973) in *Physico-Chemical Properties of Nucleic Acids*, vol. 2 (edited by Duchesne, J.), pp. 92-145, Academic Press, New York.
- van Amerongen, H., Kuil, M. E., van Mourik, F., & van Grondelle, R. (1988) *J. Mol. Biol.* **204**, 397-405.
- van Amerongen, H., Kwa, S. L. S., & van Grondelle, R. (1990) *J Mol. Biol.* **216**, 717-727.
- van Amerongen, H. & van Grondelle, R. (1989) *J. Mol. Biol.* **209**, 433-445.
- Vournakis, J. N., Poland, D., & Scheraga, H. A. (1967) *Biopolymers* **5**, 103-122.
- Wada, A. (1972) *Appl. Spectrosc. Rev.* **6**, 1-30.
- Wang, A. H. J., Quigley, G. J., Kolpak, F. K., Crawford, J. L., van Boom, J. H., van der Marel, G., & Rich, A. (1979) *Nature* **282**, 680-686.
- Warshaw, M. M. & Cantor, C. R. (1970) *Biopolymers* **9**, 1079-1103.
- Watson, J. D. & Crick, F. H. C. (1953) *Nature* **171**, 737-738.
- Woisard, A. & Fazakerley, G. V. (1986) *Biochemistry* **25**, 2672-2676.
- Wu, H. M., Dattagupta, N., & Crothers, D. M. (1981) *Proc. Natl. Acad. Sci. USA* **78**, 6808-6811.
- Yamaoka, K. & Charney, E. (1973) *Macromolecules* **6**, 66-76.
- Yamaoka, K. & Matsuda, K. (1981) *Macromolecules* **14**, 595-601.
- Yuan, H., Quintana, J., & Dickerson, R. E. (1992) *Biochemistry* **31**, 8009-8021.
- Zaloudek, F., Novros, J. S., & Clark, L. B. (1985) *J. Am. Chem. Soc.* **107**, 7344-7351.
- Zhong, L. & Johnson, W. C., Jr. (1990) *Biopolymers* **30**, 821-828.
- Zhurkin, V. B., Lysov, Y. P., & Ivanov, V. I. (1978) *Biopolymers* **17**, 377-412.

## **APPENDIX**

**Stacking Interactions of ApA Analogues  
with Modified Backbones**

**Hunseung Kang<sup>1</sup>, Ping-Jung Chou<sup>1</sup>, W. Curtis Johnson, Jr.<sup>1</sup>,  
Dwight Weller<sup>2</sup>, Sung-Ben Huang<sup>3</sup>, and James E. Summerton<sup>3</sup>**

<sup>1</sup>Department of Biochemistry and Biophysics, and <sup>2</sup>Department of  
Chemistry, Oregon State University, Corvallis, OR 97331;  
and <sup>3</sup>Summerton Antivirals Inc., 249 SW Avery Lane,  
Corvallis, OR 97333.

Published in *Biopolymers* (1992) **32**, 1351-1363

## ABSTRACT

CD spectra have been measured as a function of temperature for a number of ApA analogues with modified backbones. Oligonucleotides with these modified backbones are being used as antisense agents having potential as viral therapeutics. Results of these studies show that when a carbonyl is substituted for the phosphate to produce an uncharged backbone, the analogues that have either sugar or morpholino substitution do not stack. In contrast, when a morpholino group is substituted for the sugar and the phosphate is modified so as to be uncharged, there is strong base stacking. Stacking interaction in the phosphorus-linked morpholino analogues are at least as strong as those found in d(ApA). The stacking interactions in ApA are weak by comparison. Singular value decomposition demonstrates that the stacking is two state, and Taylor series decomposition yields a coefficient that measures base stacking interactions. The van't Hoff equation is applied to the base stacking coefficient from the Taylor series fitting to give thermodynamics parameters.

## INTRODUCTION

The unique base-base stacking interaction of polynucleotides to form a single helix is known to be one of the major driving forces in the formation of stable three-dimensional structures of RNA and DNA, and plays significant roles in various stages of gene expression. However, to get the complete conformational properties of polymers, the stacking interaction must be investigated in detail in simple model compounds because of the complexity of large biological molecules. For these reasons the conformational analysis of simple model compounds such as dinucleoside and trinucleoside phosphates has received a great deal of attention (Cantor & Tinoco, 1965; Vournakis et al., 1967; Brahms et al., 1967; Warshaw & Cantor, 1970; Lowe & Schellman, 1972; Powell et al., 1972). All of these papers studied the geometry and the thermodynamics of the stacking interaction by means of optical methods, such as UV absorption, optical rotatory dispersion, and CD. Besides these optical methods, nmr (Lee et al., 1976; Kondo & Danyluk, 1976; Ezra et al., 1977; Olsthoorn et al., 1982) and the Raman laser temperature-jump technique (Dewey & Turner, 1979, 1980; Freier et al., 1981) have also been used to get information about the backbone geometry of dinucleoside or trinucleoside phosphates, or to measure the kinetics and conformational dynamics of the single-strand stacking process.

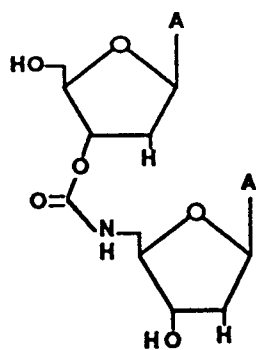
Many dimers and trimers that have some modifications in the bases, as well as those compounds with standard bases and sugar-phosphate backbone structure, have been investigated to get structural information about the stacked and unstacked conformations. In particular, CD spectra measured as a function of temperature yield thermodynamic parameters of the stacking interaction, and hence are a valuable measure of the properties of dimer and trimer molecules that exist in a stacked conformation at any temperature (Lowe & Schellman, 1972; Powell et al., 1972; Olsthoorn et al., 1980). This accurate knowledge of the thermodynamics of the intramolecular stacking equilibrium is a prerequisite

for a meaningful interpretation of the nmr spin-spin coupling constants and chemical shifts in terms of structural information about stacked and unstacked conformations.

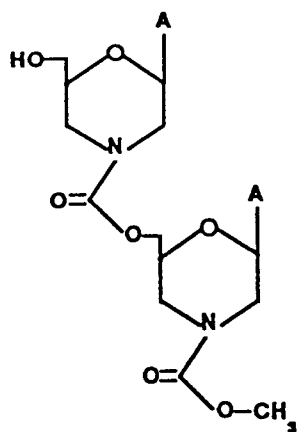
In this paper we examine the temperature dependence of the CD for dimers that have an unusual backbone structure, as shown in Figure 4.1, which also defines the Roman numerals used to symbolize the dimers. A star indicates an asymmetric center at the phosphorus, and the two stereoisomers were separated on a silica gel. The absolute configuration of the stereoisomers has not been determined, and they are denoted by their relative speed on the silica gel (fast or slow). We investigate the effect of backbone structure on stacking interaction and obtain thermodynamic parameters that describe the stacking-unstacking process. The unusual dimers studied here are being tested as model compounds related to antisense agents designed to inhibit the activity of target viruses by blocking the translation and other genetic processes. The structural information about dimer stacking reported here will provide important clues for designing different types of antisense agents.

Figure 4.1. Structures of the ApA analogues and their constituent monomers studied, showing the morpholino moiety and different linkage variations. A star indicates an asymmetric phosphorus.

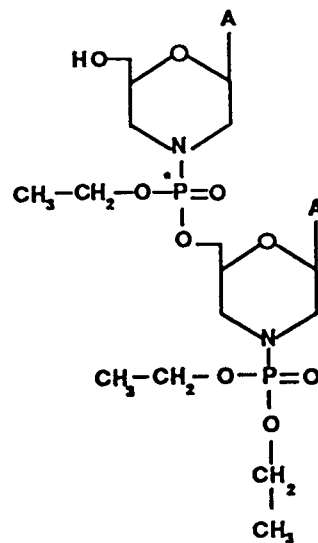




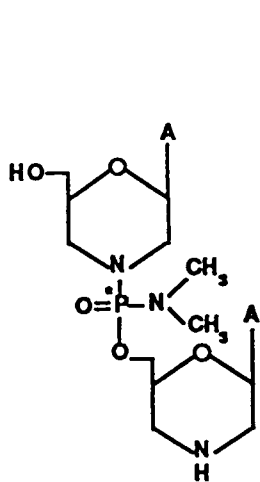
(I)



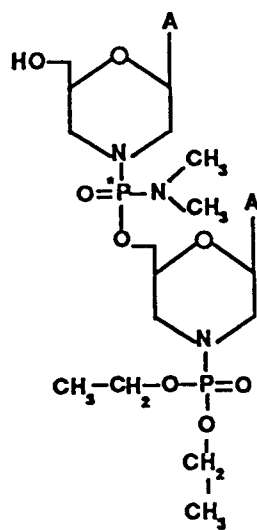
(II)



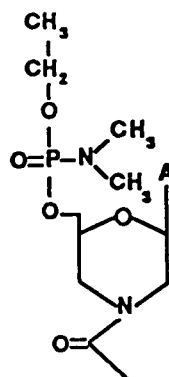
(III)



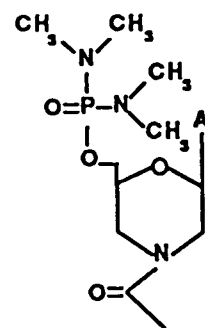
(IV)



(V)



(VI)



(VII)

Figure 4.1

## MATERIALS AND METHODS

**Materials:** ApA and d(ApA) were purchased from a Sigma, and used without further purification. All other ApA analogues and their constituent monomers were synthesized by Antiviral Inc. (Corvallis, OR). Structures are shown in Figure 4.1. All samples were dissolved in 10 mM sodium phosphate buffer, pH 7.0, at a concentration of approximately 0.1 mM in base. Concentrations were determined spectrophotometrically by assuming that the extinction coefficient of ApA analogues is the same as that of d(ApA):  $\epsilon = 12,800 \text{ M}^{-1} \text{ cm}^{-1} \text{ base}^{-1}$ .

**Spectroscopic Measurements:** All measurements were performed in 1-mm cylindrical quartz cells (Hellma). Absorption spectra were recorded on a Cary 15 spectrophotometer at ambient temperature (about 20 °C). CD spectra were measured on a Jasco J-40 CD spectrograph, which was calibrated with (+)-10-camphosulfonic acid (Aldrich) assuming  $\Delta\epsilon(290.5) = +2.37$  and  $\Delta\epsilon(192.5) = -4.9$ . The recorded spectra were digitized at 0.5-nm resolution using a PC computer. Cell temperature was regulated to 0.2 °C with a thermoelectric temperature controller. The temperature of the solution was measured in the cell with a thermistor (YSI 423, VWR Scientific). For each dimer about 10 CD spectra were recorded over the temperature range of 2 - 90 °C. Monomer CD spectra were recorded at three different temperatures (5, 25, and 90 °C). After recording a series of CD spectra, the uv absorption spectrum monitored the concentration of the sample. CD spectra were smoothed with a cubic spline algorithm.

**Singular Value Decomposition:** To investigate the number of species in equilibrium during temperature variation, singular value decomposition (SVD) was applied to an  $m \times n$  data matrix  $\mathbf{Q}$  containing the set of CD spectra, where  $m$  indexes the wavelength and  $n$  indexes the CD curves recorded as a function

of temperature. SVD decomposed this matrix as  $\mathbf{Q} = \mathbf{USV}^T$ , where  $\mathbf{U}$  and  $\mathbf{V}$  are in theory unitary  $m \times m$  and  $n \times n$  matrices, respectively (Noble & Daniel, 1977). In practice  $\mathbf{U}$  is computed as an  $m \times n$  matrix of orthonormal basis vectors.  $\mathbf{S}$  is computed as an  $n \times n$  matrix containing nonzero elements only on the main diagonal; these elements,  $s_i$ , are the singular values of  $\mathbf{Q}$ . The  $n$  rows of  $\mathbf{V}$  are the least-square coefficients for reconstituting the original data from  $\mathbf{U}$  and  $\mathbf{S}$ . The number of significant singular values in  $\mathbf{S}$  is the number of independent components, which corresponds to the number of detectable chemical species present in equilibrium.

**Taylor Series Analysis** : In order to obtain physical information about stacking interactions, measured CD curves for each dimer as a function of frequency  $\nu$  were fitted to a Taylor series expansion in the monomer absorption curve  $\epsilon_m$

$$\Delta\epsilon(\nu) = A \epsilon_m(\nu) + B \left[ \frac{d\epsilon_m(\nu)}{d\nu} - \frac{\epsilon_m(\nu)}{\nu} \right]$$

to investigate the degenerate and nondegenerate interactions of the bases in the dinucleotide. The basic theory and practical details are described by Causley et al. (1983).

The coefficient  $B$  determined from Taylor series fitting depends only on base stacking. The two-state (stacking-unstacking) equilibrium model was applied to the temperature dependence of the Taylor coefficient  $B$  to calculate thermodynamic parameters by using the van't Hoff equation (Powell et al., 1972) :

$$B(T) = B_{un} + (B_{st} - B_{un}) / [ 1 + \exp(\Delta H^\circ / RT - \Delta S^\circ / R)]$$

Using  $B(T)$ , rather than the variation of  $\Delta\epsilon$  with temperature at some wavelength, has two advantages. First, the parameter  $B(T)$  monitors the change in  $\Delta\epsilon$  with temperature at all wavelengths considered. Second, in theory  $B_{un}$  is zero, so we need only solve for three parameters instead of four. In previous work where we had data that allowed solving for all four parameters,  $B_{un}$  was indeed found to be essentially zero (Causley et al., 1983). This becomes especially important in the present work where most of the melting data is linear with no hint of curvature toward the maximum  $B_{st}$  or the minimum  $B_{un}$ . Catlin & Guschlbauer (1975) had difficulty analyzing even their highly accurate CD spectra for the four parameters in the van't Hoff when the dimer gave linear melting data. Here we show that by reducing the problem to three parameters and by using modern fitting methods, it is possible to obtain results with a low standard deviation for linear melting data.

**Fitting the Melting Data :** We transform the van't Hoff equation in the traditional way as

$$R \ln \left[ \frac{B_{st}}{B(T)} - 1 \right] = -\Delta S^\circ + \frac{\Delta H^\circ}{T}$$

We could use the best fit to the melting data as the criterion to solve for  $\Delta H^\circ$ ,  $\Delta S^\circ$ , and  $B_{st}$  simultaneously. However, the data are imperfect, and rather than fit it perfectly, it is more rational to monitor the significance of the parameters we desire ( $\Delta H^\circ$  and  $\Delta S^\circ$ ) as a function of  $B_{st}$ . Further, for a given  $B_{st}$  we can use linear regression, rather than nonlinear regression, to solve for  $\Delta H^\circ$  and  $\Delta S^\circ$  with the transformed equation. The accuracy of the fitting was monitored by calculating the sum of square error (SSQ) for the difference between the calculated and observed  $B(T)$ , and the correlation coefficient of the transformed

function  $R^2$ . The significance of  $\Delta H^\circ$  and  $\Delta S^\circ$  is given by their magnitude divided by their standard deviation for a given fit, here called  $t$ .

Figure 4.2 shows how  $\Delta H^\circ$  and  $\Delta S^\circ$  and their significance, calculated from the data for ApA, vary with  $B_{st}$ . It is easy to see that the maximum magnitude for the significance occurs at a  $B_{st}$  of 4.71. This corresponds to low but not minimum values for SSQ and  $R^2$  (Figure 4.2). Further, extrema for SSQ and  $R^2$  are not as sharp as for  $t_{\Delta H}$  and  $t_{\Delta S}$ .

Figure 4.2. Variance of (a)  $R^2$  (——) and SSQ (---), and (b)  $\Delta S^\circ$  (——),  $\Delta H^\circ$  (....),  $t_{\Delta S}$  (---), and  $t_{\Delta H}$  (— — —) as a function of  $B_{st}$  on fitting  $B(T)$  for ApA to the van't Hoff equation.

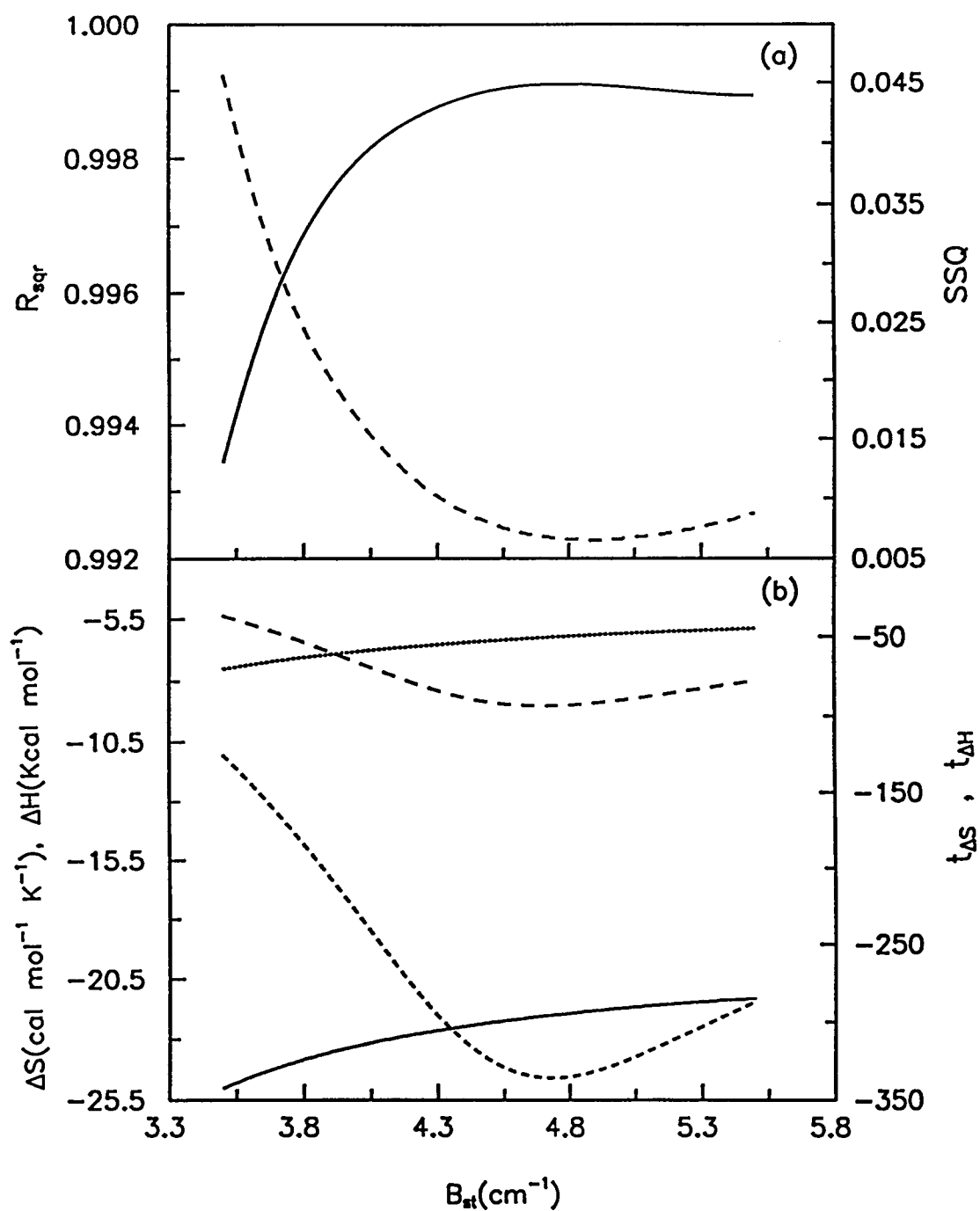


Figure 4.2

## RESULTS AND DISCUSSION

**Effect of Backbone Structure on CD :** The CD spectra of these ApA analogues at different temperatures are shown in Figures 4.3-4.6. For the sake of clarity, only a representative set of experimental spectra is shown, whereas the calculations were carried out on the complete set of data.

All dimers except the carbonyl-linked I and II show large exciton effects due to degenerate interaction from stacked bases. Splitting of the degeneracies through Coulombic interactions between the monomers yields a conservative CD that looks like the derivative of the absorption. The CD vs temperature profiles (Figures 4.3-4.6) clearly represent different CD intensities and shapes in the measured spectra. These results indicate that the nature of dimer stacking can be affected solely by the backbone structure. In these sets of spectra excellent isodichroic points are observed, which indicates that each spectrum may be represented as a linear combination of only two basis spectra. This in turn suggests that two-state model may be used to describe the stacking - unstacking equilibrium process for these dimers. We will confirm this phenomenon later with further analysis of the data.

Figures 4.5 and 4.6 also show that the CD spectra of the carbonyl-linked dimers is similar to the spectra of the constituent monomers; the monomer spectra of VI and VII appear to be a useful estimate for the CD properties of the unstacked state. Thus we see for I and II (Figures 4.3 and 4.4) that there is no significant base-base interaction present in the carbonyl-linked dimers; they are always unstacked. The discrepancy in the CD spectrum between unstacked dimer and monomer at shorter wavelength indicates that the unstacked dimer prefers to adopt one or more conformations that give interactions not present in the constituent monomers.



**Figure 4.3. Representative CD spectra of ApA, d(ApA), and dimer I in 10 mM sodium phosphate buffer, pH 7.0, between 2 and 90°C.**

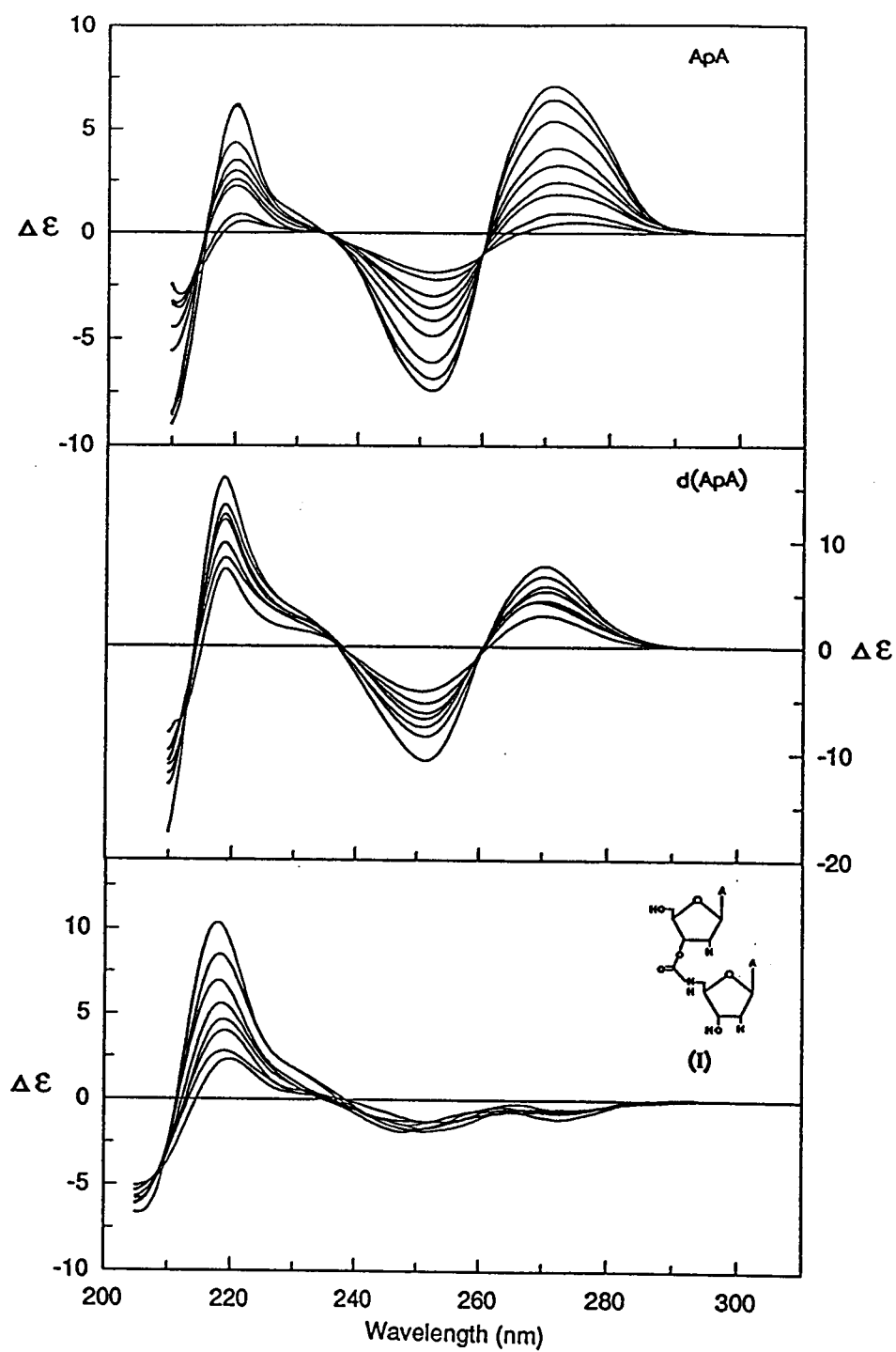


Figure 4.3

Figure 4.4. Representative CD spectra of dimer II, III-fast, and III-slow in 10 mM sodium phosphate buffer, pH 7.0, between 2 and 90°C.

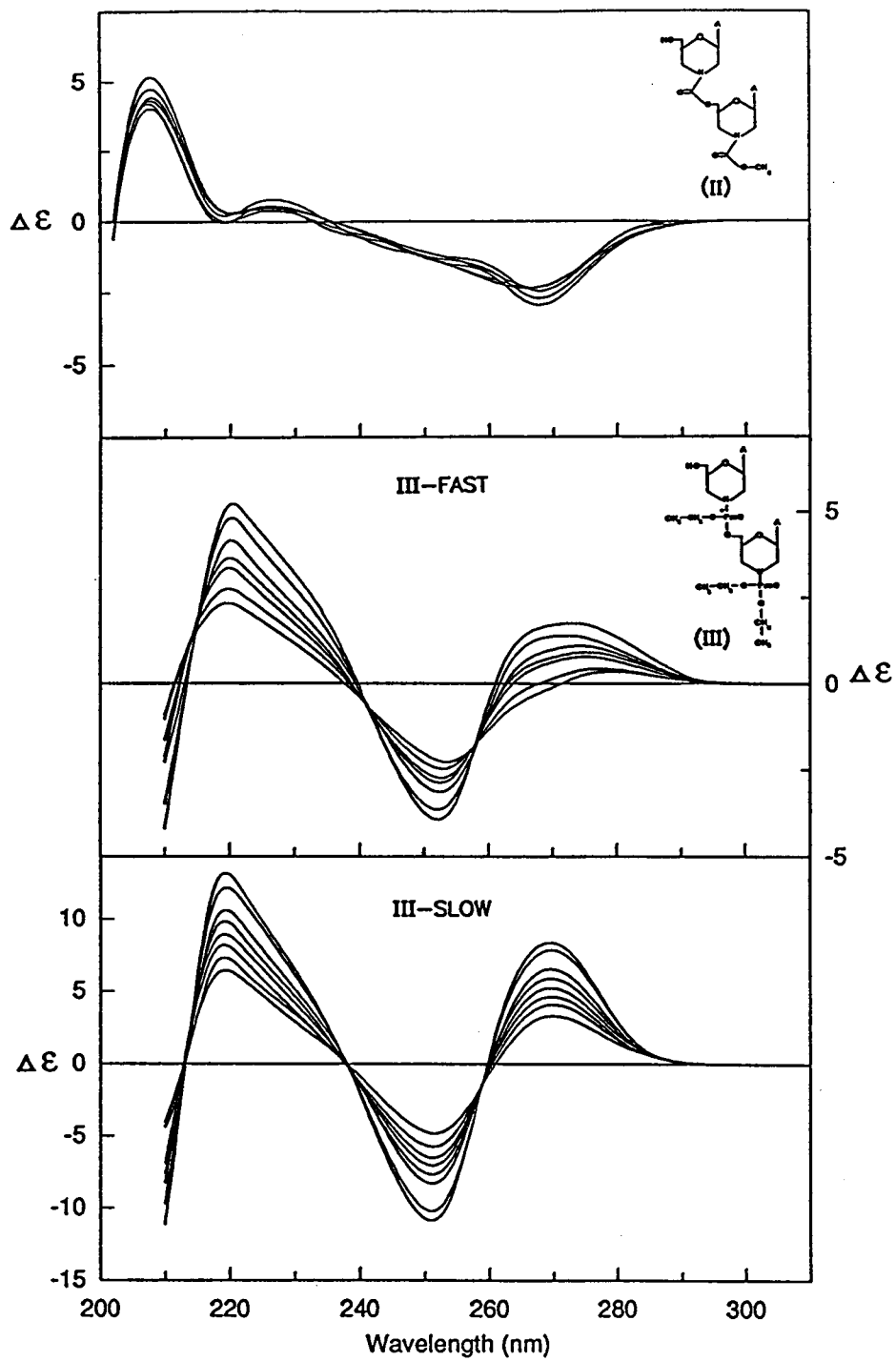


Figure 4.4

Figure 4.5. Representative CD spectra of monomer VI, and dimers IV-fast and IV-slow in 10 mM sodium phosphate buffer, pH 7.0, between 5 and 90 °C.

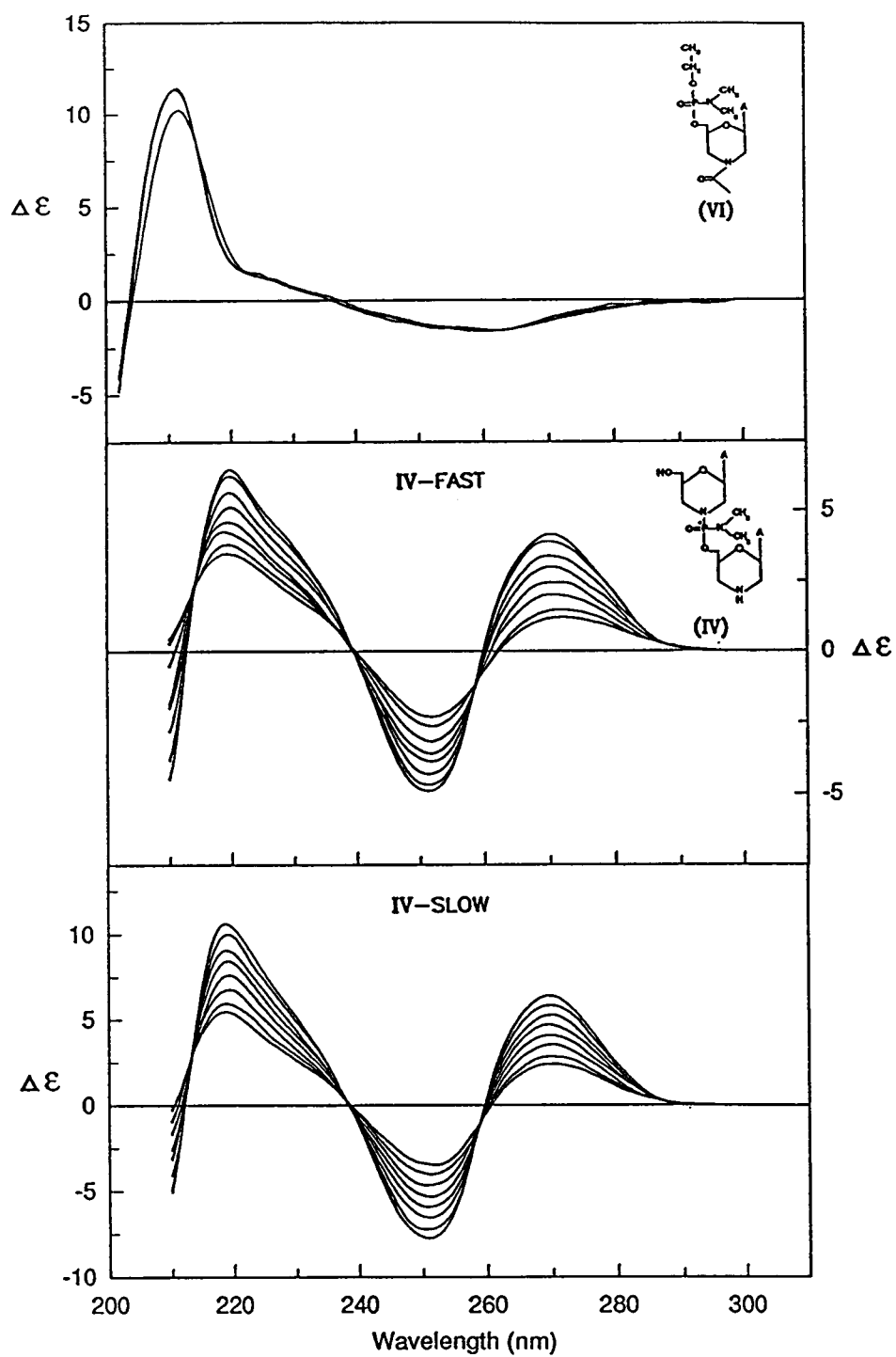


Figure 4.5

Figure 4.6. Representative CD spectra of monomer VII, and dimers V-fast and V-slow in 10 mM sodium phosphate buffer, pH 7.0, between 5 and 85 °C.

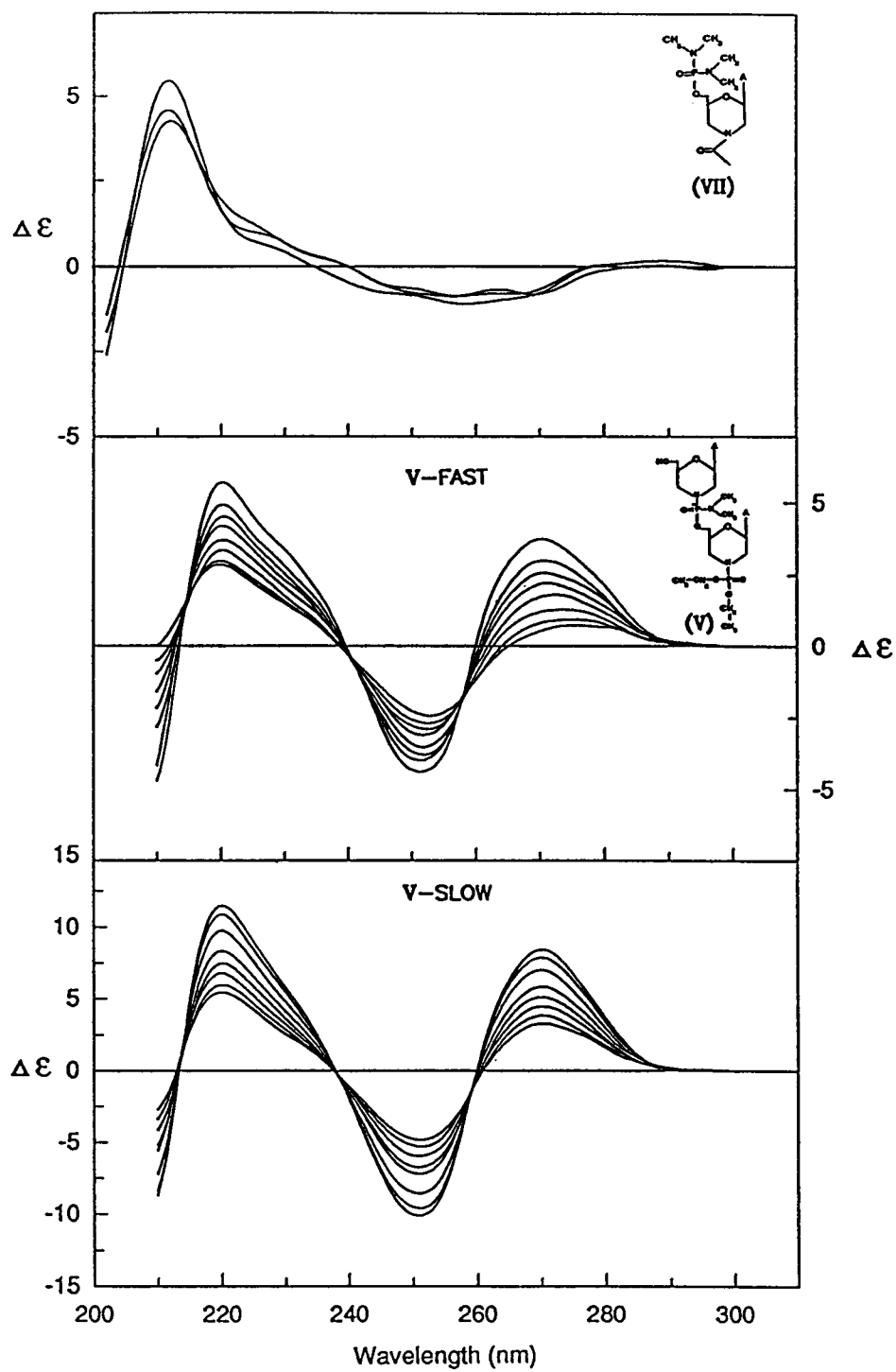


Figure 4.6



**SVD and Taylor Series Fitting** : To determine the number of significant components in equilibrium, each set of CD spectra was analyzed through SVD. We produced temperature basis vectors ( $\mathbf{SV}^T$ ) and wavelength basis vectors ( $\mathbf{US}$ ) for the stacked and unstacked dimers to visualize the number of significant components for the stacking process, some of which are shown in Figures 4.7 and 4.8.

It is obvious that only two of these curves contribute significantly to the computed basis set. For some dimers tested, the third vectors deviate from zero at short wavelength region, but this effect may be regarded as the relatively low signal-to-noise ratio in that region. The remaining vectors of the calculated sets are not represented in the figures because these are regarded as null vectors with amplitudes within the limits of the usual baseline noise over the entire wavelength range. From these results, it is concluded that the observed spectra may be represented as linear combinations of only two curves and that a two-state stacking-unstacking model can be justified for thermodynamic analysis of the spectra.

Although SVD vectors reveal the number of significant components in the data sets, they do not have any physical meaning. Taylor series fitting of the CD curve for a dimer or polymer to its monomer absorption band can be used to extract important physical parameters that have a physical meaning. Here we decompose the smoothed curves for the first positive and negative bands of dimers that stack into the Taylor series components as described by Causley et al. (1983). We use only the first two bands of the CD spectrum for each dimer as they obviously represent true degenerate stacking interactions, and the Taylor series expansion is only valid over a small wavelength region. The A and B coefficients determined for each of the dimers that stack are plotted in Figure 4.9. Stacking coefficient B represents the degree of stacking interaction between adjacent monomer bases. Each dimer has different curve for  $B(T)$ , which is higher at lower temperature and decreases as the temperature increases. The unstacked dimer studied, I and II, have an almost zero stacking

coefficient over the entire temperature range studied. The A coefficient of all dimers was nearly constant over the temperature range studied.

One striking feature of the temperature dependence of stacking coefficient  $B(T)$  for the analogues is that their values are almost linearly related with temperature. This result contrasts with work on ribonucleotide dimers (Powell et al., 1972; Olsthoorn et al., 1980; Causley et al., 1983), where unstacking is almost complete at 90 °C. Taking ApA as an example (Figure 4.9), the dependence of stacking coefficient on temperature shows considerable curvature. From this linear relationship between coefficient  $B(T)$  and temperature for the modified dimers, we will extract the enthalpy ( $\Delta H^\circ$ ) and the entropy ( $\Delta S^\circ$ ) for the stacking process, and the stacking coefficient at the fully stacked state ( $B_{st}$ ) using the van't Hoff equation.

**Thermodynamics of Stacking :** To calculate  $\Delta H^\circ$ ,  $\Delta S^\circ$ , and  $B_{st}$  for the dimers that stack, the Taylor series coefficients,  $B(T)$ , were fitted with the van't Hoff equation as described in the materials and methods section. Table 4.1 lists the stacking parameters and the melting temperature ( $T_m$ ) defined as the temperature yielding 50 % stacking. The small standard deviations for  $\Delta H^\circ$  and  $\Delta S^\circ$  indicate that our fitting is very stable. A glance at these values shows that  $\Delta H^\circ$  and  $\Delta S^\circ$  differ for each stacking dimer studied, which means the backbone structure of each dimer could affect the thermodynamic characteristics of stacking interaction. As a framework for further discussion we classify the dimers that stack according to decreasing stability as indicated by their  $T_m$  (Table 4.1). An alternate way of representing relative stability would be to arrange the dimers according to their  $\Delta G^\circ$  at a given temperature, say 25 °C. A large negative  $\Delta G^\circ$  would mean that at this temperature stacking is more favored. Since  $\Delta G^\circ$  depends on both  $\Delta H^\circ$  and  $\Delta S^\circ$ , its value will vary according to the relative contribution of  $\Delta H^\circ$  and  $\Delta S^\circ$ . The relative stability of stacking interaction according to  $\Delta G^\circ$  and  $T_m$  is similar. Arranging according to  $T_m$  (Table 4.1) we find

IV-fast > IV-slow  $\approx$  V-fast  $\approx$  III-slow  $\approx$  V-slow > III-fast  $\approx$  d(ApA) > ApA

In most cases, these ApA analogues appear more stacked than d(ApA). In addition, it is important to recognize that these unusual backbones show a higher capability for stacking than the standard ribose-phosphate backbone in ApA.

The  $T_m$  reported for ApA as calculated from thermodynamic parameters varies from -42 to +77 °C, and using CD or optical rotatory dispersion from -8 to +43 °C (Powell et al., 1972; Frechet et al., 1979; Olsthoorn et al., 1981; Causley et al., 1983). Our  $T_m$  of +10 °C for ApA is slightly lower than other recent CD work (Powell et al., 1972; Frechet et al., 1979; Causley et al., 1983), and within the experimental error of determining  $\Delta H^\circ$  and  $\Delta S^\circ$  in our earlier report (Causley et al., 1983). The  $T_m$  is considerably lower than the ApA analogues studied here, and arises in spite of a very favorable  $\Delta H^\circ$ , because of a particularly unfavorable  $\Delta S^\circ$  (Table 4.1).

For comparison, the percentage of stacking for dimers that stack was calculated from the parameters of Table 4.1 as a function of temperature (Figure 4.10). Evidently, phosphorus-linked morpholino analogues (III, IV, and V) show excellent stacking properties; more than 80 % of the molecules adopt the base stacked conformations at 0 °C. It is clear that all phosphorus-linked morpholino analogues have a greater stacking ability than ApA.

**Fitting Straight Lines :** One striking feature of the temperature dependence of the stacking coefficients  $B(T)$  for d(ApA) and the analogues is that the values are almost linearly related to temperature (Figure 4.9) over the range studied. The slope and intercept of these lines vary with the dimer studied. Thus, it is interesting to see how the thermodynamic parameters change as the slope or intercept of the straight lines is changed. As an example we produced various straight lines with different slopes and intercepts based on the measured  $B(T)$  of d(ApA) (Figure 4.11). We then fitted these

straight lines to the transformed van't Hoff equation to extract thermodynamic parameters. Table 4.2 shows results of this fitting, and we found some general trends. As the slope of the straight line increases,  $B_{st}$ ,  $\Delta H^\circ$ , and  $\Delta S^\circ$  magnitudes increase, but since  $\Delta S^\circ$  increases faster than  $\Delta H^\circ$ ,  $T_m$  decreases. In contrast, as the intercept of a straight line with constant slope increases,  $\Delta H^\circ$  and  $\Delta S^\circ$  decreases in magnitude and  $T_m$  increases because  $\Delta S^\circ$  changes faster. Here  $B_{st}$  increases also. When straight line data are multiplied by some factor, the  $\Delta H^\circ$  and  $\Delta S^\circ$  extracted from the new line are the same as from the parent line, and only the  $B_{st}$  is changed by the same factor (data not shown). This result means that a consistent error in measuring CD intensity does not affect the thermodynamic parameters. All of these results indicate that reasonable thermodynamic parameters can be extracted even from the straight lines, by fitting them to the van't Hoff equation.

**Conformation of Stacked Dimers :** The CD spectrum of a nucleotide or unstacked dinucleotide is very sensitive to the angle that the base forms with the sugar. The CD spectra of the stacked dimers presented in Figures 4.3-4.6 show conservative exciton effects (the B term), which are sensitive to the relative conformation of two stacked bases. The long wavelength band is positive, and this indicates a right-handed helical twist of the transition dipoles and therefore a right-handed helical conformation.

$B_{st}$  measures the conservative exciton effects for the fully stacked dimer. We see that the fast dimers have a  $B_{st}$  that is considerably lower than the slow dimers (Table 4.1), indicating that the fast dimers have a stacked conformation different from the slow dimers. Dimer III-fast exhibits the lowest  $B_{st}$  of the dimers studied here that stack, and the shape of its CD (Figure 4.4) is somewhat different from the other stacking dimers. Natural dimer d(ApA) has a  $B_{st}$  that is virtually the same as III-slow and V-slow, indicating similar stacked conformations. Dimer ApA has the largest  $B_{st}$ , even though it has the lowest stability of the dimers studied here that stack. Apparently, the ultimate

magnitude of the conservative exciton interaction is not directly related to stacking stability, as measured by the thermodynamic parameters.

Figure 4.7. The three most significant wavelength basis vectors (**US**) determined from singular value decomposition of CD spectra for (a) I, (b) III-slow, and (c) V-slow. Symbols: (—) first; (···) second; (— — —) third.

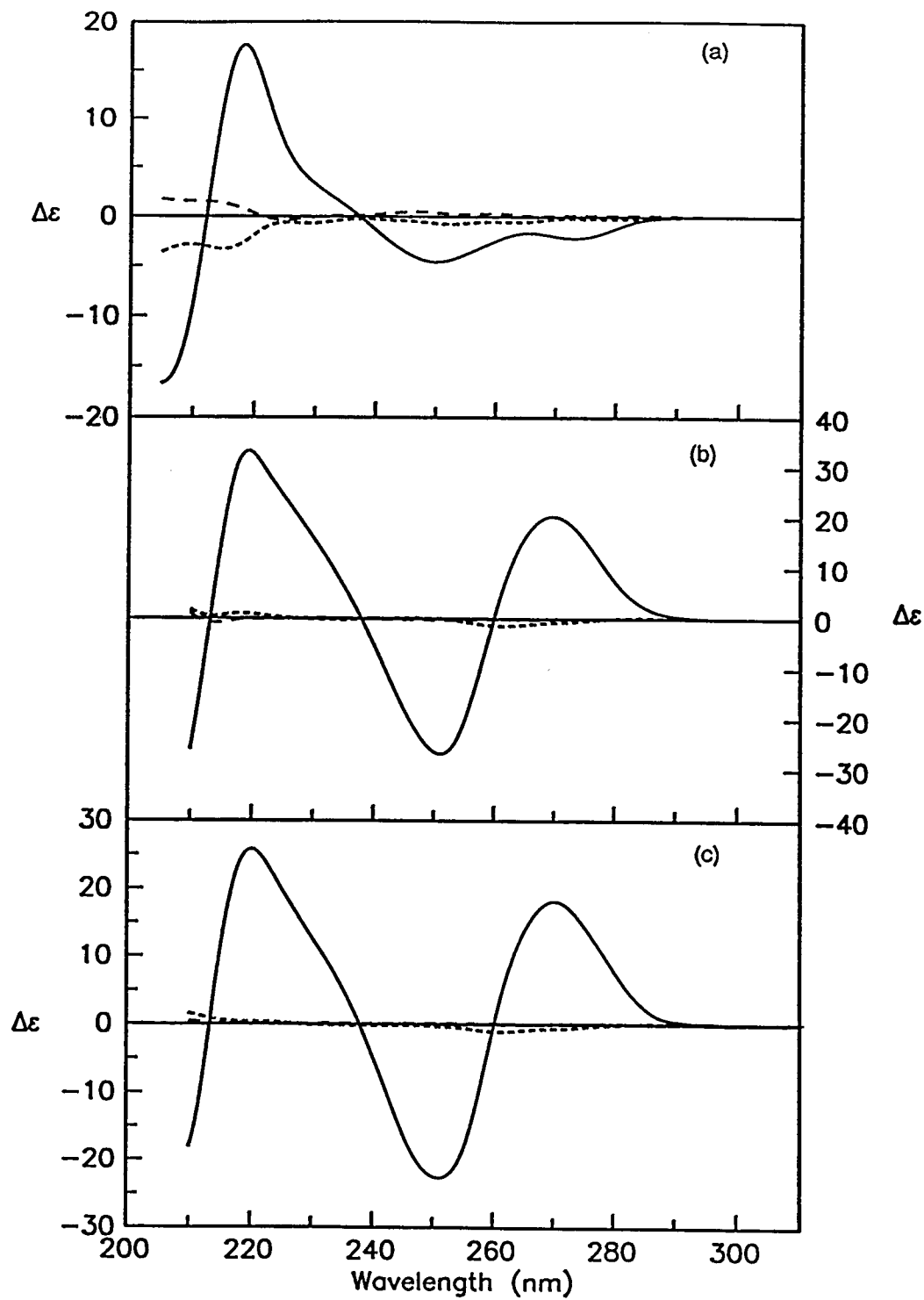


Figure 4.7

Figure 4.8. The three most significant temperature basis vectors ( $\mathbf{SV}^T$ ) determined from singular value decomposition of CD spectra for (a) I, (b) III-slow, and (c) V-slow. Symbols:  $\square$ , first;  $\Delta$ , second; +, third.



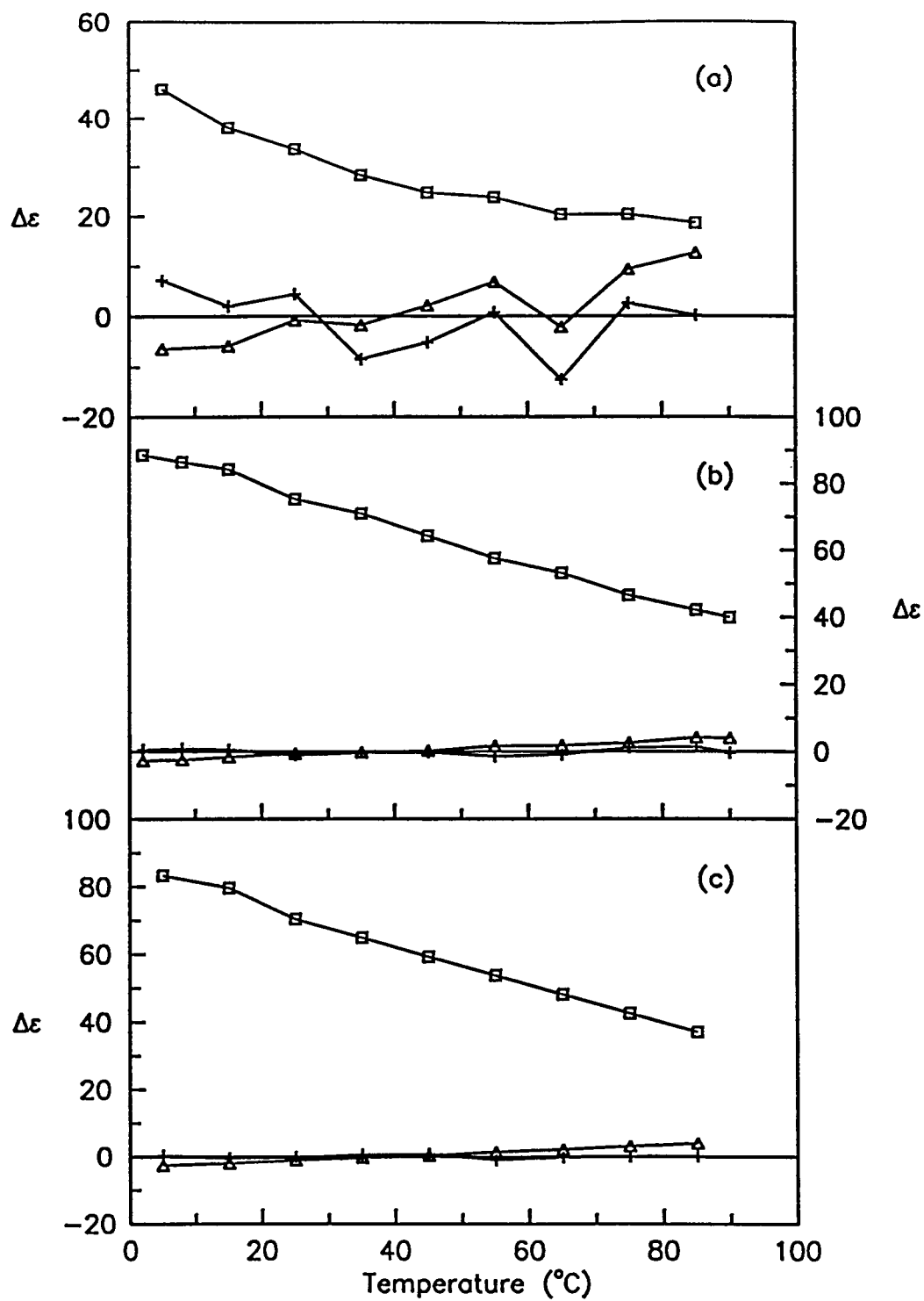


Figure 4.8

Figure 4.9. Taylor series coefficients A and B vs temperature for d(ApA)

(+), ApA ( $\times$ ), I ( $\diamond$ ), II ( $\oplus$ ), III-fast ( $\square$ ), III-slow ( $\blacksquare$ ), IV-fast ( $\circ$ ),  
IV-slow ( $\bullet$ ), V-fast ( $\triangle$ ), and V-slow ( $\blacktriangle$ ).

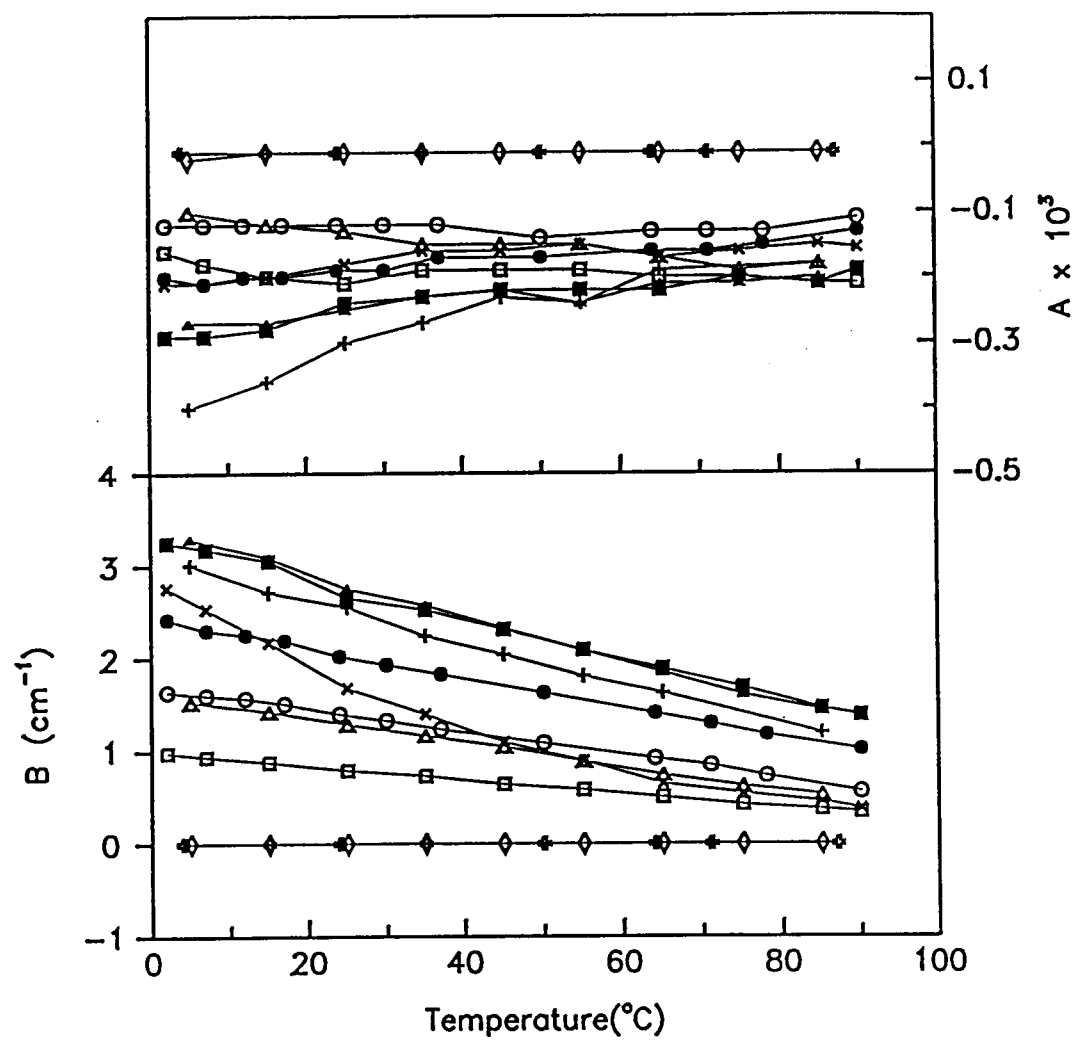


Figure 4.9

Figure 4.10. Percentage of stacking vs temperature for dimers that stack, calculated from the parameters of Table 4.1. Symbols are same as in Figure 4.9.

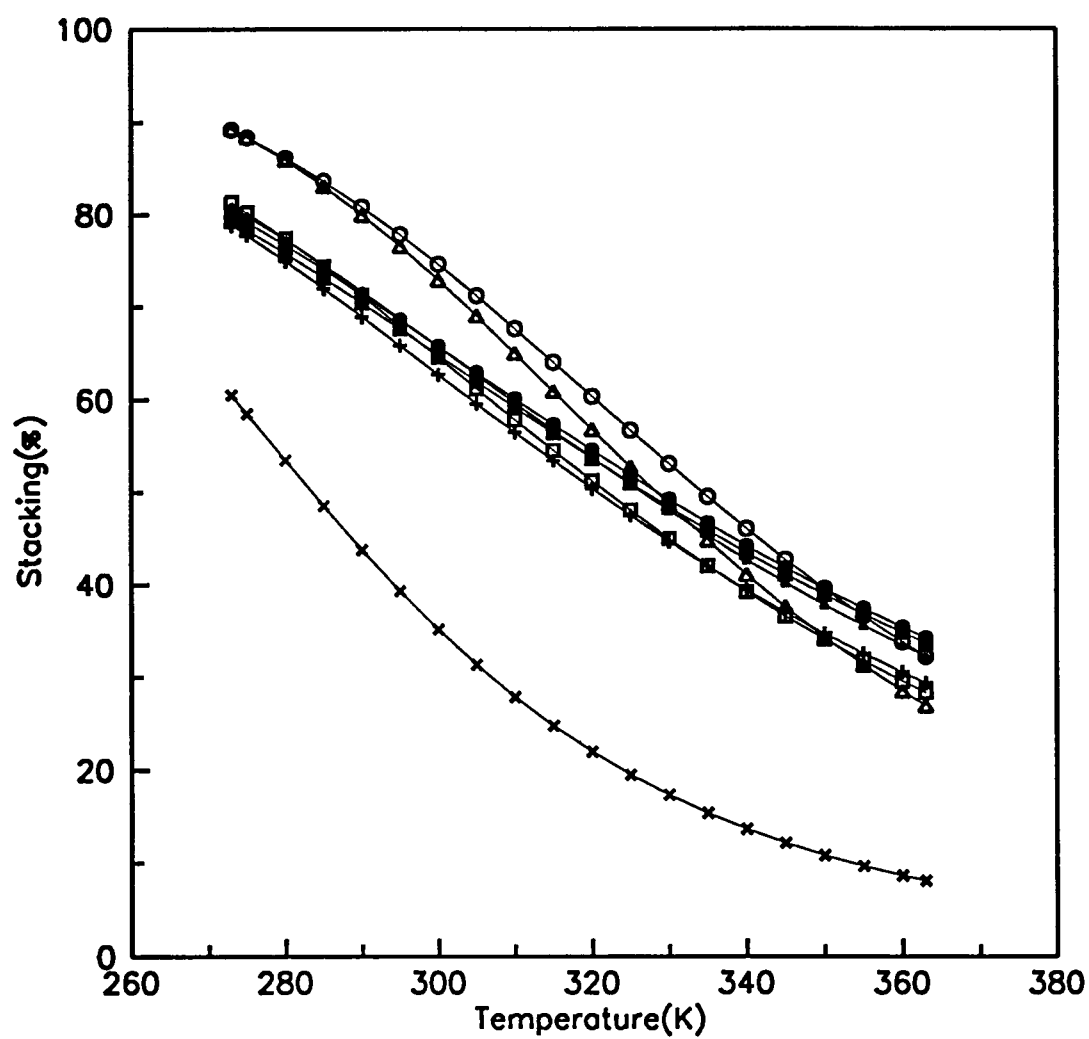


Figure 4.10

Figure 4.11. Taylor coefficients  $B$  vs temperature for various straight lines with different slopes and intercepts. These lines were produced based on the measured  $B(T)$  of  $d(\text{ApA})$ . The lines  $\bullet$  (top) and  $\circ$  (bottom) are similar to those measured for  $B(T)$  of  $d(\text{ApA})$ .

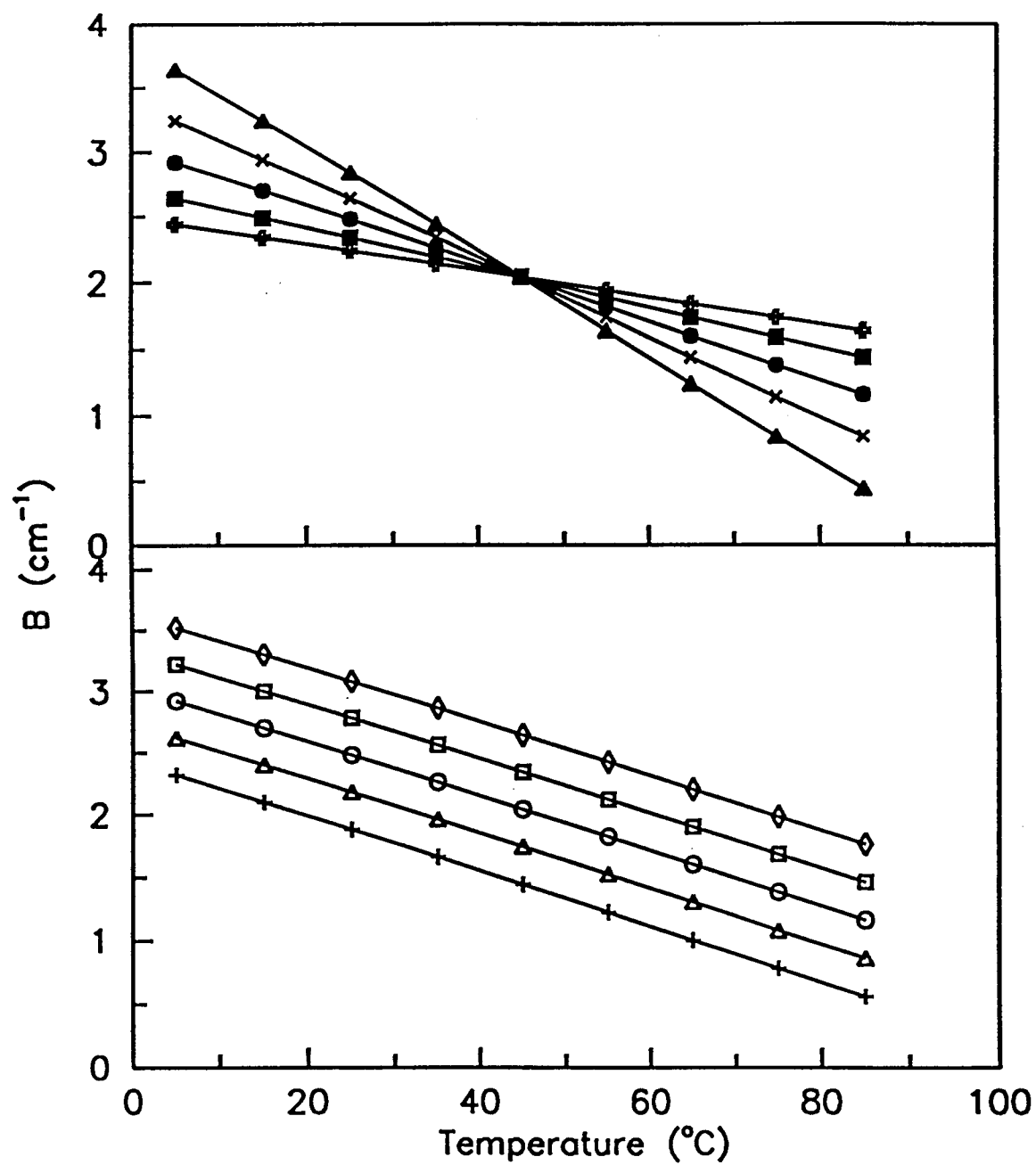


Figure 4.11

Table 4.1. Thermodynamic Parameters for Intramolecular Stacking











Sample	$B_{st}$ ( $\text{cm}^{-1}$ )	$\Delta H^\circ$ ( $\text{kcal mol}^{-1}$ )	$\Delta S^\circ$ ( $\text{cal mol}^{-1}\text{K}^{-1}$ )	$T_m$ ( $^\circ\text{C}$ )	$\Delta G^\circ{}^b$ ( $\text{cal mol}^{-1}$ )
III-fast	1.22	$-5.23 \pm 0.06^a$	$-16.26 \pm 0.05^a$	49	-384.5
III-slow	4.18	$-4.41 \pm 0.10$	$-13.50 \pm 0.10$	54	-387.0
IV-fast	1.86	$-6.23 \pm 0.12$	$-18.65 \pm 0.12$	61	-672.3
IV-slow	3.04	$-4.47 \pm 0.07$	$-13.61 \pm 0.06$	55	-414.2
V-fast	1.76	$-6.81 \pm 0.08$	$-20.74 \pm 0.06$	55	-629.5
V-slow	4.21	$-4.77 \pm 0.07$	$-14.62 \pm 0.06$	53	-413.2
d(ApA)	3.94	$-4.79 \pm 0.10$	$-14.93 \pm 0.07$	48	-340.9
ApA	4.71	$-6.24 \pm 0.07$	$-22.02 \pm 0.07$	10	-322.0

<sup>a</sup> Standard deviation.

<sup>b</sup>  $\Delta G^\circ = \Delta H^\circ - T\Delta S^\circ$  at  $25^\circ\text{C}$ .



Table 4.2. Results of Fitting Various Straight Lines (Figure 4.11) with Different Slopes and Intercepts to the van't Hoff Equation

Line	$B_{st}$ ( $\text{cm}^{-1}$ )	$\Delta H^\circ$ ( $\text{kcal mol}^{-1}$ )	$\Delta S^\circ$ ( $\text{cal mol}^{-1}\text{K}^{-1}$ )	$T_m$ ( $^\circ\text{C}$ )
-  -	2.99	$-3.17 \pm 0.01$	$-8.47 \pm 0.01$	102
-  -	3.24	$-4.15 \pm 0.03$	$-12.01 \pm 0.02$	73
-  -	3.51	$-5.55 \pm 0.07$	$-16.81 \pm 0.05$	57
-  -	3.74	$-7.32 \pm 0.16$	$-22.72 \pm 0.13$	49
-  -	3.98	$-10.05 \pm 0.43$	$-31.65 \pm 0.34$	44
-  -	2.66	$-7.61 \pm 0.18$	$-23.67 \pm 0.14$	49
-  -	3.09	$-6.37 \pm 0.11$	$-19.56 \pm 0.08$	53
-  -	3.51	$-5.55 \pm 0.07$	$-16.81 \pm 0.05$	57
-  -	3.91	$-4.98 \pm 0.05$	$-14.88 \pm 0.04$	62
-  -	4.31	$-4.53 \pm 0.04$	$-13.34 \pm 0.03$	66

## **ACKNOWLEDGEMENTS**

This work was supported by National Science Foundation grant DMB-8803281 from the Biophysics Program.

## REFERENCES

- Brahms, J., Maurizot, J. C., & Michelson, A. M. (1967) *J. Mol. Biol.* **25**, 481-495.
- Cantor, C. R. & Tinoco, I., Jr. (1965) *J. Mol. Biol.* **13**, 65-77.
- Catlin, J. T. & Guschlbauer, W. (1975) *Biopolymers* **14**, 51-72.
- Causley, G. C., Staskus, P. W., & Johnson, W. C., Jr. (1983) *Biopolymers* **22**, 945-967.
- Dewey, T. G. & Turner, D. H. (1979) *Biochemistry* **18**, 5757-5762.
- Dewey, T. G. & Turner, D. H. (1980) *Biochemistry* **19**, 1681-1685.
- Ezra, F. S., Lee, C. H., Kondo, N. S., Danyluk, S. S., & Sarma, R. H. (1977) *Biochemistry* **16**, 1977-1987.
- Frechet, D., Ehrlich, R., & Remy, P. (1979) *Nucleic Acids Res.* **7**, 1981-2001.
- Freier, S. M., Hill, K. O., Dewey, T. G., Marky, L. A., Breslauer, K. J., & Turner, D. H. (1981) *Biochemistry* **20**, 1419-1426.
- Kondo, N. S. & Danyluk, S. S. (1976) *Biochemistry* **15**, 756-768.
- Lee, C. H., Ezra, F. S., Kondo, N. S., Sarma, R. H., & Danyluk, S. S. (1976) *Biochemistry* **15**, 3627-3639.
- Lowe, M. J. & Schellman, J. A. (1972) *J. Mol. Biol.* **65**, 91-109.
- Noble, B. & Daniel, J. W. (1977) *Applied Linear Algebra*, Prentice-Hall, Englewood Cliffs, NJ.
- Olsthoorn, C. S. M., Bostelaar, L. J., de Rooij, J. F. M., van Boom, J. H., & Altona, C. (1981) *Eur. J. Biochem.* **115**, 309-321.
- Olsthoorn, C. S. M., Doornbos, J., de Leeuw, H. P. M., & Altona, C. (1982) *Eur. J. Biochem.* **125**, 367-382.
- Olsthoorn, C. S. M., Haasnoot, C. A. G., & Altona, C. (1980) *Eur. J. Biochem.* **106**, 85-95.
- Powell, J. T., Richards, E. G., & Gratzner, W. B. (1972) *Biopolymers* **11**,

235-250.

Vournakis, J. N., Poland, D., & Scheraga, H. A. (1967) *Biopolymers* **5**, 103-122.

Warshaw, M. M. & Cantor, C. R. (1970) *Biopolymers* **9**, 1079-1103.